High Speed Weighing System Analysis via Mathematical Modelling

A thesis presented in partial fulfilment of

the requirements for a degree of

Masters of Engineering

Mechatronics

at

Massey University,

Albany, Auckland,

New Zealand

Rami Elbeltagi

2011

Abstract

In-process electronic high speed weighing systems play an important role in the highly automated, continuously evolving industrial world of today. They are an essential component in sorting, grading and quality control within a diverse range of industries, including; robotics, automotive and food. Load cells are considered to be the definitive force sensor for industrial weighing systems. Load cell output is in the form of an oscillatory response in which the measurand contributes to the response characteristics. Current methods require the oscillatory response to settle in order to achieve an accurate measurement. This is time consuming and speed limiting.

The focus of this paper is to find alternative weighing analysis methods for a system which utilises two load cells, placed either side of a carrier travelling on a chain conveyor, running at speeds of 10 items a second. It is necessary to determine the value of the measurand in the fastest time possible to speed up the process and increase throughput. This has been approached by mathematically modelling the system to allow accurate prediction of the weights passing the load cells before the settling time of the oscillatory response. Models of harmonic motion have been considered for the motion of a load cell.

An experimental system was built and weighing data collected for different speeds and loads. Spectral analysis of the weighing data was analysed to determine dominant frequencies and estimate system parameters.

This thesis describes the work done on load cell modelling and improving an in-process electronic weighing system by successfully predicting the weight during the transient period of the oscillatory response. The assumptions and results of both simulations and experimental data are presented.

Acknowledgments

I would like to thank everyone who has helped and supported me through this project. I would firstly like to thank my family; Osama Elbeltagi, Hala Elattar and Moemen Elbeltagi, who have provided me with encouragement and loving support. They made sure I believed I could achieve whatever I put my mind to.

My deep and sincere gratitude to my mentor, Dr. Alona Ben-Tal, B.Sc., M.Sc., Ph.D., College of Sciences, Institute of Information & Mathematical Sciences, Massey University. Her encouragement, personal guidance and understanding have provided a good basis for the thesis. Her wide knowledge and logical way of thinking have been of great value to me.

I am deeply grateful to my supervisor, Dr. Johan Potgieter, B.Sc., M.Sc., Ph.D., College of Sciences, Institute of Technology & Engineering, Massey University, for his detailed and constructive comments, and for his excellent advice during the preparation of this thesis.

I would like to express my warm and earnest thanks to Marcus Davies, R&D Mechanical Development Manager, Compac Sorting Equipment, who introduced me to the potential of this project and has guided me during the first steps. His ideals and concepts have had a remarkable influence on my entire career as a Mechanical R&D Design Engineer.

During this work I have collaborated with many colleagues, David Williamson, Oliver Grant, Nathan Vissers, Frazer Noble and James Scholz, to whom I have great regard, and would like to extend my heartfelt thanks. They allowed me to discuss problems and gave me untiring help during my difficult moments.

The financial support of Compac Sorting Equipment as well as providing me with a chance to do further study is gratefully acknowledged.

I am much thankful for the liberality of Dick and Mary Earle for providing me with a munificent scholarship. Their interest in this project has been immense and their input has been very beneficial.

Table of Contents

List of Figures

List of Tables

Chapter 1: Introduction

The strain gauge based load cell is the most common weighing device which uses a thin foil resistor as the primary sensing element (Muller, de Brito, Pereira, & Brusamarello, 2010). A load cell is a transducer which converts force into a measurable electrical output. The strain gauges are bonded on elastic materials and change their resistance according to the deformation of the spring element when under stress. The resistance is proportional to the intensity of the applied force. The strain gauges are usually assembled in a Wheatstone bridge configuration where the measurement is indirect by the detection of the differential voltage in the centre of the bridge. This eliminates the offset voltage that naturally occurs in a simple resistance-to-voltage converter. A typical setup is having a Wheatstone bridge using 1, 2 or 4 strain gauges then adding an amplifier and filter for conditioning.

The strain gauges are sensitive to mechanical stress, temperature variations as well as to unwanted noise and vibration interferences (Muller, et al., 2010). As the demand for higher throughput increases, higher processing speeds are needed. However, higher speeds introduce additional noise and vibrations and therefore diminish the accuracy of the measurements. This is why the need for new high speed weighing methods is becoming increasingly important.

In addition, government bodies internationally are trying to maintain high standards of weighing by introducing legal requirements and regulations for weighing. This is beneficial to both the customers and the producers. The producer's manufacturing efficiency is increased and hence profitability whilst packing quality and quantity are assured to the customer's satisfaction (Balachandran et al., 1995). As a result of these two trends, new high speed weighing methods are becoming increasingly important.

Load cell output is in the form of an oscillatory response in which the measurand contributes to the response characteristics. Current methods require the oscillatory response to settle down before an accurate measurement is achievable. It is necessary to determine the value of the measurand in the fastest time possible to speed up the process of measurement.

Compac Sorting Equipment Ltd is a New Zealand owned company established in 1984 by Hamish Kennedy. Compac specialises in produce sorting and handling equipment and is now the world leader in fruit sorting technology. Compac designs, manufactures, assembles,

installs and maintains machines which are termed sizers to sort and pack fruit all over the world. Compac's success has been based on the application of leading edge technology through the collaboration of mechanical, electrical and software solutions. The machines sort produce by size, colour, defect, sweetness and weight. Compac exports worldwide to Australia, North and South America, Europe, Asia and South Africa, and manufactures in four countries; New Zealand, Uruguay, Italy and Korea. Compac employs over 100 employees in New Zealand and over 300 employees worldwide.

One of Compac's main inspection systems is the weighing hence expressing interest and sponsoring my Master's project. Compac's dependency on this system has caused them to invest in research work being conducted in the past, such as presenting the project to Mathematics in Industry Study Group (MISG) in 2005. MISG form a workshop whereby Mathematicians and Engineers tackle real world complex problems and suggest solutions to the various industries. The suggestions from the workshop in 2005 have guided me in this research.

1.1 Objectives

The objective of the project is to improve a high speed weighing system. This has been tackled through mathematically modelling the system and inferring various methods to calculate the weight. Disturbances and interferences with acquiring the weights while using these methods were investigated. This allowed for a great deal to be learned about the real-life counterpart and increased the opportunity to understand the problem and its results, and provide sound conclusions.

A high speed weighing system has been configured and assembled to allow testing to be performed. It consists of a weighing inspection section with a dual load cell system surrounded by a chain conveyor based machine that transports carriers onto the dual load cell system. Items are placed onto the carriers and allowed to settle prior to the weighing inspection section. Through this, different methods can be used to determine the weight of unknown items at high speeds of up to 10 items a second.

1.2 Literature Review

The purpose of this literature review is to provide an overarching of the work done on load cell modelling and weighing analysis methods , as well as the various techniques used to face the weighing problem.

Several methods have been proposed to improve the weighing measurements from a load cell. They can be classified into three areas; frequency compensation, model parameter estimation and neural network modelling.

1.2.1 Frequency Compensation

Due to noise introduced on the weigh measurement output, it is necessary to find a suitable filter technique that will cope with the variations in the frequency of system noise. The filter needs to extract the desired part of the signal, giving both a fast transient response and stable, robust weighing result. Adaptive filters are used to handle wide variety of masses to compensate for changes in natural frequency by adjusting its transfer function depending on an optimisation algorithm. Compensation for imperfections in load cell captures is an imperative aspect of sensor research, as there is influence of unwanted signals, non-ideal frequency response, nonlinearity, cross sensitivity and parameter drift defects occurring in primary sensors (Jafaripanah, Al-Hashimi, & White, 2005).

Calpe et al. (2002) present, while looking at high speed weighing of fruit, the use of more advanced pre-processing method to have a ±2g deviation at 16fruit/sec for a fruit range up to 250g. The work presents a two step process of filtering and having the resulting signal deconvoluted. The purpose of the filtering is to soften vibrator oscillations produced by the mechanical system and to remove of power line interference.

In this approach it was assumed that the load cell functions as a second order system. Through the use of adaptive filtering, they have shown that there was improvement in the graph's oscillations by using a least mean squared (LMS) algorithm to adjust an adaptive filter coefficient used in the method of steepest descent. They have also shown that better results can be obtained by using an averaged least means squares (ALMS) variant.

Oscillations were still evident in their graphs after the adaptive filtering so they investigated the path of modelling the oscillations using another model from a single input record of a step

function. The model was a second order, zero-phase system with zero delay, so it equalises the system response (Frances et al., 2000). They called it the ARMA model.

The results of the ARMA model produced a plateau around the actual weight, including a 20g error range. The average of the plateau was thought to be an accurate enough estimation of the weight. The plateau's length varied depending on the weight and speed at which the fruits were travelling. To determine the length of the plateau, first the end limit was obtained by using a pulse from an optical encoder. This encoder was used for synchronization to mark the moment when the cup exits the weighing platform. Next, the start of the plateau was determined by using a look-up-table which contained lengths of plateaus obtained for different speeds.

Due to unspecified mechanical restrictions of the machine, they were only able to run at 16 fruit a second, and they could not maintain that speed for a long duration. This limitation confined them to obtain results of only 10 measurements for 6 fruit weights; 0g (empty carrier), 50g, 100g, 150g, 200g and 250g. Furthermore, to obtain these results, the fruit were manually placed at a distance to the weighing platform to stabilise the fruit and avoid superfluous vibrations. At least two empty cups were left between consecutive pieces. The results are summarised in Table 1. They show a maximum error of 0.57% for the 250g weights.

Real Value (g)	0	50	100	150	200	250
Mean (g)	-0.02	49.95	100.21	150.32	199.31	248.58
Standard Deviation (g)	0.2	0.31	0.44	0.50	0.56	0.68
Maximum Deviation (g)	0.61	0.82	1.02	1.32	0.86	1.4

Table 1: Weigh results of 10 samples of weights between 0g and 250g

Halimic & Balachandran (1995) proposed the use of a Kalman filter to take these superfluous vibrations into account. The aim was to use improved filtration to allow an increase in speed and enhanced measurement accuracy of weighing. They stated that the main constraint in

increasing the throughput rate and achieving higher accuracy was the noise superimposed on the signal from the system noise, which predominantly came from the mechanical and electrical part of the weighing system and from the type of product. Another contributing factor is the speed of the conveyor as the level and frequency of noise varied with it.

Their weighing system was based on a belt conveyor transporting various sized products onto a load cell system. Due to variations in the product length coming onto the weighing area, weighing was time varying and this caused change in the values of the model parameters therefore requiring an adaptive filter.

When a Finite Impulse Response (FIR) filter with a smooth cut-off frequency characteristics and a linear phase response with a Hann's window was used, results for a single weighing measurement have shown improvement of 150%, and for repeated measurements only a 5% improvement was shown. This was due to the fluctuation of the DC level with very low frequency from measurement to measurement hence proposing the Kalman filter. The Kalman filter is a useful tool for reducing the effects of noise in measurements by estimating the true value of a set of variables from a set of noisy measurements.

To design the Kalman filter, mathematical models were employed to examine the suitability of the chosen filter. Automatic methods where the parameters of the filter are optimised using the performance indices as the quality of the filter, were found to be less time consuming than using an analytical method, and trial and error technique. The input to the load cell was modelled as a ramp function to simulate a rigid type input such as a plastic container or a carton box, and as a sinusoidal or cosinusoidal function to represent a plastic film bag filled with powder. They modelled the load cell as a damped spring system having the following equation;

$$(w(t)+m_1)\ddot{\theta}(t)+c\dot{\theta}(t)+k\theta(t)=w(t)g \qquad (1.1)$$

Where $w(t)$ is the mass of the product, m_1 is the mass of the load cell, c is the damping coefficient, k is spring constant, $\emptyset$ is the position of the weighable and g is the acceleration due to gravity.

This is used to estimate what the required variables in a Kalman filter will be, based on estimates of the time varying parameters.

The results obtained by applying the Kalman filter on real measurement data from the weighing system produced a 300% improvement as a result of single weighing measurement. Repeated measurements showed that a 50% improvement was attained. Therefore, this shows that a Kalman filter could be effective with increased speed given that all influences of the system and measurement noise are known. Unfortunately, the weight values were not stated and therefore the absolute accuracy is unknown.

1.2.2 Model Parameters

The load cell is frequently used to determine the weight by evaluating the step response due to an object exerting a force (weight) causing deflection in the load cell. The voltage output from the load cell is proportional to the input load (i.e. the weight).

Shu (1993) considers the weigher as a second order mass spring damper system similar to Halimic & Balachandran (1995) (Equation (1.1)). It was demonstrated that the mass can be estimated from the model parameters which are acquired through fitting the model to a measured transient weighing signal to have the least-squared errors.

The unknown mass of the product was derived from the z transformation by looking at the limit of the discrete values at infinity. This means that the unknown mass was found from the latter part of the weigh graph, avoiding the initial transient at the input side due to the sliding and springing of the package on the weighing platform.

Shu (1993) emphasised that determining the mass was independent of the initial conditions. The mechanical system that was used had noise in the measurements as a result of sliding or spring-like motion of the package on the load cell platform. The initial conditions affected the appearance of the start of the weigh graph signals. The end values were unchanged, hence determining the mass from the limit of the equations looking at the latter part of the weigh graphs.

In addition to the initial noise, the electrical elements such as the sensor and the amplifier contribute noise interference in the whole weighing process. Shu (1993) mentions that these can be minimised with a well designed system and the use of either a software low pass filter with a cut-off greater than the highest possible natural frequency of the weigher, or a hardware filter at the output side.

The method for finding the weight involved a recursive calculation of an algorithm. When this was used on two simulated noise-free signals of a 100g weight from the same parameters but under different initial conditions, they gave similar results. These results were not provided in the article. One of the signals was then corrupted with white-Gaussian noise and was found to converge in 180 steps to a value of 102.5539g using the recursive calculation, and when using a filter it converged in 50 steps to 99.77757g. This shows that it is more effective using a filter. Results are presented in Table 2.

Without a filter		With a filter	
Number of recursion steps	Estimated Weight (g)	Number of recursion steps	Estimated Weight (g)
60	105.1959	10	111.2408
90	99.91519	20	100.1327
120	103.912	30	98.95274
150	102.972	40	99.22825
180	102.5539	50	99.77757

Table 2: Results on two noise-free simulated signals

This has been further supported with real measurements by using a 36.2g, 100g and a 173.8g iron weights as test weights. A third order digital Infinite Impulse Response (IIR) low-pass filter with a third order was used to eliminate the input noise. Furthermore, the first 40 points of the measurement were eliminated to avoid input noise caused by sliding or springing of the weights on the platform.

The results to a 1% accuracy, showed that the weights can be acquired in less than 20% of the time needed while calculating it using the traditional static method. As the traditional static method required at least more than 1000 data points, whereas using the recursive algorithm meant that the weight can be found in approximately 200 data points.

Another concept of using the load cell as a weigher involves impact (Gilman & Bailey, 2006). Impact was performed by dropping the objects to be weighed onto a load cell, therefore exerting relatively large forces on each other for a short time. The load cell's

movement in response to external excitation force was, once again, modelled using Newton's second law; similar to the modelling performed by Halimic & Balachandran (1995) and Shu (1993) (refer to Equation (1.1)).

Given that the objects to be weighed are dropped onto the load cell, the impact event is approximated using the principle of conservation of momentum as the system is isolated and closed. The impact force causes an impulse which is equal to the change in momentum of the load cell. The mass can then be found in terms of the impulse and the impact velocity of the object by using the following equation;

$$m(J, v_m) = \frac{MJ}{M(1+e)v_m - J} \qquad (1.2)$$

Where M is the mass of the load cell, J is the impulse, v_m is the impact velocity and e is the coefficient of restitution (fractional value representing the ratio of speeds after and before an impact).

J can be found from the load cell output as it is approximated by a Dirac delta function scaled by J. Therefore the system output is assumed to be a scaled impulse response, $Jh(t)$. To determine the velocity of a falling object, the time (t_T) and distance (d) which the object experiences are measured. Then, assuming that the object is being accelerated solely by the force of gravity (g), the impact velocity becomes a function of t_T and d;

$$v_m(t_T, d) = \frac{d}{t_T} + \frac{1}{2} g t_T \qquad (1.3)$$

This approach assumes that the object rebounds in the opposite direction after collision with the load cell, with no significant change to the position or orientation of the object or the load cell during impact. Furthermore, it assumes the initial velocity of the load cell is zero and it assumes the effects of gravity, restoration and damping forces on the velocity of the load cell are negligible.

To test the relationship between impact and velocity, two steel balls with an 11.7g and 2.7g were dropped from varying heights on the load cells. The results indicated that there was a linear relationship between the measured size of the impulse and the impact velocity of dropped objects. Knowing the impact of an object, the velocity can be found using the linear

relationship; therefore the mass can be determined using Equation (1.2). Another experiment to test the time interval required to make each measurement was performed by dropping three almost identical objects with the same weight (~2.2g) at 250ms intervals. Results showed that a time interval of approximately 50ms was required to make each measurement, giving a theoretical measurement rate of 20 measurements per second for high speed weighing.

There was a lot of uncertainty due to the assumptions that have been made to simplify the analysis. They do not hold in real systems and this was evident in the high speed testing, especially due to the assumption that the load cell velocity prior to impact is zero.

It was also mentioned that for faster weighing, impact is not ideal due to constraints in the weighing process i.e. it was hard to control having the preceding item removed from the environment to avoid interference with the following item.

1.2.3 Artificial Neural Networks

Yasin & White (1999) investigated the application of neural network method to predict the weight by considering the feeding mechanism of a load onto a tri-beam load cell. This load sensor is based on three cantilevered beams coupled together. The load cell was considered as a non-linear mapping box where the input is the unknown load, and the output is the electrical signal generated due to the input load.

Through system simulation they have used three successive extreme points along with the time intervals between successive peaks to represent the input neurons. This was feasible as they showed that three successive points have sufficient information to determine the final value, the output neuron.

Simulated testing was performed by using a set of 100 patterns for training the neural network which was generated by choosing masses that were uniformly distributed over the range of 100g to 1000g. This was done for 10 different initial conditions that were chosen randomly. The neural network learns the behaviour of the sensor from the set of training patterns. For testing purposes, patterns were simulated by using 150g, 350g, 550g, 750g and 950g. These masses were purposely chosen to be different than those used for training. Results of the simulation for the testing weights showed an error of $\pm 1.5\%$,. The error was random across the testing weights, and it was considered small.

The simulated results were verified with real measurements by performing a practical experiment on the tri-beam load cell. A load set of 330 sample weights varying between 0g and 975.7g were used for training the network. Three weights of 148.29g, 542.3g and 832.2g were used to test the network. The training procedure was repeated many times with different conditions and each time the maximum error from the testing data was calculated. It was shown that if the number of training samples was greater than 30, the maximum error was less than $\pm 1.5\%$, similar to what was seen in the simulation.

Bahar & Horrocks (1997) investigated a multi-layer perceptron artificial neural network to obtain the weight from a finite segment of the load cell data from a weighing system. The idea of a finite segment was to allow for high speed weighing without having to wait for the transient effects. Furthermore, the neural network used backpropagation learning, whereby, it used an iterative method to minimise the error between the actual and the desired outputs of the network in response to given inputs.

Similar to Gilman & Bailey (2006), Shu (1993) and Halimic & Balachandran (1995), the article presented by Bahar & Horrocks (1997) proposed using Equation (1.1). They mention that an ideal weighing platform can be modelled by a mass-spring-damping structure with an underdamped step response, governed by the solution of the second order differential equation.

To simulate the network, Bahar & Horrocks (1997) used the solution to the model to generate data. They first used 200 noise-free input samples of applied masses that were uniformly chosen to cover the range 1kg to 100kg for training the network. It was assumed that the input is a step function. Results indicated that a linear relationship between applied masses and estimated output masses were evident as the errors were small. The average noise error in the linearity was 0.1187% and the root mean square (RMS) error was 0.0772kg between the applied and estimated masses. These verified that an artificial neural network is capable to accurately model the non-linear relationship between the load cell time series data and the corresponding applied mass.

Next they simulated noisy input samples by mixing the aforementioned training samples with random measurement noise having a 2% amplitude of the steady state mass. The results presented in Table 3 show an RMS error and average error of 0.4208kg and 0.5641% respectively for the testing data, and 0.4534kg and 0.4593% respectively for the training data.

The small difference between the training and testing data verified that a beneficial “noise averaging” is performed by the Artificial Neural Network.

Data	RMS error (kg)	Average error
Training	0.4208	0.5641%
Testing	0.4534	0.4593%

Table 3: Simulated testing and training data errors

Finally, experimental data were obtained from an industrial load cell to train an Artificial Neural Network. Applied masses of 5 to 45kg in steps of 1kg were used to train the network, except for 10kg, 20kg, 30kg and 40kg which were used as the testing data. Training was performed in a typical noisy laboratory environment. Testing data was applied by dropping the masses onto the load cell from a height of typically 2cm. The results presented in Table 4 shows that the testing applied masses can be predicted accurately even when noise is present.

Applied mass to the weighing platform (kg)	Estimated mass of the Artificial Neural Network	Error between applied and estimated masses (kg)
10	9.8814	0.1186
20	19.8137	0.1863
30	30.1190	0.1190
40	40.9231	0.9230

Table 4: Experimental results of the applied masses

1.2.4 Literature review Discussion

Accurate, fast and reliable dynamic weighing is important in the modern world. Several methods have been proposed to get an accurate measurement from a load cell. The output of the load cell was found to be highly sensitive to excitation factors all of which had a significant effect on the accuracy of the weighing measurements, as well as, mechanical and electrical inaccuracies influencing the output measurement results.

The methods reviewed have been split into three classifications of frequency compensation, model parameters estimation and neural networks.

Frequency compensation methods have been based on using adaptive filters which tracks variations in the measurand, as opposed to only having a fixed filter that is only valid at one specific load value. This is performed through the use of digital filtering, exhibiting the reciprocal characteristic of the load cell being cascaded with it. The transfer function of the filter is usually identified assuming that the sensor can be modelled as a linear system. Furthermore, an adaptive rule is needed and is a crucial element for automatic updating of the parameters of the filter to suit different measurands.

The literature review first investigated frequency compensation using an adaptive filter with an ALMS algorithm as proposed by Calpe et al. (2002). Their research showed that they acquired ±2g for a speed of 16 cups per second in a very controlled environment. This was possible as the graphs had a long time to settle as the effect of neighbouring cups was not taken into account by having at least two empty cups between consecutive fruit. It was mentioned that external interferences in the form of oscillations were evident in the measurements. These oscillations were attempted to be compensated for using Kalman Filter by Halimic & Balachandran (1995) and it seemed to be quite effective when looking at a single weighing measurement with an improvement of 300%. Repeated measurements were not as effective only showing a 50% improvement, possibly due to interferences between the items. Unfortunately, Halimic & Balachandran (1995) did not provide details of the apparatus used to perform the measurements, nor did they provide information on the weights or speed for testing. These oscillations were also noted by McGuinness et al. (2005) when analysing the power spectrum noticing there were usually two, or sometimes three, frequencies that were dominating in each spectra. It was mentioned that the lower frequency oscillations corresponded to the bouncing which decreased in frequency value yet increased in amplitude as the weight increased.

Model parameters estimation method developed a parametric model for the sensor (load cell) through experimental data or analytical means. This was commonly performed using a mass spring damper system. This method depended on extraction of parameters from a short duration of the response in each measurement. The value of the measurand was determined from the parameters of the model. This method was different depending on the model chosen and the procedure that was used to find parameters of the model.

The literature review investigated model parameter estimation methods where a suitable algorithm was used to estimate or predict the weight. Shu (1993) and Gilman & Bailey (2006) considered a second order system to acquire their algorithms. Shu (1993) utilised a recursive calculation of an algorithm to acquire a 1% accuracy in determining the weight from 20% of the data measurements. These results were from running 36.2g, 100g and 173.8g over the load cell. Unfortunately, the speed at which the items were run was not provided. Gilman & Bailey (2006) used a different method of applying the load by using impact rather than sliding. Time had to be given between objects being dropped on the load cell and assumptions had to be made to simplify the analysis. Results showed that weights can be calculated in 50ms periods, although this could not be done continuously as time was needed between loads in order to acquire the measurements accurately.

Neural Network method was based on a black box model that assumed a new system output can be predicted from the past inputs of the system. It used a collection of elements, called neurons, to learn through training by presenting the system with known weights (training data) and corresponding desired responses which perform generalisations about testing data. The Neural network was capable of ‘representing’ any known function to any level of accuracy assuming a sufficient number of layers (Windrow & Lehr, 1990).

Neural Networks analysis by Yasin & White (1999) were capable of accurately predicting an applied mass in a noisy environment on a tri-beam load cell system, while the weighing platform was still in transient mode to accuracies of 1.5%. This method was highly dependent on the training of the neurons with 330 sample weights needed to make generalisations. Bahar & Horrocks (1997) investigated the usage of Neural Network on a load cell system whereby the masses are dropped onto the load cell. Simulations verified that the neural network was capable to accurately model the relationship between the load cell and the applied mass, while performing noise averaging. Experimental results showed that the

applied masses were predicted when noise was present, with maximum error of 2.3% while applying a 40g weight.

1.3 Project Approach

Taking all these different research material into account, this project aims at improving a high speed weighing system's calculation through the model parameters approach. Similar to Gilman & Bailey (2006), Bahar & Horrocks (1997), Halimic & Balachandran (1995) and Shu (1993) the load cell model is considered as a second order equation using Newton's second law. This project however presents different methods than those previously suggested, whereby the initial oscillations are used to predict the unknown mass. The methods presented require estimation of the load cell parameters. They are referred to as the Frequency and Damping methods (Chapter 3). These are compared to the Averaging method which is currently used by Compac.

This approach been chosen as it has a number of benefits over the frequency compensation and neural network approaches. Modelling the system mathematically provides a systematic approach to problem solving, allowing analyses and understanding of the problem.

The neural network approach depends on a "black box" model that is developed to satisfactorily represent the input-output performance of the system with no insight into the system structure. It is difficult to analyse the source of the problem in detail and to diagnose the issues if it is dependent on trial and error through a learning system.

The system that will be experimented on already has electronics designed specifically for the application which includes filters and therefore, the Frequency compensation methods were not investigated further.

M. McGuiness et al. (2005) have already done a substantial amount of analysis as part of the Mathematics in Industry Study Group (MISG). Their findings are considered and built upon throughout the context of this project. Specifically, the Frequency method was suggested. This, as well as the Averaging method, are studied in detail and tested in this thesis. In addition to this, the Damping method is developed, tested and compared to the other methods.

Chapter 2: The Weighing System

The in process electronic high speed weighing system being analyzed consists of a dual load cell system whereby chain driven carriers travel over two load cells at high speeds up to 10 carriers a second. The desired item to be weighed is placed on a carrier, which is a Compac patented product. Dual load cells are used for stability of the items on the carriers. Furthermore, as each load cell is only subjected to half the weight of the item it has the advantage of not being over-stressed. The carrier has four contact points. Two points on each side of the carrier slide along a hardened stainless steel plate mounted on a load cell. The load cells are cantilevered to allow deflection.

Figure 1: Compac Carrier

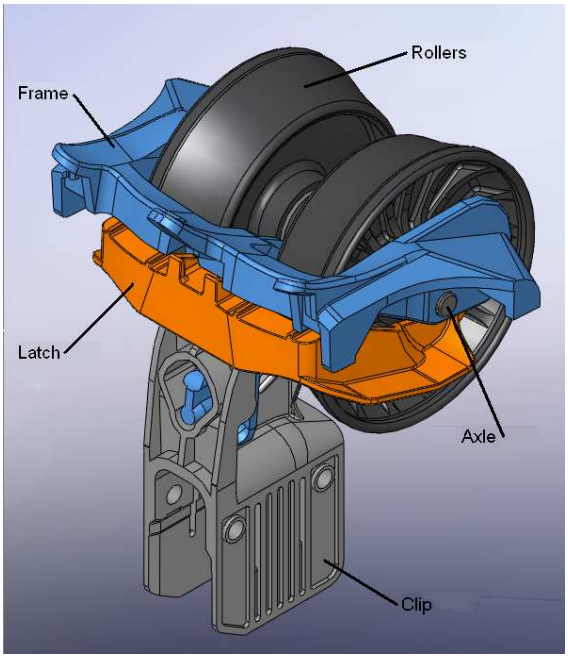

Figure 2: Carrier Components in Solidworks

The load cells used are Vishay low profile single point with a 6kg capacity. They have an accuracy class (NTEP/OIML) of C3 with a maximum number of intervals of 3000 and a Y value (Emax/Vmin) of 6000. Therefore for the 6kg load cell, it has an accuracy of ±1g. The Data Sheet is presented in Appendix A. Further research could have been spent searching for other load cells with higher Y value to increase the resolution, and with increased stiffness.

Figure 3: Apples on a Vishay Load Cell

Stiffness is advantageous when weighing heavier items, as the oscillations would reach steady state faster. Although due to the weights of the items we are interested in, the 6kg load cells are sufficient and will be reactive to small changes of weight, as well as being cheaper.

Load cell output is in the form of an oscillatory response of current and is dependent on the amount of deflection it experiences due to the added weight. This current output (4-20mA) is passed through an instrumentation amplifier, and filtered using a 5th order Butterworth filter. This is then passed through a current to voltage converter and sampled at 4 kHz by a 12bit Analogue to Digital Converter (ADC). Figure 4 shows a typical weigh graph of three carriers from the load cell output.

Figure 4: Typical Weigh Graph

The Load Cell system is designed such that each carrier exerts pressure on both load cells at the same time. The graphs are introduced with an overshoot as each carrier exerts pressure on the load cell plate. The load cell plate is made out of hardened stainless steel and is cut to the shape of a z to allow contact points on the carrier to exert pressure on the load cell for the maximum allowed time (refer to Figure 42). The overshoot then dampens into oscillations which would eventually reach steady state if enough time is given.

The item to be weighed travels along two load cells on a carrier for a short period of time depending on the speed of the motor driving the chain. The outputs from the two associated load cells are summed and the carrier weight is subtracted to give the desired weight of the item.

Due to the possibility of interferences propagating through machine components, this system is placed on a weighing structure isolated from the whole machine. This weighing structure is bolted down to the floor. The only point of contact between the weighing system and the rest of the machine is the carriers with the desired items to be weighed. Figure 5 is of the experimental machine modelled in Solidworks.

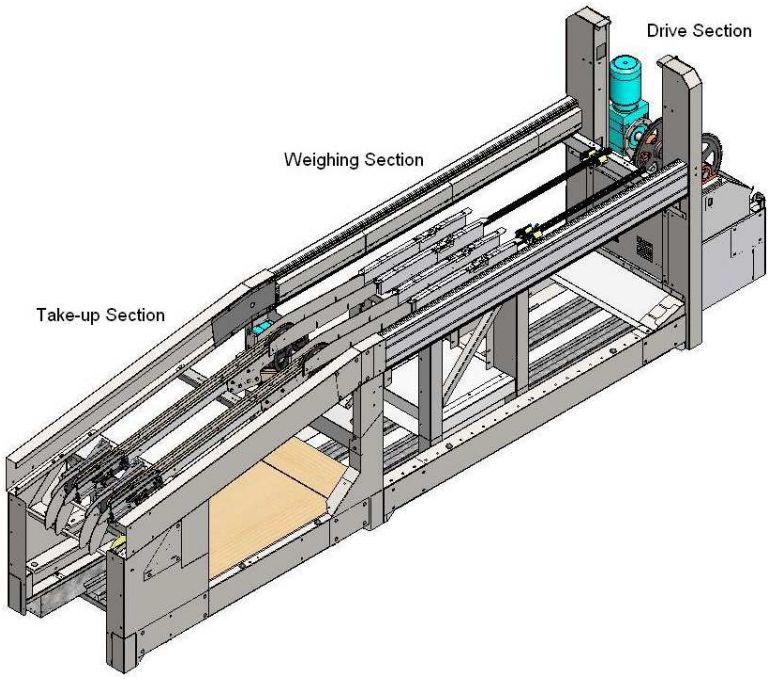

Figure 5: The Weighing Machine

Solidworks was used for the design as it is a very powerful 3D modelling tool which has intuitive 3D design software with built-in intelligence to allow collaboration while designing. It allows speed design while ensuring accuracy starting from individual parts to top level

assemblies. Having the machine model design and the flexibility of viewing and editing individual parts allows for testing real world conditions to make sure it is right before building (Solidworks 2011).

The machine that has been configured and built for experimentation purposes to allow access to weighing data for analysis consists of two lanes with a take-up, a weighing and a drive section. Two lanes have been chosen so comparison tests can be done simultaneously. This saves time having to redo each test twice, and has helped with determining variations and errors to be expected between the lanes. The take-up section is where the items to be weighed are placed on the carriers. This is two meters long to allow easy placement of the items to stabilize on the carriers before entering the weighing section. Unstable items on carriers may cause false readings due to not having all its weight exerted on the load cell, or adding additional force onto the load cell due to gravity and kinetic inertia.

The weighing section contains the dual load cell system arrangement for each lane of carriers. It is isolated from the rest of the machine by being bolted to the floor with the load cell system being the only point of contact with the carriers. This is to avoid unnecessary vibrations interfering with the weighing.

The Drive section contains a 3kW Bonfiglioli motor to drive the chain conveyors at fast speeds up to 600 carriers a minute (10 items a second) using a Lenze variable speed drive (VSD) to control and obtain the desired speed.

The carriers have a floating feature to further isolate the item to be weighed from the rest of the machine as the carriers travel over the weighbridge section (refer to Figure 6). When in floating position, only the frame, rollers, axle and latch are weighed along with any item on top. These items are easily subtracted from the overall weight of the carrier to obtain the weight of the item of interest. While in floating position, the only point of contact between the clip and the rest of the carrier is in the horizontal axis along the direction of travel. The clip attaches to the chain, which is driven by the motor.

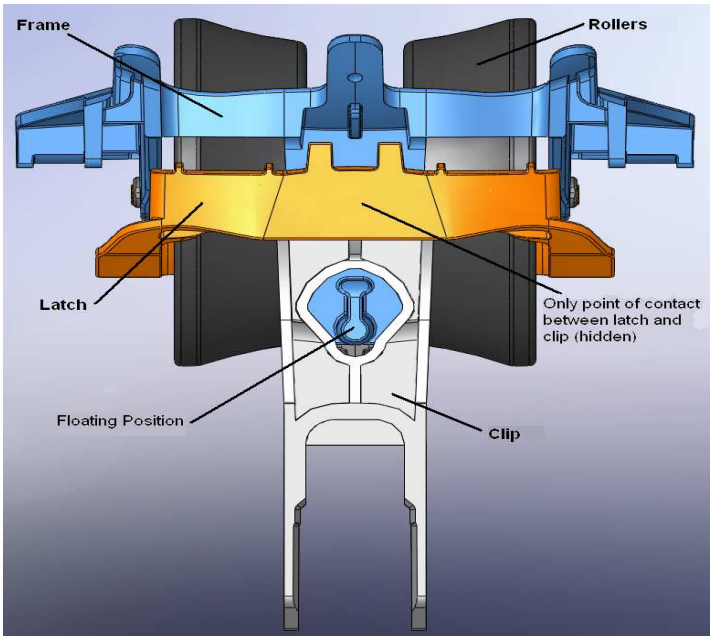

Figure 6: Carrier in floating position

Due to variations in manufacturing, the frame, rollers, axle and latch might vary slightly within tolerance. The weights of every component of 40 carriers from this machine have been weighed separately and presented in Appendix B. They are summarised in Table 5. It is evident that there is a variance of 1.8g that has to be taken into account when calculating the weights of items run on the carriers. Therefore each carrier's weight is known during an initial tare of the machine and recorded to be subtracted as it runs over the weigh bridge section.

	Summary of 40 Carrier Components			
	mean (g)	min (g)	max (g)	Range (g)
Frame	51.22665	50.912	52.004	1.092
Latch	16.435825	16.301	16.469	0.168
Roller & axle	75.40575	74.92	75.78	0.86
Clip	30.72005	30.628	30.836	0.208
Total Calculated weight (all components)	173.788275	172.901	174.719	1.818
Total Calculated weighing weight (floating components)	143.068225	142.249	144.083	1.834

Table 5: Carrier Component Weights

Chapter 3: Modelling

To calculate the weight of an item, three methods are investigated and compared; an "Averaging" method, a "Frequency" method and a "Damping" method. These methods have been accrued through mathematically modelling the system. Compac currently utilise the Averaging method. This chapter details the mathematical model and the details of each of these methods. Advantages and disadvantages of each method are also portrayed.

To test these methods, a model of the load cell system has been simulated on Matlab (refer to Chapter 5). The model's user interface allows for entering the parameters of the load cell. It outputs the inferred weight using all three methods with their error percentages.

3.1 Mathematical Model of the system

The model of the load cell is represented by Figure 7 as a Mass Spring Damper (MSD) system, where m is the mass of the desired item subjected to the load cell. M is the equivalent mass of the load cell that is attached to a mass-less spring with spring constant k. As the load is applied to the load cell, a counteracting force produced by the spring due to an offset x from equilibrium is defined by Hooke's law as $f_s = -kx$.

This would be sufficient to model the load cell in a static equilibrium, but in analysing the dynamic characteristics, it is important to take into account the damping. Viscous damping is assumed, where the damping force is proportional to the velocity: $f_D = -c\frac{dx}{dt}$, where c is the damping coefficient. By using Newton's second law the following differential equation is obtained:

$$(M+m)\frac{dx^2}{dt^2} = -c\frac{dx}{dt} - kx + mg + Mg \qquad (3.1)$$

Where g is the average acceleration produced by Earth's gravity.

The solution of Equation (3.1) has the form:

$$x = c_1 e^{-\mu t}\cos(\omega t) + c_2 e^{-\mu t}\sin(\omega t) + \frac{(M+m)g}{k} \qquad (3.2)$$

Where c1 and c2 are constants which depend on the initial conditions. The damping factor (μ) is:

$$\mu = \frac{c}{2(M+m)} \qquad (3.3)$$

and the frequency ω is:

$$\omega = \frac{1}{2}\sqrt{\frac{4k(M+m)-c^2}{(M+m)^2}} \qquad (3.4)$$

We see from Equation (3.4) that with heavier weight, the frequency decreases and from Equation (3.2) that amplitude of oscillations would increase with heavier weight.

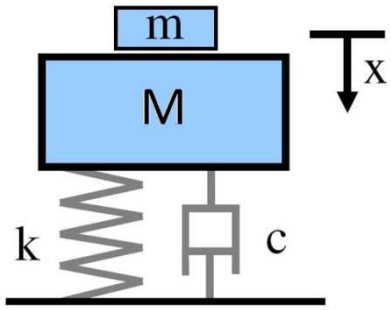

Figure 7: Mass Spring Damper (MSD) System

The output of the load cell from the machine was either converted to grams or given in terms of deflection of the load cells i.e. millimetres. When the output from the machine is not in terms of grams, a conversion factor needs to be taken into account. Therefore the new solution is in the form of;

$$\hat{x} = \alpha\left(c_1 e^{-\mu t}\cos(\omega t) + c_2 e^{-\mu t}\sin(\omega t) + \frac{(M+m)g}{k}\right) \qquad (3.5)$$

Where α is a conversion factor (millimetres to grams).

Equation (3.1) is used in cases where the deflection is from a steady state that is not solely by the mass of the load cell, i.e. $m \neq 0$. This would be evident from an offset in the graphs before a mass is applied to the system as shown in Figure 8.

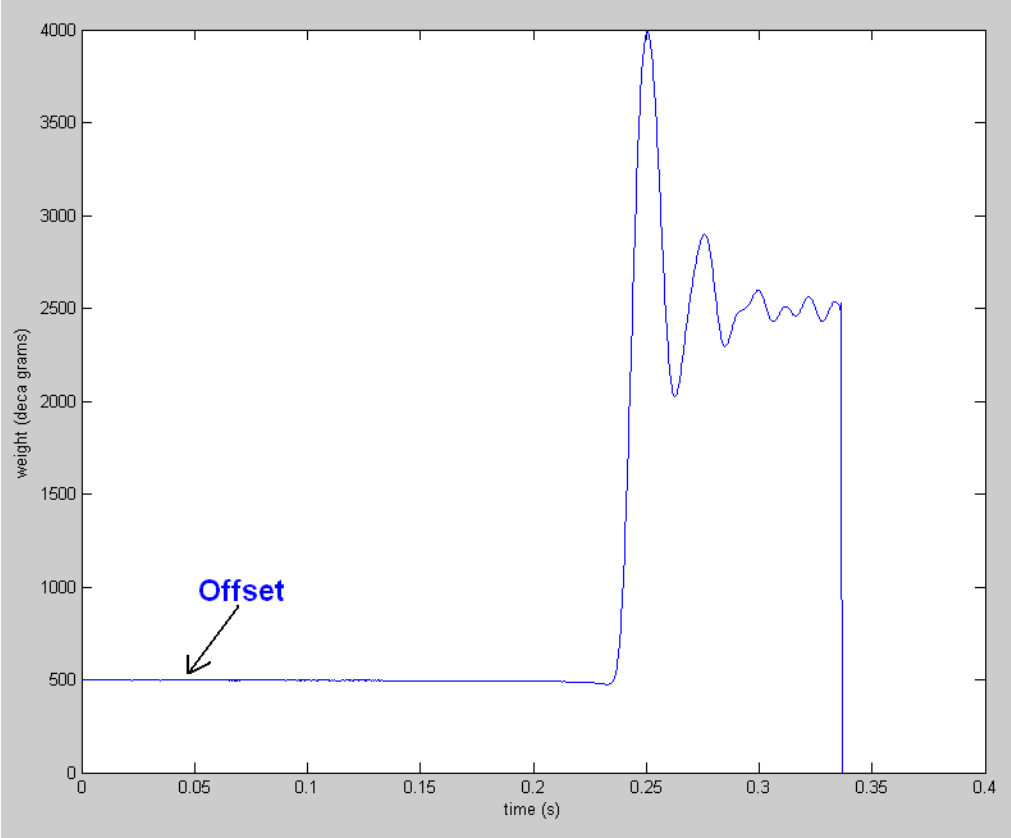

Figure 8: Offset on a Weigh Graph

In cases where the offset is 0, Equation (3.6) is used.

$$(M+m)\frac{d\tilde{x}^2}{dt^2} = -c\frac{d\tilde{x}}{dt} - k\tilde{x} + mg \qquad (3.6)$$

This has the following solution;

$$\tilde{x} = c_1 e^{-\mu t}\cos(\omega t) + c_2 e^{-\mu t}\sin(\omega t) + \frac{mg}{k} \qquad (3.7)$$

Where μ and ω are the same as they were defined in Equations (3.3) and (3.4) above.

Note that Equation (3.6) can be derived from Equation (3.1) by defining $\tilde{x} = x - \frac{Mg}{k}$. That is, $\tilde{x}$ is the displacement from the steady state when m=0.

3.2 "Averaging" Method

The averaging method is based on the assumption that the oscillatory response has enough time to settle down. The weight can be found from the value of the graph when it has become stable.

The two solutions are considered. The first is where the deflection is from steady state not solely by the mass of the load cell with the conversion factor taken into account (Equation (3.5)). The second is where the deflection is from steady state when m= 0 (Equation (3.7)).

Considering the limit of the first solution to the model (Equation (3.5));

$$\lim_{t\to\infty} x(t) = \alpha\frac{(m+M)g}{k} \qquad (3.8)$$

Note that this equation with α =1 is the solution to the model where there is no conversion to millimetres and the deflection is from an unloaded spring.

Similarly, considering the limit of the second solution to the model (Equation (3.7);

$$\lim_{t\to\infty} x(t) = \frac{mg}{k} \qquad (3.9)$$

Figure 9 shows the limit of an oscillating graph where β is a constant multiplier to the mass being weighed shown in the two equations above.

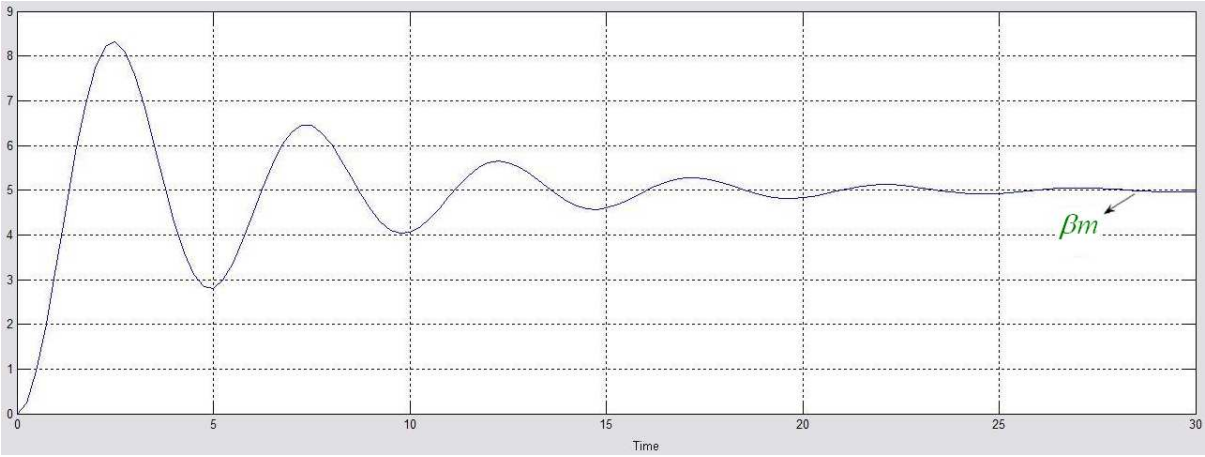

Figure 9: Limit of an oscillating Weigh Graph

To find the unknown mass when run over a load cell, Equation (3.8) can be rearranged to;

$$m = \frac{k \lim_{t \to \infty} x(t)}{\alpha g} - M \qquad (3.10)$$

Similarly, Equation (3.9) can be rearranged to find the unknown mass (m) by having;

$$m = \frac{k \lim_{t \to \infty} x(t)}{g} \qquad (3.11)$$

In this method the last 35% of the data measurements of each carrier with the desired item to be weighed are averaged. An average of these measurements is taken to compensate for the cases where the graphs are still oscillating in the time allocated to acquire the weight. As each carrier travels over two load cells, two average measurements are obtained for each carrier. The two measurements are then summed and the weight of the associated carrier is subtracted to get the weight of the desired item.

This method relies on the settling of the oscillatory response from the load cells to acquire an accurate measurement of the desired weight. This becomes less efficient when the speed of the carriers increases as the time for which the dual load cell system is subjected to the carriers is decreased. Furthermore, having heavier items on the carriers would require more time for the response to settle as the deflection of the load cells is greater. This method is therefore time-consuming and speed limiting.

3.3 "Frequency" Methods

In the next two sections, the weight of the item of interest is predicted from the initial oscillations of the weigh graphs. The method described in this section has been named the Frequency method as the unknown mass is predicted by rearranging the frequency equation (Equation (3.4)). Similarly, the Damping method described in the next section is named as such because the unknown mass is predicted by rearranging the damping factor equation (Equation (3.3)) as will be seen later in this chapter.

As each load cell has its unique properties, it is required to find the parameters of each load cell which are its mass (M), spring constant (k) and damping coefficient (c). The parameters M, k and c are calculated only once as they are unique to each load cell.

The weight can then be calculated, using these parameters, by measuring the first two successive peaks in the load cell output, using the fact that the frequency (ω) can be

calculated from the time difference between the two peaks (refer to Equation (3.18)) and using Equation (3.4) to solve for m:

$$m = \frac{k + \sqrt{k^2 - \left(\frac{2\pi}{t_2 - t_1}\right)^2 c^2}}{2\left(\frac{2\pi}{t_2 - t_1}\right)^2} - M \qquad (3.12)$$

Similar to the Averaging method, both Equation (3.5) and Equation (3.7) are used when calculating the parameters. When considering the solution given by Equation (3.7), one possible procedure for deducing the parameters is performed by running a known mass over the system and measuring the load cell output. The spring constant (k) can be calculated by rearranging Equation (3.9);

$$k = \frac{(m)g}{\lim_{t \to \infty} x(t)} \qquad (3.13)$$

Calculating the damping factor (μ) requires measuring any two successive peaks or two maximum amplitudes of the same phase (t_1, y_1) and (t_2, y_2) as in Figure 10.

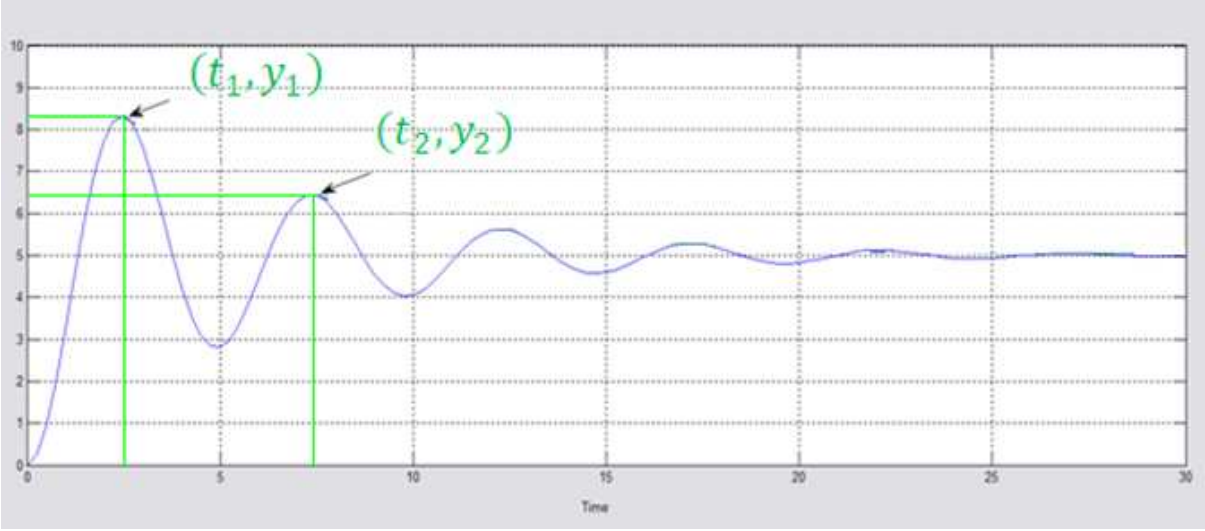

Figure 10: Two Successive Peaks

From Equation (3.7), these points are at

$$y_1 = Ae^{-\mu t_1}\sin(\omega t_1 - \varphi) + \frac{mg}{k} \qquad (3.14)$$

$$y_2 = Ae^{-\mu t_2}\sin(\omega t_2 - \varphi) + \frac{mg}{k} \qquad (3.15)$$

As both points are in-phase, subtracting $\frac{mg}{k}$ from both sides and dividing both equations to get;

$$\frac{y_1 - \frac{mg}{k}}{y_2 - \frac{mg}{k}} = \frac{e^{-\mu t_1}}{e^{-\mu t_2}} \qquad (3.16)$$

Therefore μ can be calculated, knowing the mass (m), spring constant (k) and coordinates of the two successive peaks using;

$$\mu = \frac{1}{(t_2 - t_1)} \ln\left[\frac{y_1 - \frac{mg}{k}}{y_2 - \frac{mg}{k}}\right] \qquad (3.17)$$

The two successive peaks have been chosen such that the angular frequency can be calculated easily by using;

$$\omega = 2\pi f = \frac{2\pi}{t_2 - t_1} \qquad (3.18)$$

The next step is finding the damping coefficient (c) and the mass of the load cell (M). This involves solving the two simultaneous equations given for the damping factor (μ), and the frequency (ω) (Equations (3.3) and (3.4)) giving;

$$\underline{M} = \frac{k}{\omega^2 + \mu^2} \qquad (3.19)$$

and

$$c = 2\mu\underline{M} \qquad (3.20)$$

Where;

$$\underline{M} = M + m \qquad (3.21)$$

One possible procedure to get the parameters of the load cell when considering Equation (3.5) requires two known masses that run over the load cell separately (m_1 and m_2). Firstly the mass of the load cell (M) can be calculated from looking at the limits of both graphs at the values when the oscillations reach steady state.

$$\lim_{t\to\infty} x_1(t) = \frac{\alpha(M+m_1)g}{k} = L_1 \qquad (3.22)$$

$$\lim_{t\to\infty} x_2(t) = \frac{\alpha(M+m_2)g}{k} = L_2 \qquad (3.23)$$

Dividing them and rearranging for Mass of the load cell (M) gives;

$$M = \frac{1}{L_1 - L_2}(-L_1 m_2 + L_2 m_1) \qquad (3.24)$$

Note that this was good in eliminating the factor α. To get the other parameters (k and c), the frequencies of the graphs of both masses are considered.

$$\omega_1 = \frac{1}{2}\sqrt{\frac{4k(M+m_1)-c^2}{(M+m_1)^2}} \Rightarrow 4\omega_1^2(M+m_1)^2 = 4k(M+m_1) - c^2 \qquad (3.25)$$

$$\omega_2 = \frac{1}{2}\sqrt{\frac{4k(M+m_2)-c^2}{(M+m_2)^2}} \Rightarrow 4\omega_2^2(M+m_2)^2 = 4k(M+m_2) - c^2 \qquad (3.26)$$

As ω_1 and ω_2 can be calculated using Equation (3.18), and the masses (m and M) are known, the parameters k and c can be found to be;

$$k = \frac{1}{(m_2 - m_1)}\left(\omega_2^2(M+m_2)^2 - \omega_1^2(M+m_1)^2\right) \qquad (3.27)$$

$$c = \sqrt{\frac{1}{(m_2 - m_1)}\left((M+m_1)4\omega_2^2(M+m_2)^2 - (M+m_2)4\omega_1^2(M+m_1)^2\right)} \qquad (3.28)$$

These are based on solving two simultaneous straight line equations;

$$b_1 = a_1 x - y \qquad (3.29)$$

$$b_2 = a_2 x - y \qquad (3.30)$$

Which have the following solutions;

$$x = \frac{1}{a_2 - a_1}(b_2 - b_1) \qquad (3.31)$$

$$y = \frac{1}{a_2 - a_1}(a_1 b_2 - a_2 b_1) \qquad (3.32)$$

(Where $b_1 = 4\omega_1^2 (M + m_1)^2, b_2 = 4\omega_2^2 (M + m_2)^2, a_1 = 4(M + m_1), a_2 = 4(M + m_2), x = k, y = c^2$)

Therefore as mentioned earlier, the unknown mass can be calculated using Equation (3.12) knowing the parameters of the load cell (M, k and c).

To summarise for the Frequency method; finding the parameters of a load cell when no offset is present only requires one known mass, otherwise two masses are required. Once the load cell parameters are known, measuring any two successive peaks or two amplitudes of the same phase could be used to predict the mass of the item that passes the load cell without the need to wait for the oscillations to settle down to steady state. Therefore this method saves time and only limits the speed when the peaks of two oscillations cannot be acquired accurately.

3.4 "Damping" Method

Considering the model of the load cell system presented in Figure 7. Another solution to finding the mass involves the analysis of the first three peaks. The analysis will be performed on Equation (3.5) which is the solution to the model of the load cell when the deflection is from an unloaded spring, and a conversion factor to get the output in grams is required. Applying the same procedure on the solution given by Equation (3.7) will give the same results as these factors are eradicated as will be seen later in this section.

Therefore from Equation (3.5), the first three peak's are at:

$$y_1=\alpha\left(Ae^{-\mu t_1}\sin(\omega t_1-\varphi)+\frac{(m+M)g}{k}\right) \qquad (3.33)$$

$$y_2=\alpha\left(Ae^{-\mu t_2}\sin(\omega t_2-\varphi)+\frac{(m+M)g}{k}\right) \qquad (3.34)$$

$$y_3=\alpha\left(Ae^{-\mu t_3}\sin(\omega t_3-\varphi)+\frac{(m+M)g}{k}\right) \qquad (3.35)$$

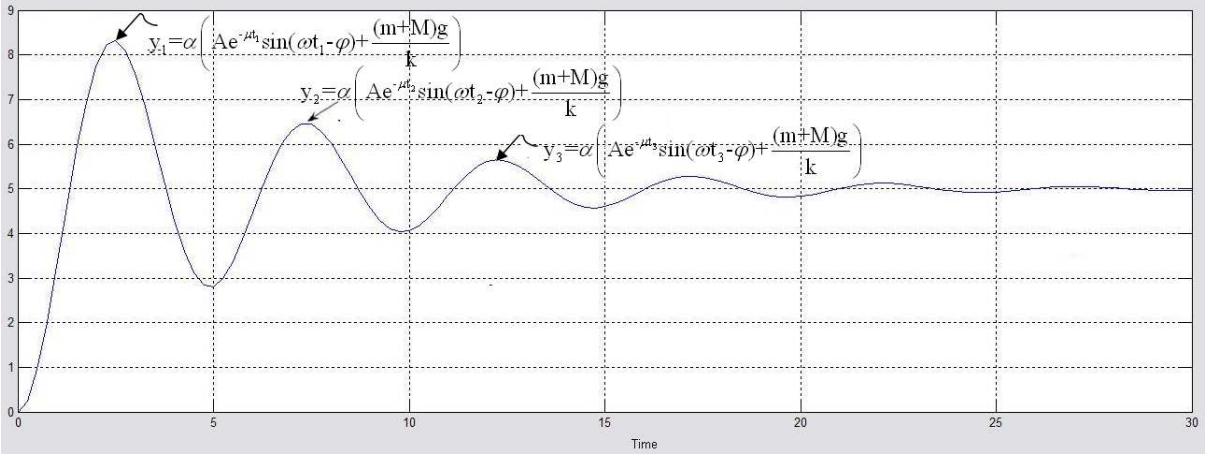

Figure 11: Three Successive Peaks

As the output from the load cells are in the form of a decaying oscillations then it is possible to deduce the damping factor from the three peaks and the time between them. Considering the ratio of their difference;

$$y_1-y_2=\alpha AF[e^{-\mu t_1}-e^{-\mu t_2}] \qquad (3.36)$$

$$y_2-y_3=\alpha AF[e^{-\mu t_2}-e^{-\mu t_3}] \qquad (3.37)$$

$$\frac{y_1-y_2}{y_2-y_3}=\frac{e^{-\mu t_1}-e^{-\mu t_2}}{e^{-\mu t_2}-e^{-\mu t_3}} \qquad (3.38)$$

Where $F=\sin(\omega t_1-\varphi)=\sin(\omega t_2-\varphi)=\sin(\omega t_3-\varphi)$ as three consecutive peaks have been chosen. Note that this was good in eliminating the factor α and the mass of the load cell (M). Therefore, as mentioned earlier, applying these equations on the solutions given by Equation (3.7) and Equation (3.5) will give the same results.

Taking the ratio of their differences as $\Delta y = \frac{y_1 - y_2}{y_2 - y_3}$ and simplifying the equation results in;

$$\Delta y(e^{-\mu t_2} - e^{-\mu t_3}) = e^{-\mu t_1} - e^{-\mu t_2} \qquad (3.39)$$

$$\Rightarrow e^{-\mu t_2}(\Delta y + 1) = e^{-\mu t_1} - \Delta y e^{-\mu t_3} \qquad (3.40)$$

$$\Rightarrow \Delta y + 1 = e^{\mu(t_2 - t_1)} - \Delta y e^{\mu(t_2 - t_3)} \qquad (3.41)$$

Knowing that $t_3 > t_2 > t_1$ therefore this can be simplified further to;

$$\Rightarrow \Delta y + 1 = e^{\mu(\Delta t)} - \Delta y e^{-\mu(\Delta t)} \qquad (3.42)$$

Grouping Δy together gives;

$$\Delta y(1 - e^{-\mu \Delta t}) = e^{\mu \Delta t} - 1 \qquad (3.43)$$

$$\Rightarrow \Delta y\left(\frac{e^{\mu \Delta t} - 1}{e^{\mu \Delta t}}\right) = e^{\mu \Delta t} - 1 \qquad (3.44)$$

As there are common terms on both sides of the equation, an equation for Δy in terms of μ and Δt can be found;

$$\Delta y\left(\frac{1}{e^{\mu \Delta t}}\right) = 1 \qquad (3.45)$$

$$\Rightarrow \Delta y = e^{\mu \Delta t} \qquad (3.46)$$

And therefore deducing the damping factor (μ) by taking the natural log of both sides is possible;

$$\mu = \frac{\ln(\Delta y)}{\Delta t} \qquad (3.47)$$

The damping factor (μ) is used to calculate the damping coefficient (c) of each load cell by running a known mass (m) and rearranging Equation (3.3) to give;

$$c = 2\mu(M + m) \qquad (3.48)$$

Knowing the parameters M, c and μ, Equation (3.3) can be rearranged to predict any unknown mass;

$$m = \frac{c}{2\mu} - M \qquad (3.49)$$

To summarise; for the Damping method, finding the parameters of a load cell requires running only one known mass over the load cell. Once the load cell parameters are known, measuring the ratio of any three successive peaks or three amplitudes of the same phase could be used to predict the mass of the item that passes the load cell without the need of waiting for the oscillations to settle down to steady state. Therefore, similar to the Frequency method, this method saves time and only limits the speed of the machine when the peaks of three oscillations cannot be acquired accurately.

Chapter 4: Simulation and Analysis

A program has been written in Matlab to simulate weigh graphs and allow applying the three methods to deduce the weight of an item. The user interface is shown in Figure 12. Input parameters of the Load cell including the load cell mass (M), spring constant (k) and damping factor (c) could be entered. The acceleration produced by earth's gravity (g) and time interval (t) were also required to be applied for the visual graph to be shown depending on the mass of the item of interest (m). The time interval is entered in the form of a vector, where in Figure 12 for example, the time is from 0 to 150ms, with Δt of 0.025ms. Results are displayed at the bottom of the user interface for calculating the weight from the output graph using all three methods, as well as their error percentages from the actual weight of the item. This allowed easy and quick comparison between the three methods.

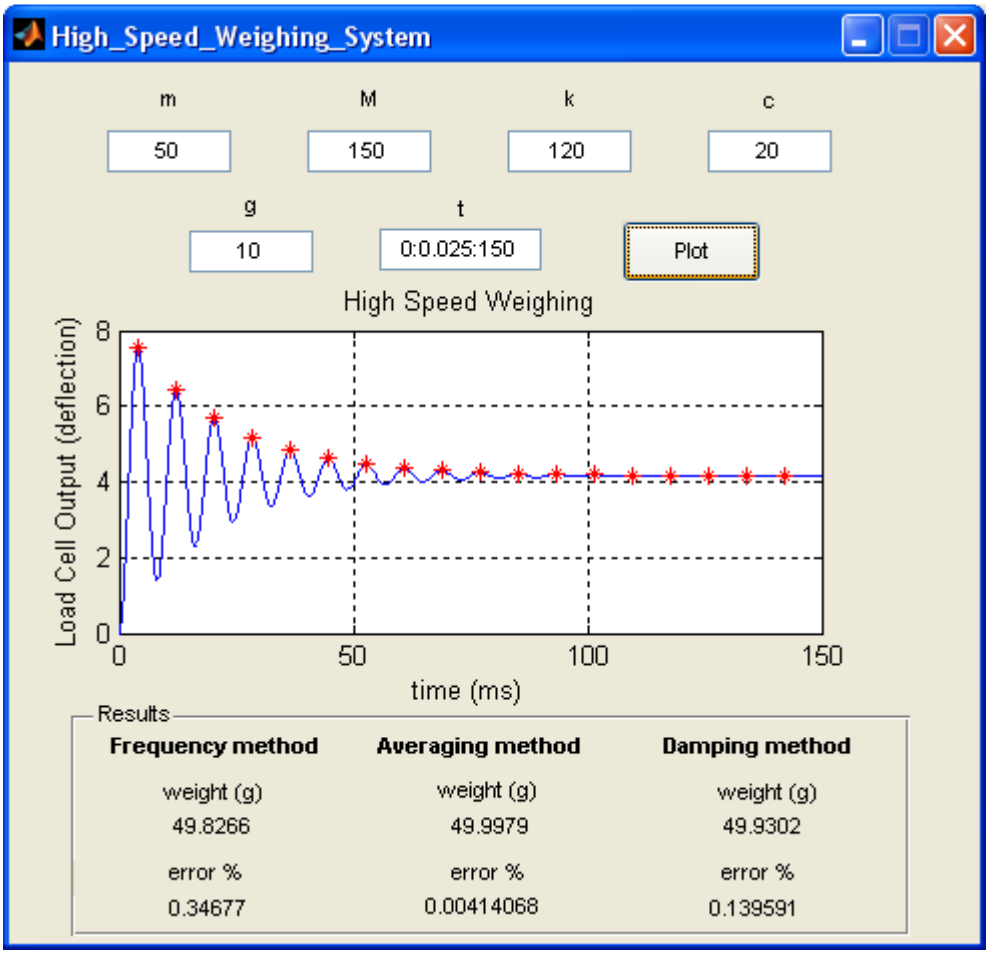

Figure 12: User Interface

Matlab was used as it encompasses a numerical computing environment which allows the implementation of algorithms, plotting of functions and data, creation of user interfaces and interfacing with programs written in other languages (Mathworks, 2011).

For investigating the effects of different load cells, the damping coefficient and spring constant values were varied. This had a great effect on the Load Cell's output. Figure 13 compares 10kg/s to a 20kg/s damping coefficient on a 150g load cell with 120N/m spring constant using a 50g load.

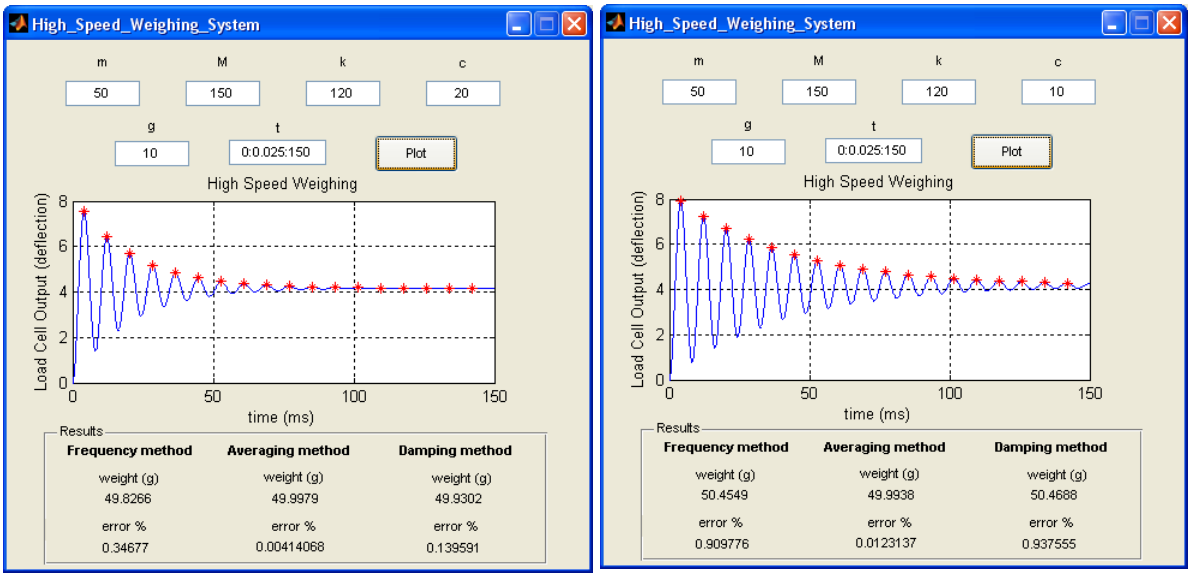

Figure 13: Comparing Weigh Graphs with different Damping coefficients

The effect of increasing the damping coefficient during a 150ms period resulted in the oscillations reaching steady state faster. As the damping coefficient (c) and the damping factor (μ) have a linear relationship denoted by Equation (3.20), the deflection of the load cell is affected by a factor of a negative exponential elucidated in Equation (3.14).

To simulate a stiffer load cell, Figure 14 illustrates running a load over a two load cells with one having half the spring constant value of the other. The graphs are from using a spring constant of 120N/m vs 60N/m while running a 50g weight over a 150g load cell with a damping coefficient of 10kg/s. The stiffer load cell has less deflection as expected from Equation (3.7).

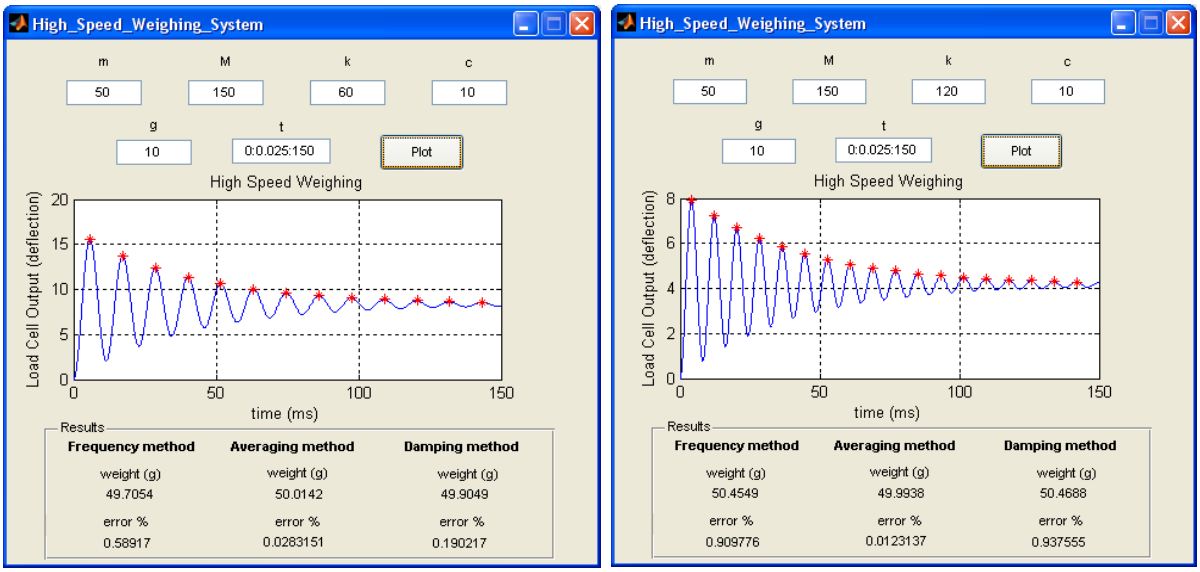

Figure 14: Comparing Weigh Graphs with Different Spring Constants

Note the different scales of the y-axis.

To compare the three methods, six weights of 57g, 145g, 197g, 242g, 272g and 378g were run through the simulation and their weigh graphs captured within 250ms using a spring constant of 60N/m with 3kg/s as the damping coefficient. The results are presented in Table 6.

Actual Weight	Frequency Method	Averaging Method	Damping Method	Freq Method error	Averaging Method error	Damping Method error	Freq Method error %	Averaging Method error %	Damping Method error %
57	57.122	56.709	57.179	0.1222	0.2907	0.1787	0.2144	0.5100	0.3135
145	144.660	144.050	145.590	0.3363	0.9521	0.5918	0.2319	0.6566	0.4081
197	197.640	194.780	196.270	0.6446	2.2234	0.7302	0.3272	1.1286	0.3706
242	242.690	245.490	241.100	0.6920	3.4922	0.9005	0.2859	1.4430	0.3721
272	272.560	267.400	272.960	0.5564	4.5960	0.9649	0.2046	1.6897	0.3548
378	377.170	366.730	376.360	0.8270	11.2710	1.6396	0.2188	2.9818	0.4337

Table 6: Results of 57, 145, 197, 242, 272 and 378g during a 250ms period

As presented, the results from the Frequency and Damping methods are more accurate than the Averaging method. As well as being more accurate, only a fraction of the time is needed to calculate the weight as it is predicted from the first two peaks for the Frequency method and the first three peaks for the Damping method. Whereas the averaging method requires all the data to average the last 35% hoping it is steady enough to get an accurate measurement. The averaging method's error increases with increasing weight. The Frequency method's error percentage is consistent between 0.2% and 0.35%. Similarly, the Damping method error

percentage is between 0.3% and 0.45%. The Damping method is slightly less accurate than the Frequency method as three peaks are required to be determined accurately as opposed to only two peaks in the Frequency method. This is affected by the resolution of capturing the data, discussed later in this chapter.

The averaging method is highly dependent on the start and finish positions as the nature of the weigh graph is oscillating about a multiple of the mass as shown from Equation (3.7) of the system. The value of the graph at steady state is given by Equation (3.9). Therefore this method would be most accurate if the start and end points are chosen as such that the values above the desired weight cancel with the values below. Choosing a multiple of periodic intervals would give the least error.

Unlike the Averaging method which depends on the graph oscillations settling down to a steady state to get better accuracy, the Frequency and Damping methods rely on the peaks of the first few oscillations. While running at the same machine speed, the data is sampled at the same frequency rate in the same duration of time regardless of the weight.

Investigating different speeds has been performed by modifying the capture time of the weigh graphs. 250ms time capture used previously is simulating running the machine at 4 items a second consecutively, which equates to 240 items a minute. To simulate running the machine at 600 items a minute, a time capture of 0.1s is required. Table 7 shows the results when running 57, 145, 197, 242, 272 and 378g weights at a faster machine speed of 600items a minute (10items a second) using a spring constant of 60N/m and a damping coefficient of 3kg/s.

Actual Weight	Frequency Method	Averaging Method	Damping Method	Freq Method error	Averaging Method error	Damping Method error	Freq Method error %	Averaging Method error %	Damping Method error %
57	57.122	57.3777	57.179	0.1222	0.3777	0.17867	0.21439	0.662631579	0.31346
145	144.66	146.649	145.59	0.33629	1.649	0.5918	0.23193	1.137241379	0.40814
197	197.64	200.162	196.27	0.64455	3.162	0.73015	0.32719	1.605076142	0.37063
242	242.69	237.534	241.1	0.69195	4.466	0.90053	0.28593	1.845454545	0.37212
272	272.56	264.107	272.96	0.55637	7.893	0.96494	0.20455	2.901838235	0.35476
378	377.17	390.196	376.36	0.82697	12.196	1.6396	0.21878	3.226455026	0.43374

Table 7: Results of 57, 145, 197, 242, 272 and 378g while running at 600cpm

Comparing these results to the ones obtained in Table 6; the weights calculated using the Damping and Frequency methods were not affected, whereas the weights calculated using the Averaging method had decreased in accuracy due to the increased speed.

As the speed increases, the time for which the items are subjected to the load cell decreases. Therefore the oscillations have less time to settle to a steady state. As the Averaging method is highly dependent on the oscillations reaching steady state, it has been highly affected whereas the peaks for the Damping and Frequency methods are from the first three oscillations which were not affected by having a shorter time.

To further investigate the errors; a Snapshot of the error between 600g and 925g for a timeframe of 250ms using the Averaging method better illustrates the periodic behaviour;

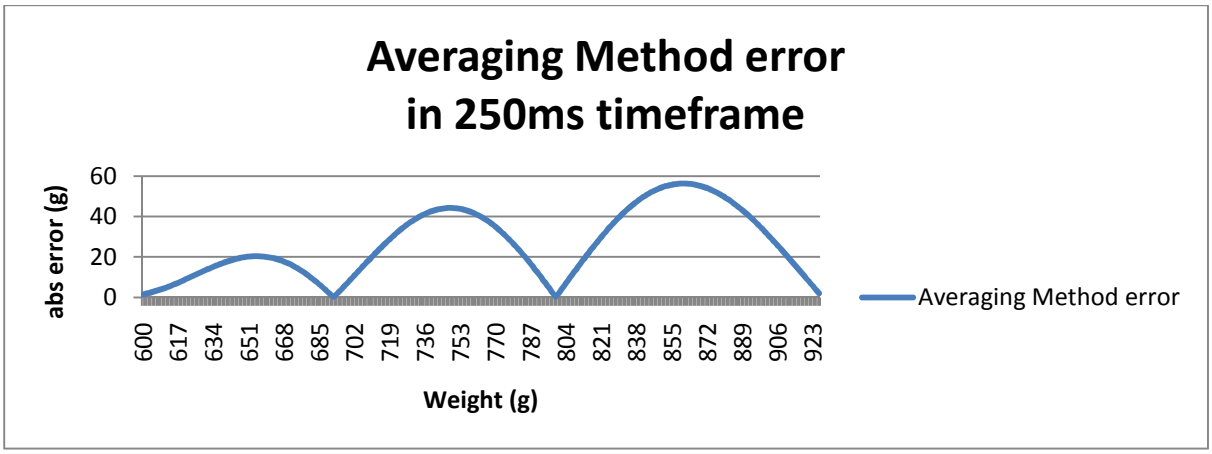

Figure 15: Averaging Method Error in 250ms

Depending on the starting point of calculating the weight, if there are more points above the desired weight then it accrues a higher positive error therefore falsely stating the weight is heavier. Similarly, if more points are below the desired weight then it portrays a lighter weight. Therefore if we inspect the averaging method on a larger scale, the error would oscillate and increase as shown in Figure 16.

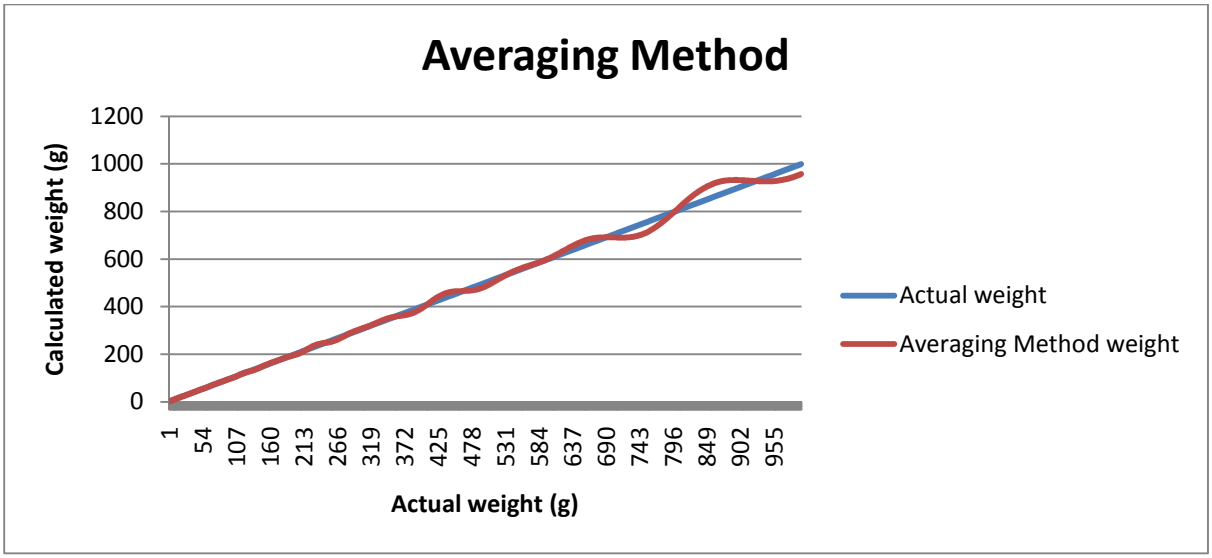

Figure 16: Averaging Method error on Larger Scale

The error increases in value as weight increases due to the amplitude of the graphs increasing and the frequency and damping of the oscillations decreasing, hence taking a longer time to settle to a steady state value. This can be seen from Equation (3.7); as the mass increases x(t) increases in amplitude. Also, from Equation (3.3); as the mass increases the damping decreases and from Equation (3.4); as the mass increases the frequency decreases.

Running an example through the simulation of a 100g vs 300g weights over a load cell with the same parameters of spring constant = 15N/m, damping coefficient = 10Kg/s over a 250ms period is illustrated below to further explain this;

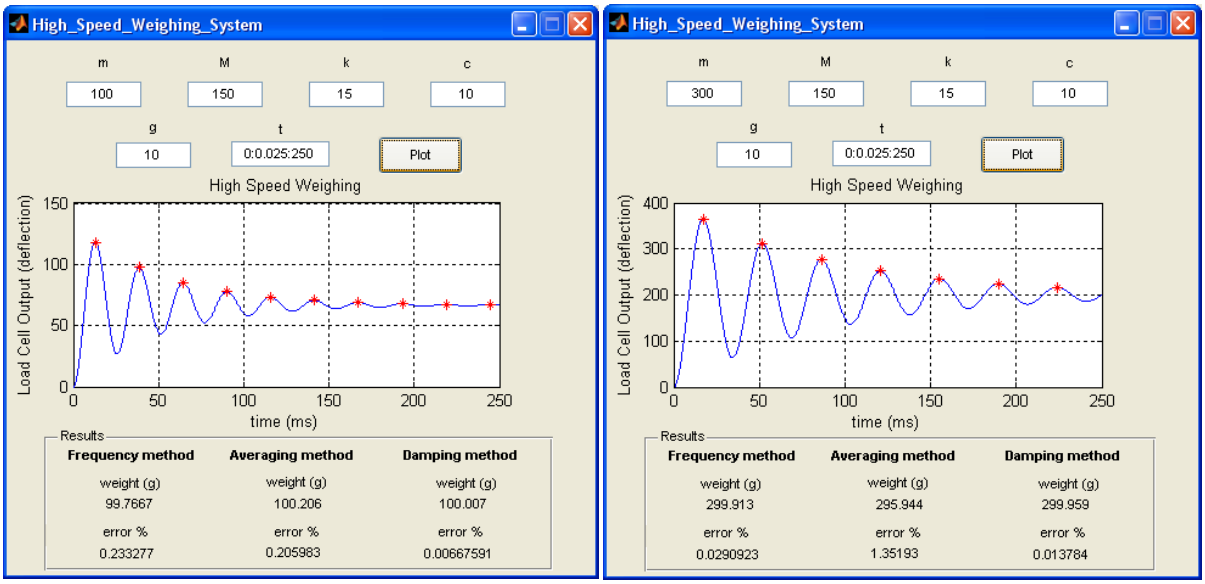

Figure 17: 100g vs 300g Weights Over a Load Cell

Notice the 100g weight has lower amplitude, higher frequency and higher damping of oscillations than the 300g weight.

On a large scale, all three methods tend to decrease in accuracy with increased weight, as seen by analysis of the linear trend line on the graphs produced by running the simulation for all values between 600g and 925g. All trend lines have a positive increasing slope.

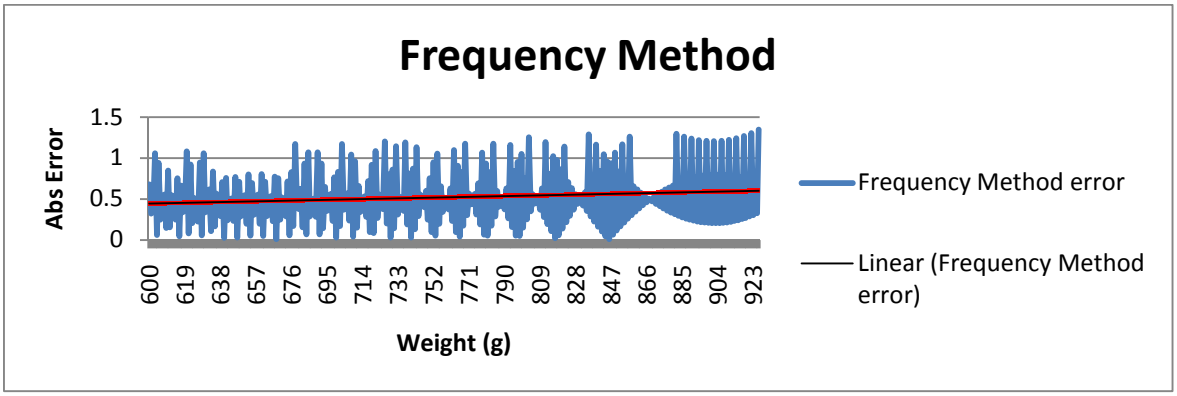

Figure 18: Frequency Method error

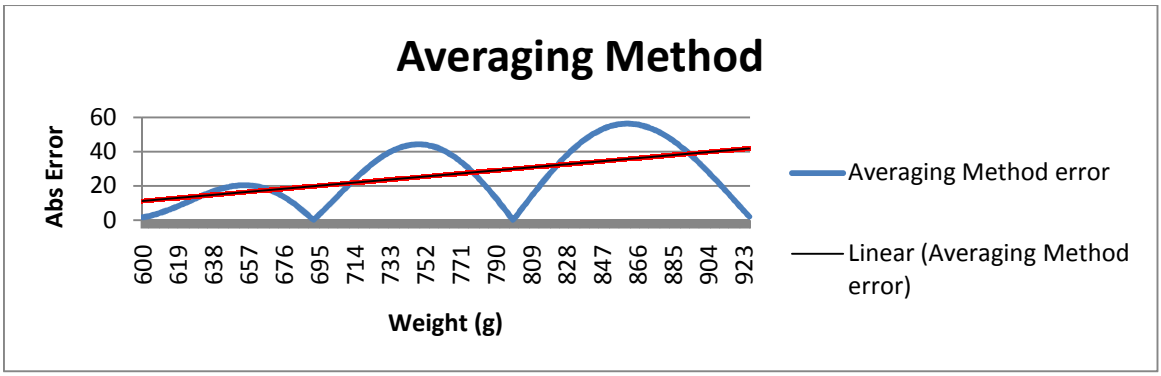

Figure 19: Averaging Method error

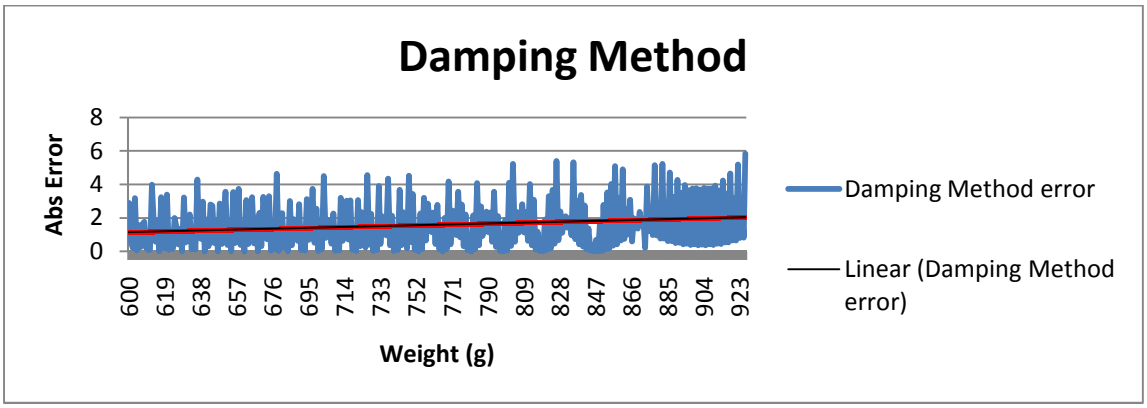

Figure 20: Damping Method error

Further to the interesting fact that the error increases with increasing weight for all three methods, looking at the trend line for the error percentages, it shows that it decreases when using the Frequency and Damping methods, but still increases when using the Averaging method.

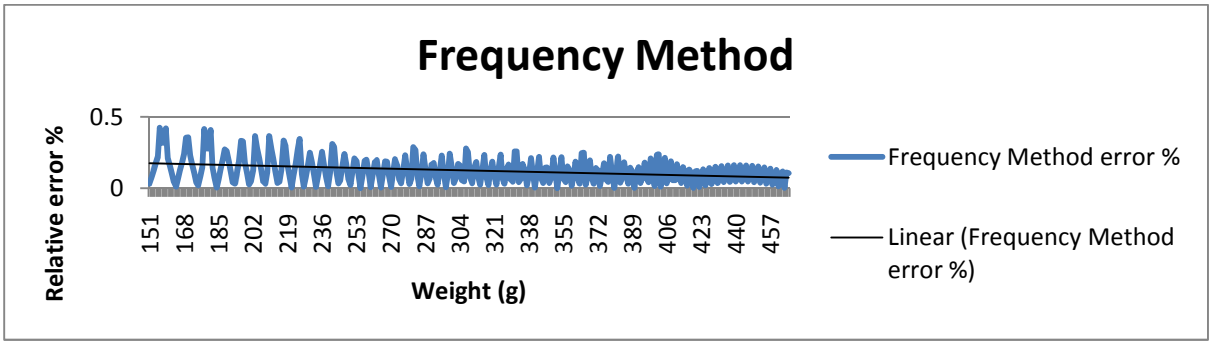

Figure 21: Frequency Method Trend Line for error Percentages

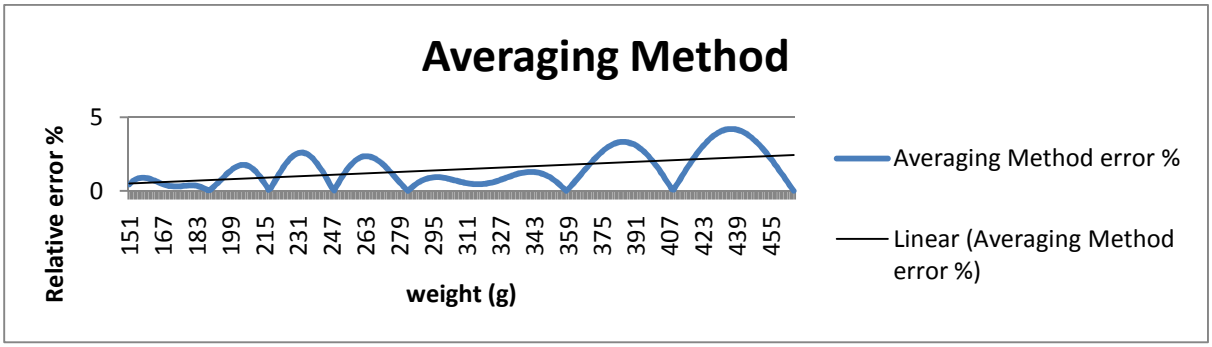

Figure 22: Averaging Method Trend Line for error Percentages

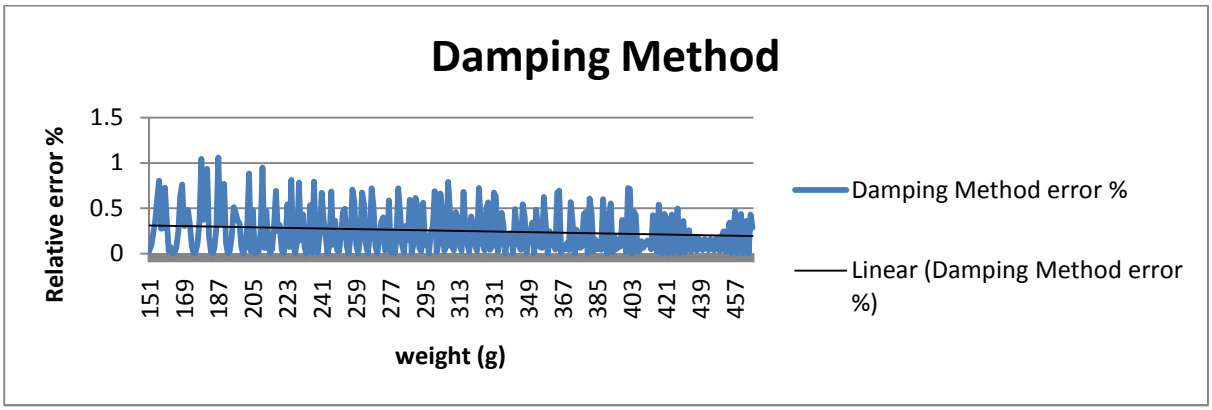

Figure 23: Damping Method Trend Line for error Percentages

Chapter 5: Weighing System Testing & Analysis

5.1 Setup

Various experiments have been performed on the weighing system which is outlined in this chapter. To perform the experiments a few preliminary installation steps had to be done to ensure that the system performed accurately. These are outlined in this section.

The whole machine should be leveled across the machine axle, especially the chain extrusion before and after the weighbridge section. Also, the Weighing section must be centred between the machine's side extrusions.

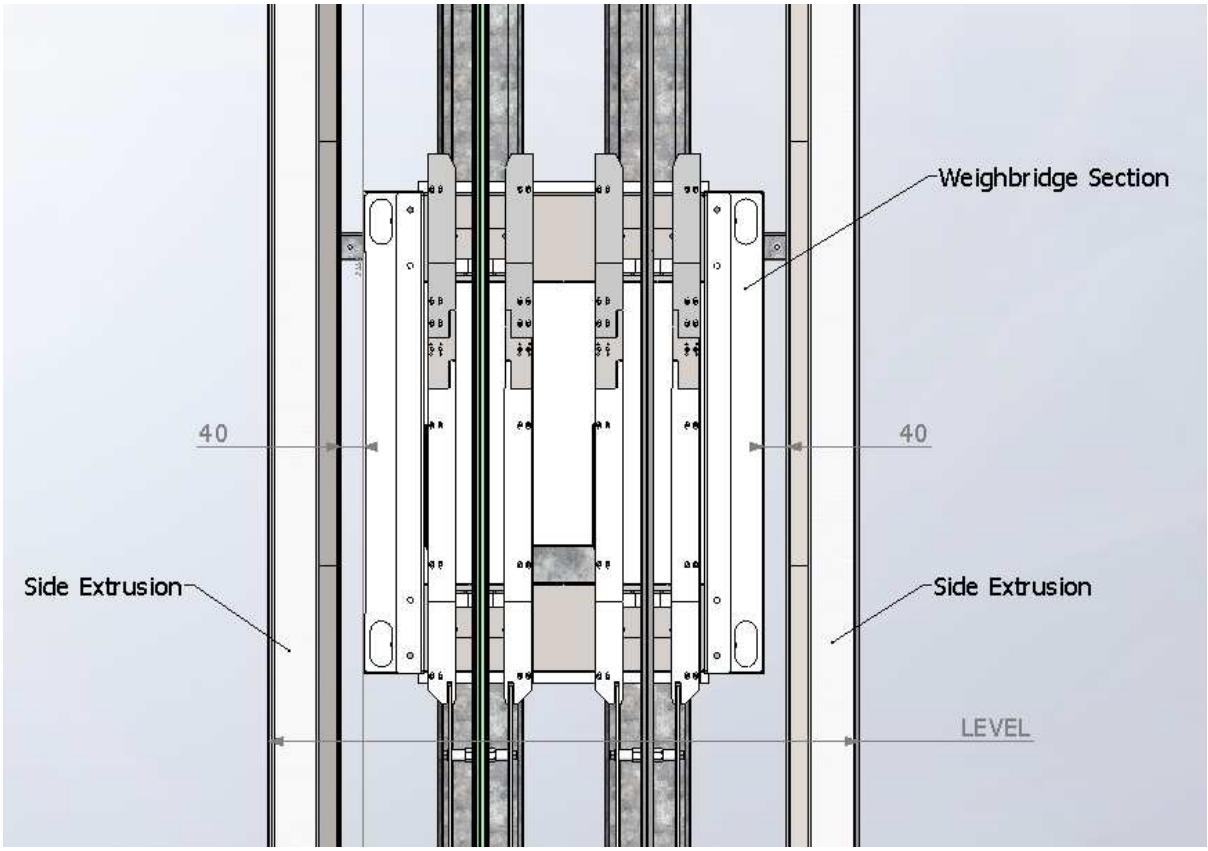

Figure 24: Centred Weigh Bridge Section

The transition plates transfer the carriers to the floating position for the most accurate weighing. There are slots in the incoming weigh plates to allow a smooth transfer of the carriers to the weighbridge section. To ensure the carriers are transitioned at the correct height onto the incoming weigh plate, the transition plates must be at a 10mm height from the bottom of the chain extrusion. This can be set using a 10mm spacer (M10 Hex Nut).

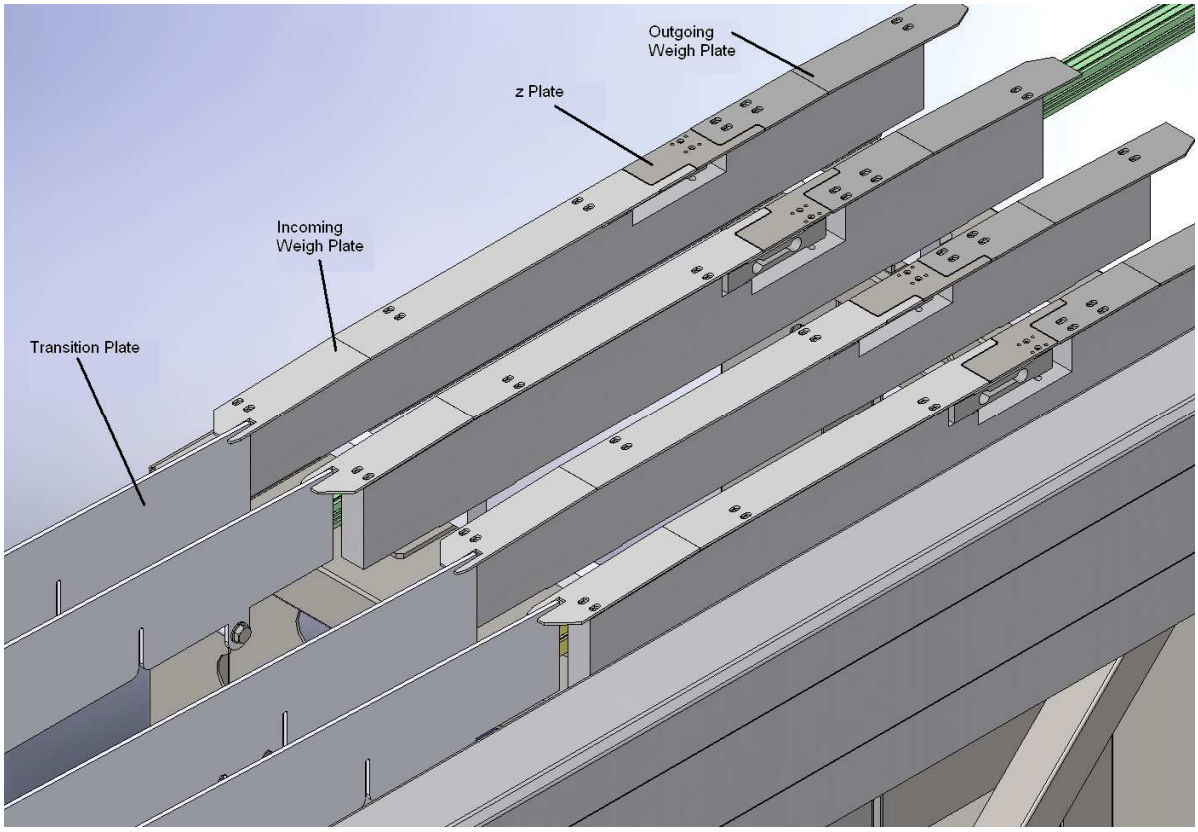

Figure 25: Transition plates onto the Weighing System

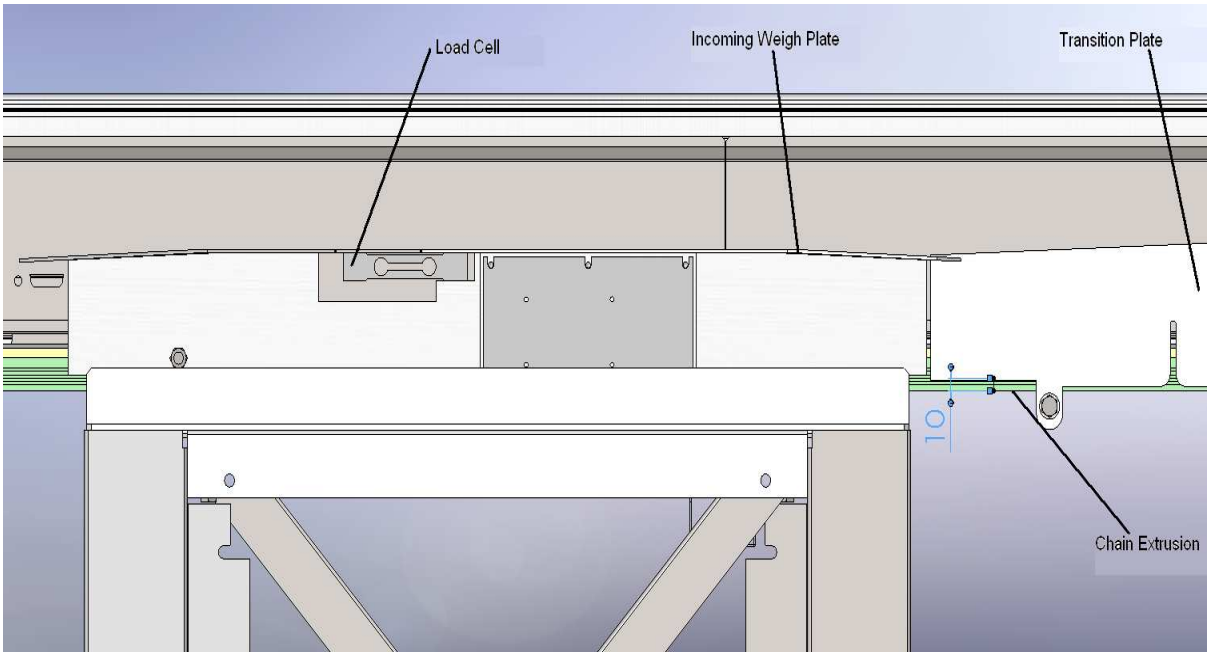

Figure 26: Transition plate height

To ensure the carriers are at the correct height as they travel along the Load Cells, there needs to be a 2mm gap between the top of the Weigh bar mounting plate and the bottom of the

chain extrusion. This places the carriers in their floating position to avoid added or removed weight. Additional weight of the chain is introduced when the gap between the weigh bar mounting bracket and the bottom of the extrusion is more than 2mm. This causes the carrier latch to touch the top of the slot in the carrier clip. When this distance is less than 2mm, the carriers are not able to exert full force of the items to be weighed onto the load cell as the carrier latch touches the bottom of the slot in the carrier clip; therefore the weight measured is calculated inaccurately to be less than the actual.

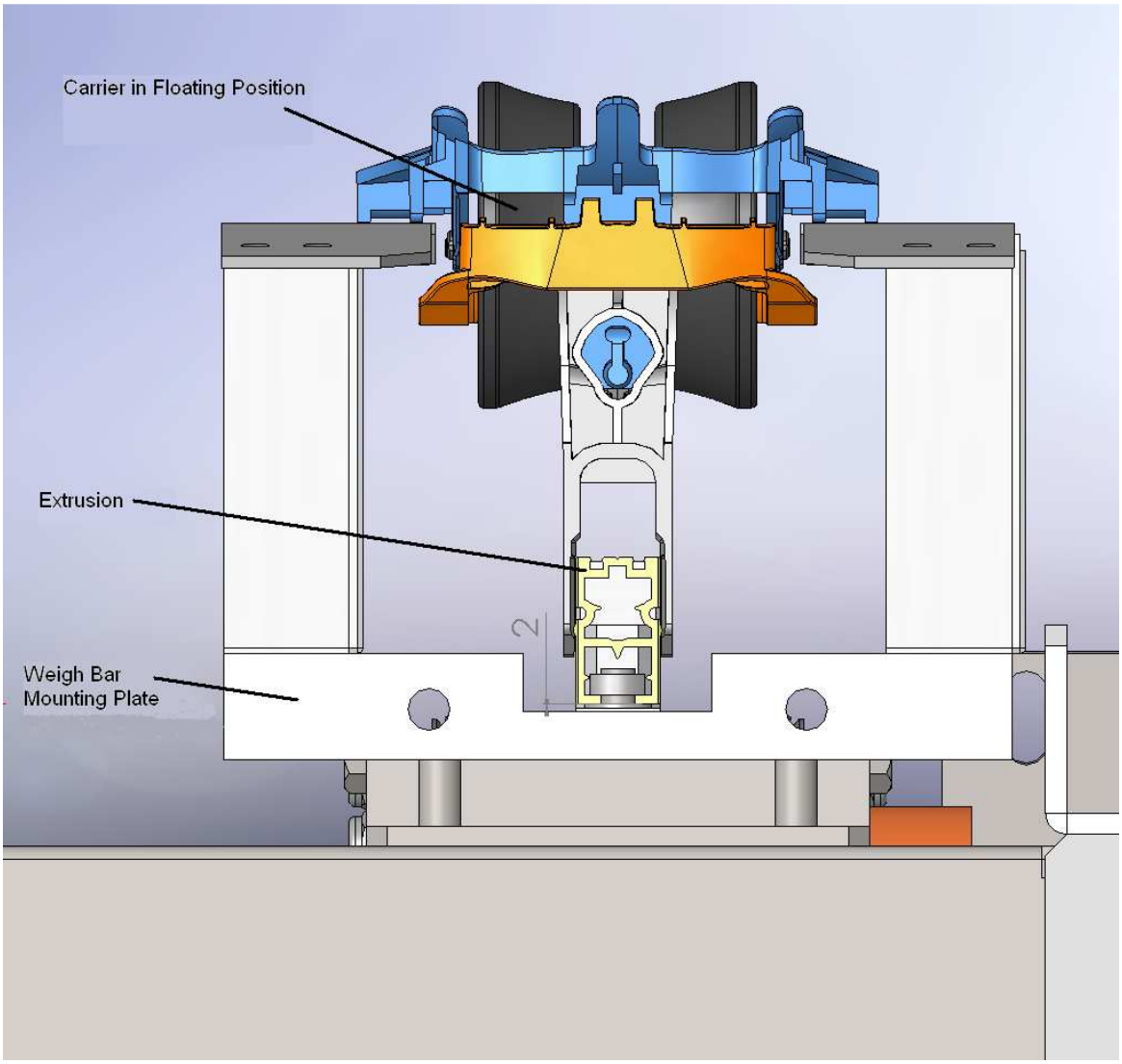

Figure 27: Weighing plate height

A jig has been designed for ease of ensuring the 2mm gap is achieved. This has been designed to be machined out of black oxide mild steel flat bar for accuracy. In addition to ensuring the height is correct, it also serves the purpose of making sure the chain extrusion is centred to the weigh bar system as it has been designed to have the same width as the

mounting block. The jig simply slides in and out between the mounting block and the chain extrusion.

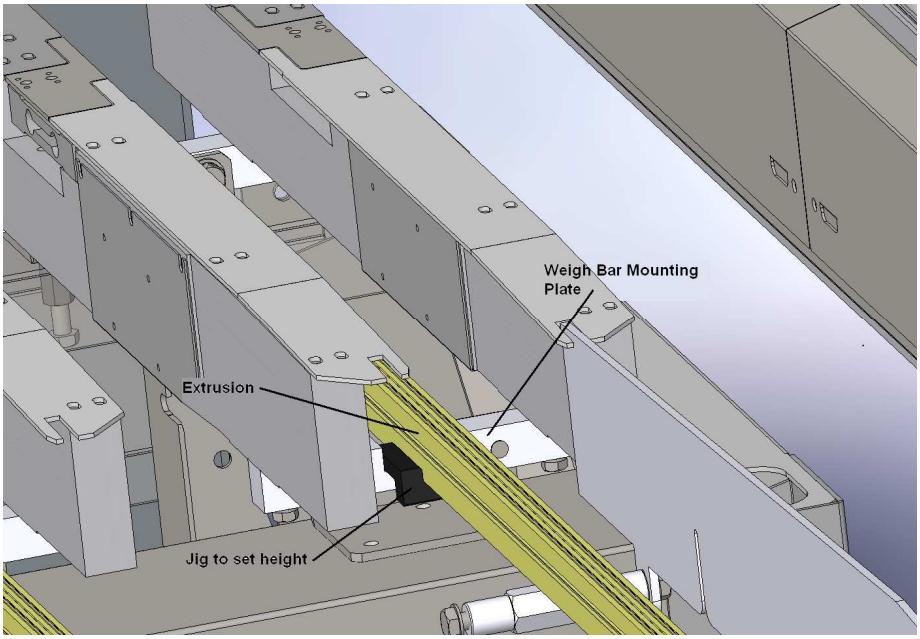

Figure 28: Weigh Bar jig in place

The height of the weigh bar pair is adjusted using a simple system whereby two locking M10x25mm bolts are loosened and two M10x70mm bolts at the bottom of the mounting bracket are either screwed in to decrease the distance between the mounting block and the chain extrusion or screwed out to increase this distance.

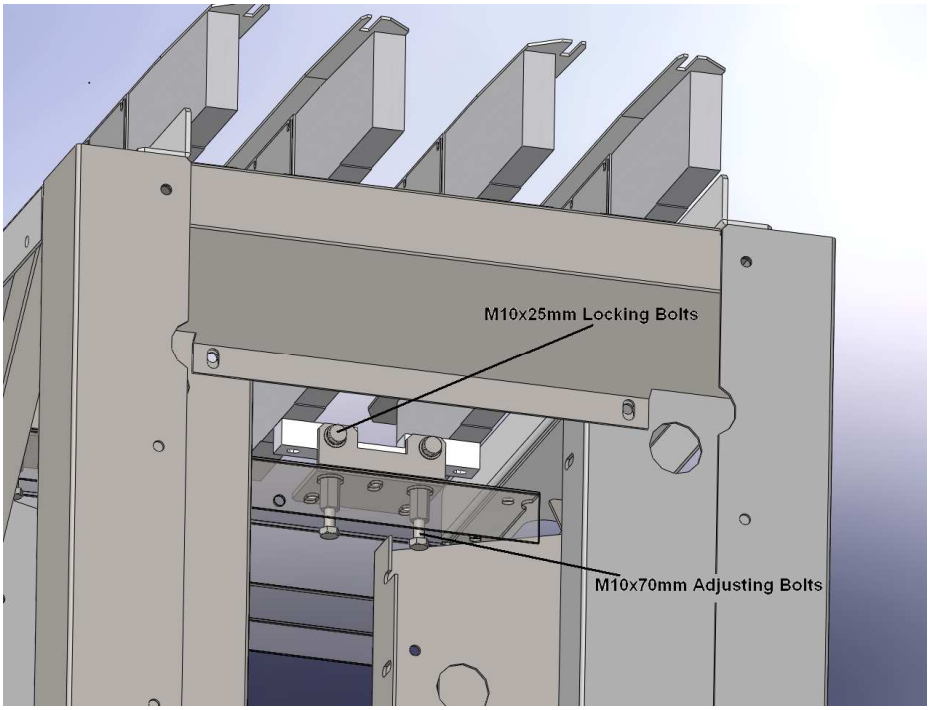

Figure 29: Position of Adjustment Bolts

To minimise the external disturbances from the machine, the weighing section must be isolated from the rest of the machine and bolted down to the floor. The only points of contact between the machine and the weighing section are the carriers.

Further to these preliminary installation steps, regular checks had to be made before tests were performed to ensure the best performance. These included the following;

- Ensuring all the chain extrusions are centred and set up correctly using the jig
    - Ensuring the jig slid in and out the mounting blocks slots with little or no friction
- Ensuring the gap between the bottom of the extrusion and the bottom of the transition plates is 10 mm
- Ensuring the gap between Transition plates and the incoming weigh plates' slots are evenly spaced
- Ensuring nothing is interfering with the Weigh Bridge, including the base wooden covers

The Compac software allowed data to be exported to an excel spreadsheet. These files are opened by Matlab and analysed using various software algorithms that will be detailed in the following sections. A sample file is in Appendix C. The files exported can have up to five

columns dependent on the number of load cells chosen. There are four load cells on this machine, due to having two lanes; therefore the last four columns are assigned to these. The first column is always the sample number.

5.2 Sampling Restrictions

The sample number is not precise as the Analogue to Digital Converter (ADC) samples at a rate of 4 kHz, but this has small variations (±4096 samples per second). Furthermore, the software caps at 2047 samples per capture of carrier weigh graphs. Depending on the number of carriers chosen, the software would average the samples obtained over the samples chosen. For example, if a capture of three carriers was chosen, and the machine was running at 300 carriers per minute (cpm), then three carriers would be captured in 0.6 seconds. This equates to 2457.6 samples. As the maximum number of samples per capture through the software is 2047, the difference is 410.6 samples. These are averaged over the 2047 samples; therefore, each sample on the software graph is an average of 1.2 samples from the ADC.

The opposite could happen where the number of cups chosen to be captured would utilise more samples in the limited time (depending on the speed of the machine) than the maximum 2047 samples. Therefore inaccuracies occur. To avoid this, the maximum carriers to capture during the allocated time due to speed have been tabulated below;

Speed (cpm)	carriers	Samples
300	5	4096
400	6	3686
500	8	3932
600	10	4096
700	11	3861

Table 8: Samples due to Speed and Readings

This is from the detailed analysis shown in Appendix D.

If another carrier is chosen to be captured at the speeds shown in Table 8, then samples would be missed as presented in Table 9.

Speed (cpm)	Carriers	Missed Samples
300	6	819
400	7	204
500	9	327
600	11	409
700	12	117

Table 9: Missed Samples

5.3 Averaging Method

Tests have been performed to find the accuracy of the system using the Averaging method at different speeds and weights. Five items weighing 164g, 226g, 379g, 528g and 711g were run over the weighing system at 300 and 600 carriers per minute (cpm).

As the weighing section consists of a dual load cell system for every lane, the load is split between the load cells, therefore each load cell was subjected to approximately 82g, 113g, 189.5g, 264g and 355.5g load. The results are presented in Table 10 while running the machine at 300cpm and Table 11 while running at 600cpm.

Weight of item (g)	Calculated weight (g)	error (g)	error %
82	81.40	0.60	0.73
113	114.10	1.10	0.97
189.5	191.40	1.90	1.00
264	261.10	2.90	1.10
355.5	360.30	4.80	1.35

Table 10: Results while running at 300cpm

Weight of item (g)	Calculated weight (g)	error (g)	error %
82	82.70	0.70	0.85
113	114.60	1.60	1.42
189.5	192.03	2.53	1.34
264	260.10	3.90	1.48
355.5	371.30	15.80	4.44

Table 11: Results while running at 600cpm

The tables show that accuracy decreases with increasing weight and speed. This method relies on the settling of the oscillatory response from the load cells to acquire an accurate measurement of the desired weight. This becomes less efficient when the speed of the carriers increases as the time for which the dual load cell system is subjected to the carriers and weight is decreased. Furthermore, having heavier items on the carriers would require more time for the response to settle as the deflection of the load cells is greater. This is evident from higher amplitudes as well as the frequency and damping of oscillations decreasing as seen in Figure 17.

To test the reliability of the load cells, one item weighing 100g was run on the carriers over the load cells 15 times repeatedly at 300, 400, 500 and 600cpm. The results are presented in Table 12.

Running 100g weight over Weighing System 15 times			
Speed (cpm)	Mean (g)	StdDev	Range (g)
300	100.66	0.92	2.9
400	100.71	1.01	3.7
500	100.78	1.57	5.4
600	101.01	1.83	6.5

Table 12: Reliability test of a 166g weight on a Carrier

It is evident that there are external factors affecting the accuracy of the system. If the system was not affected by external disturbances then there would not have been a range evident when running the same item a number of times at the same speed over the weighing system. It is interesting to note that as speed increases the reliability decreases. This is investigated further in this chapter.

To further investigate the inconsistency, empty carriers have been run on the dual load cell system at 300, 400, 500 and 600cpm. The components of the carriers that are weighed are the frame, latch, rollers and axle. They add up to a total of 143g. The z-plate on top of the load cell has to be taken into account as it is calculated as part of the weight. The z-plate weighs 87g. Therefore when empty carriers are run there is a total of 230g over the weighing system. The results are shown in Table 13.

Running 15 230g Carriers over Weighing System			
Speed (cpm)	Mean (g)	StdDev	Range (g)
300	230.04	0.71	2.2
400	230.36	0.71	2.3
500	230.39	0.74	2.4
600	230.52	0.77	2.6

Table 13: Accuracy of empty Carriers

This shows that the carriers and z-plate have a slight variation that occurs during manufacturing. These variations affect the accuracy of the system when trying to calculate the weight. The inaccuracy is not as high as that of Table 12 There are other factors that affect the accuracy of calculating the weight that are explained and investigated further in this chapter.

If the averaging method is applied on a weigh graph like that of Figure 30, it would give an inaccurate weight as a disturbance is evident at the last 35% of the weigh graph data causing it to increase. The weight calculated through the averaging method for this item is 143.3g. The item's weight was actually 283g and it was run at 399cpm over the dual load cell system;

therefore the weight should have been estimated to be about 141.5g. This gives an error of 1.8g, which equates to about 1.27%.

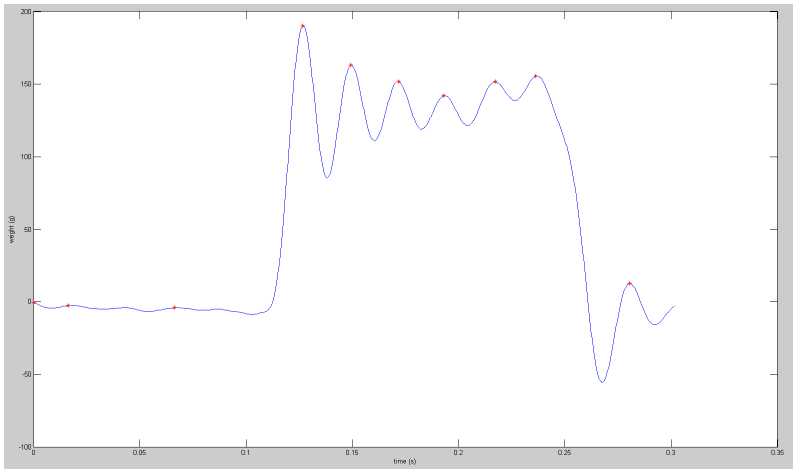

Figure 30: Graph with disturbance in the final 35%

This same weight is analysed using the Damping and Frequency methods.

5.4 Damping Method

The next section is the experiments conducted on getting the weight of an unknown item, and deducing the accuracy using the Damping method. There are various factors that influence the output of the load cell, and hence provide a misleading outcome to the weight. These factors are discussed.

Firstly, the parameters of both load cells on a lane were needed to be determined. To get the parameters of the load cell an experiment was conducted whereby a known load (200g) was placed onto the z-plate on top of each load cell statically on the second lane, presented in Figure 31and Figure 32. The response of the load cells were captured and peaks detected. In order to capture the data statically, a rod simulator was used to deceive the software into thinking the machine was running at 290cpm. From this, the x-axis time scale can be determined accurately.

Data was collected from each of the load cells from the second lane and uploaded into the Matlab software. The known mass and gravitational constant were specified. The code is presented in Appendix F.

It was essential to be able to capture the peak values of the oscillations accurately as the methods depend on them to deduce the weight. The Algorithm “Peakdet” has been written as

a function, presented in Appendix E, to allow it to be called from within any program throughout the tests to capture the peaks and troughs of any graph. The peaks in Figure 31 and Figure 32 have been signified with black crosses.

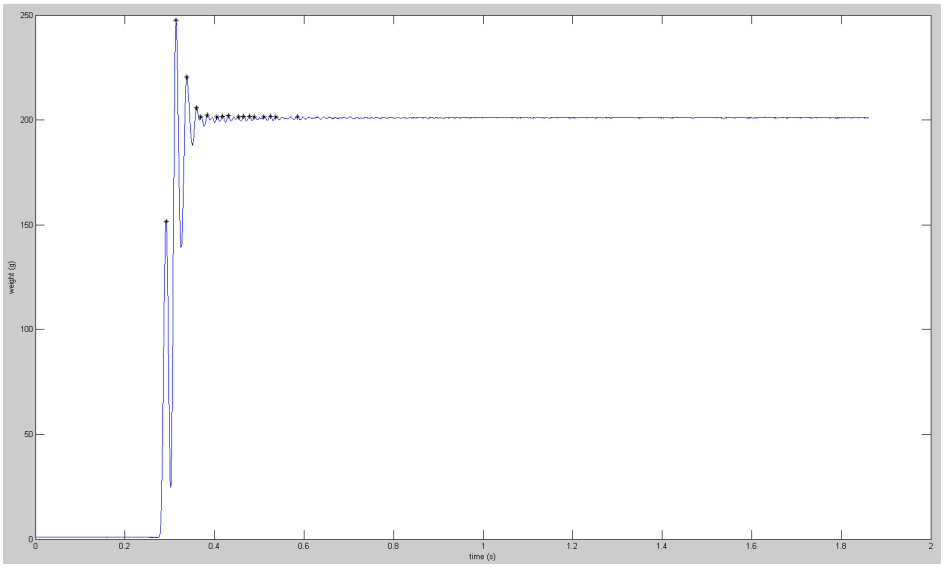

Figure 31: Weigh Graph of a 200g weight on first load cell

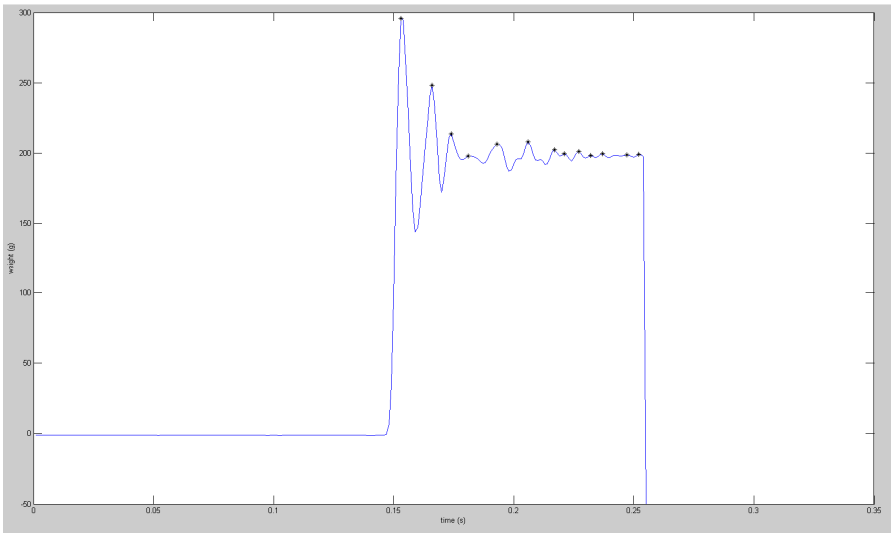

Figure 32: Weigh Graph of a 200g weight on second load cell

The peaks that were of interest are the highest three that happen as a result of placing the weight onto the load cell. This data was used to get the damping factor (μ) by taking the ratio of the amplitude of these peaks, as well as the average time between the peaks, then using Equation (3.47) to calculate it. This is summarised in Table 14.

Load Cell	1st Peak	2nd Peak	3rd Peak	Ratio of peaks	Average time (s)	Damping factor
1	(0.3137, 247.6)	(0.3380, 220.4)	(0.3595, 205.9)	1.8793	0.0229	27.5805
2	(0.1530, 295.9)	(0.1660, 248.3)	(0.1740, 213.7)	1.3757	0.0105	30.379

Table 14: 200g load cell data

The damping coefficient (c) is calculated from the damping factor (μ) using Equation (3.48), and equated to be 1.2152e4 kg/s for the first load cell and 1.1032e4 kg/s for the second load cell.

Through reverse Engineering, a check was made using the parameters to see if the mass can be returned and it came out to be 200g as expected using these parameters.

In order to test these parameters, an item with a 283g weight (unknown weight) is run at 399cpm on a carrier over the dual load cell system and its data captured. The weight of the carrier was removed and the weigh data was used to predict the weight using the Damping method on the load cells with the graphs presented in Figure 33 and Figure 34. Peaks have been denoted with red crosses.

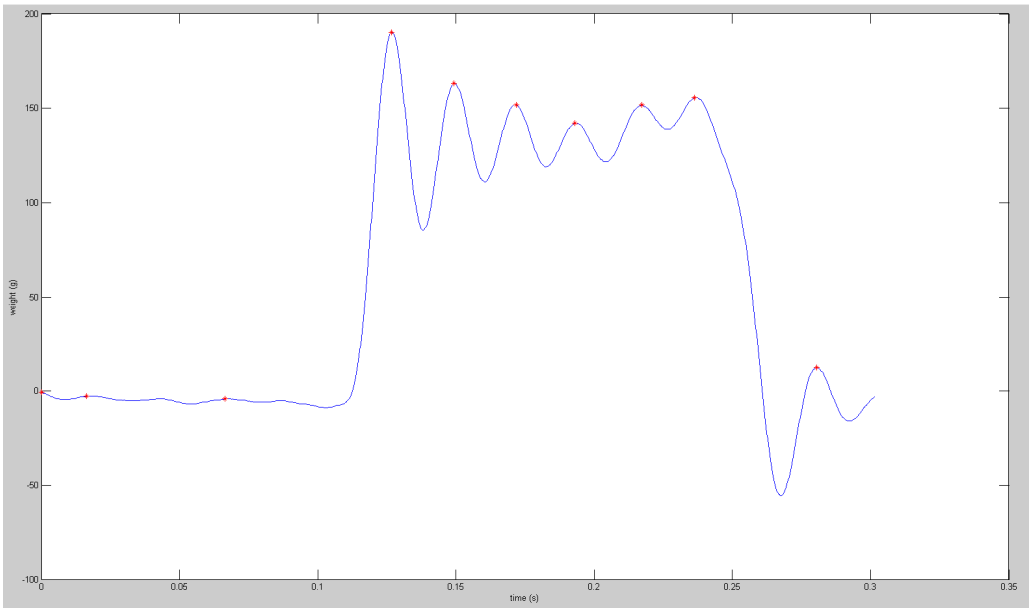

Figure 33: Weigh Graph of a 283g weight running at 400cpm on first load cell

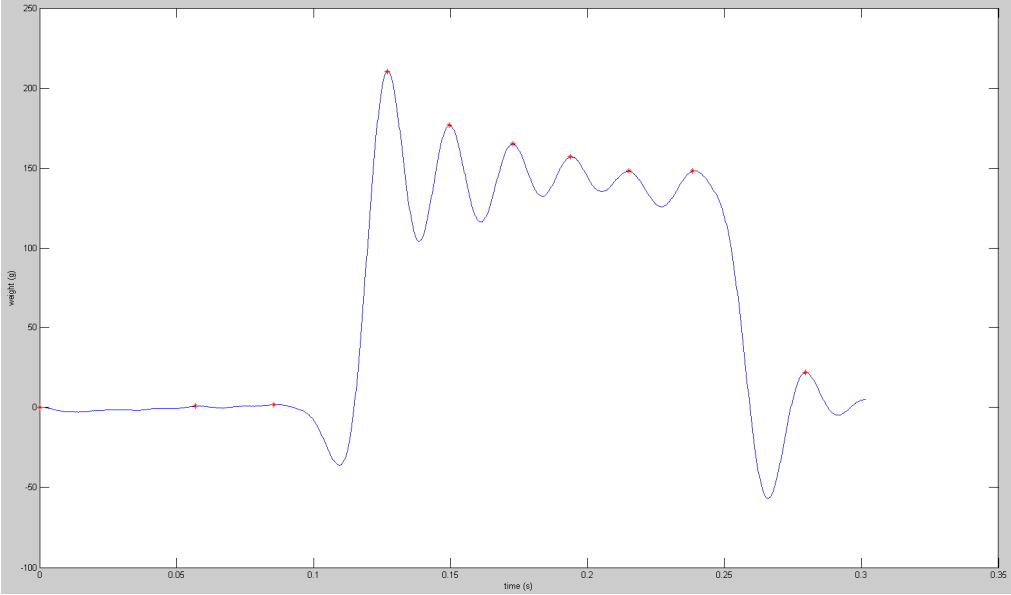

Figure 34: Weigh Graph of a 283g weight running at 400cpm on second load cell

The peaks that are of interest are stored in an array starting at the overshoot peak. This was after the initial fluctuations at the 0g weight, hence polling in the code for a peak above 50, shown in Appendix F. The damping factor was found from the ratio of the peaks and the average time difference by using Equation (3.47). The graph's three peaks were used to find the ratio of the difference of amplitudes of the second & third to the second & first peaks, and the average time difference. Finally, the mass was calculated using Equation (3.49). This is all summarised in Table 15.

Load Cell	1st Peak	2nd Peak	3rd Peak	Ratio of peaks	Average time (s)	Damping factor	Predicted weight (g)
1	(0.1268, 190.2075)	(0.1492, 163.2075)	(0.1718, 151.9575)	2.4	0.0225	38.9097	141.7668
2	(0.1270, 208.0075	(0.1495, 176.8875)	(0.1727, 165.1375)	2.6	0.0225	43.2888	140.3549

Table 15: 283g load cell data

Assuming the item on the carrier was stable, the weights would have been expected to either be divided equally between them (141.5g on each load cell) or compensated by one load cell

more than the other due to the shape of the item being weighed. Either case should give the total weight of the item when both load cell's acquired weights are summed.

Summing the masses from both load cells gives the total predicted mass of the 283g item as 282.1217g. Therefore there is an error of 0.8783g while using the Damping method. This equates to 0.31%. This is a similar result to the simulations.

Testing with other masses gave conflicting results to the simulation in some cases. These are outlined in Table 16 and Table 17;

Speed (cpm)	Actual Weight (g)	1st peak	2nd peak	3rd peak	Predicted weight (g)	error (g)	error %
300	82	(0.2093, 102.9)	(0.2585, 87.7)	(0.2957, 86.8)	84.30	2.30	2.81
300	113	(0.3144,129.1)	(0.3350, 121.43)	(0.3619, 119.3)	112.68	0.32	0.29
300	189.5	(0.3365, 247.7)	(0.3672, 211.7)	(0.3941, 198.2)	190.30	0.80	0.42
300	264	(0.3331,342.9)	(0.3605, 309.1)	(0.3898, 291.2)	270.69	6.69	2.53
300	355.5	(0.4056, 441)	(0.4368, 408.6)	(0.4680, 389.4)	362.28	6.78	1.91

Table 16: Weight prediction while being run at 300cpm

Speed (cpm)	Actual Weight (g)	1st peak	2nd peak	3rd peak	Predicted weight (g)	error (g)	error %
600	82	(0.1790, 137.6)	(0.2026, 107.4)	(0.2230, 100.2)	84.49	2.49	3.03
600	113	(0.0912, 123.7)	(0.1158, 116.3)	(0.1341, 113.9)	115.70	2.70	2.39
600	189.5	(0.1819, 296.3)	(0.2078, 242.2)	(0.2359, 217.3)	191.93	2.43	1.28
600	264	(0.0818, 363.9)	(0.1133, 297.5)	(0.1462, 266.1)	260.92	3.08	1.17
600	355.5	(0.0756,493.9)	(0.1025,443)	(0.1301, 409)	372.39	16.89	4.75

Table 17: Weight prediction while being run at 600cpm

These results are not consistent as seen in the simulation. The accuracy has a general tendency to decrease with increasing weight and also decrease with increasing speed. The inconsistency in the results is due to disturbances causing the graphs not to act as a second order harmonic oscillator as assumed by the system model due to disturbances that are investigated further in this chapter.

To further explain the discrepancies, the expected graph from the output of the model has been overlaid onto the actual graph for the 189.5g load while running at 300cpm in Figure 35, and while running at 600cpm in Figure 36.

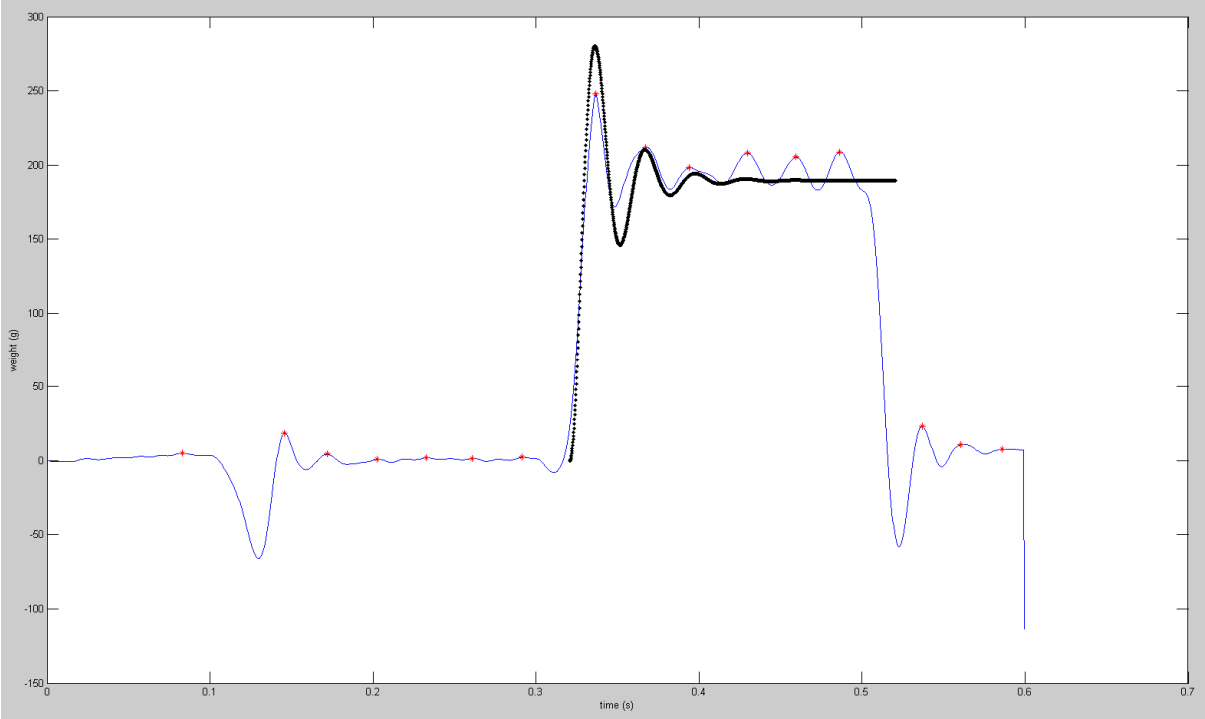

Figure 35: Actual vs Predicted for 189.5g at 300cpm

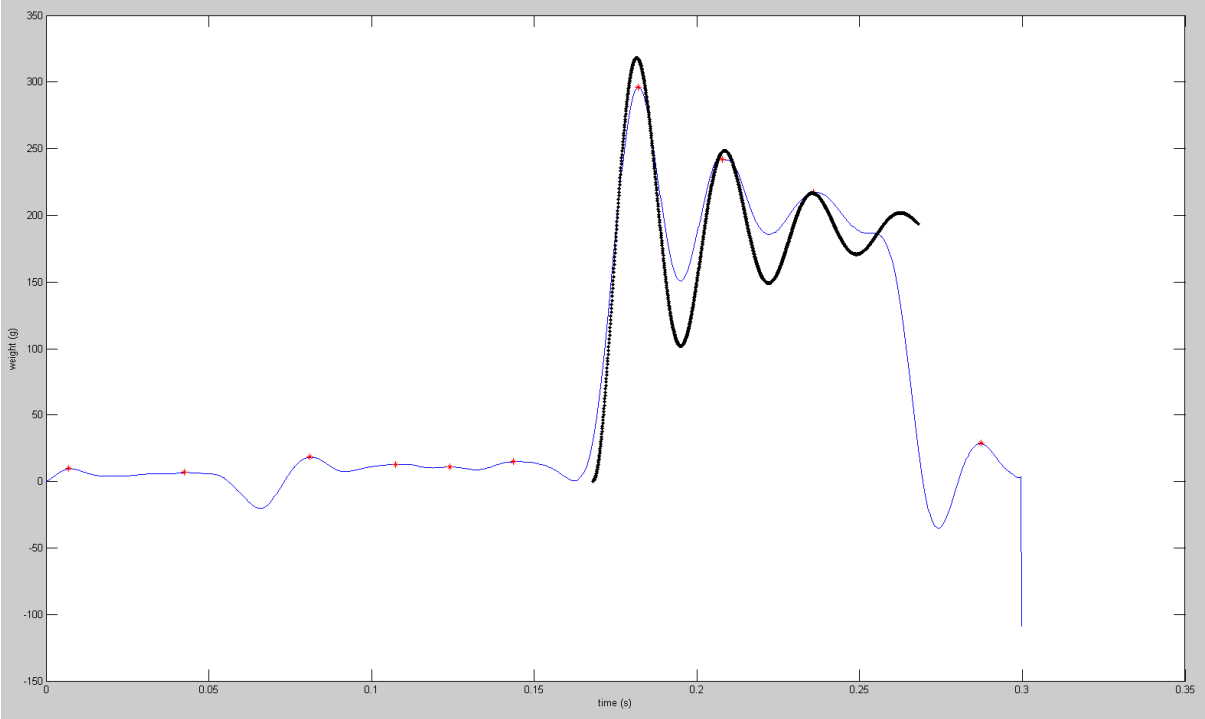

Figure 36: Actual vs Predicted for 189.5g at 600cpm

The model graphs are not exactly overlaid onto the output graphs from the weighing system. While running at 300cpm, the first peak of the oscillations had a lower value than the expected output from the model, although this was counteracted by having the second and

third peaks with a higher value than the expected model. Therefore, the overall weight prediction was higher than the actual weight by 0.8g. While running at 600cpm, the first and second peaks were lower than the expected outcome from the model, but the third was higher which lead to the 2.43g difference.

Similarly, when investigating the graphs for the 264g weight, Figure 37 and Figure 40 represent running the weight at 300cpm and 600cpm respectively. As presented, the model graph is a closer fit while running at 600cpm than it is while running at 300cpm. This lead to a better accuracy at 600cpm with 3g error, while at 300cpm there was a 6.7g error.

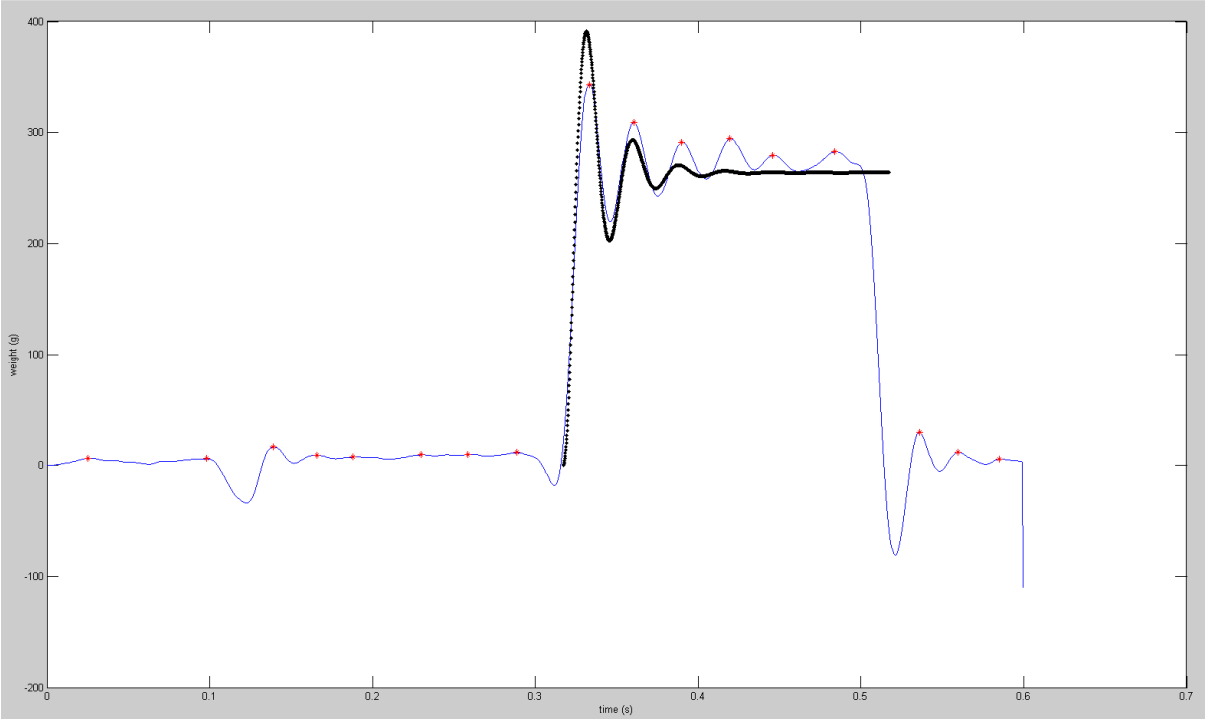

Figure 37: Actual vs Predicted for 264g at 300cpm

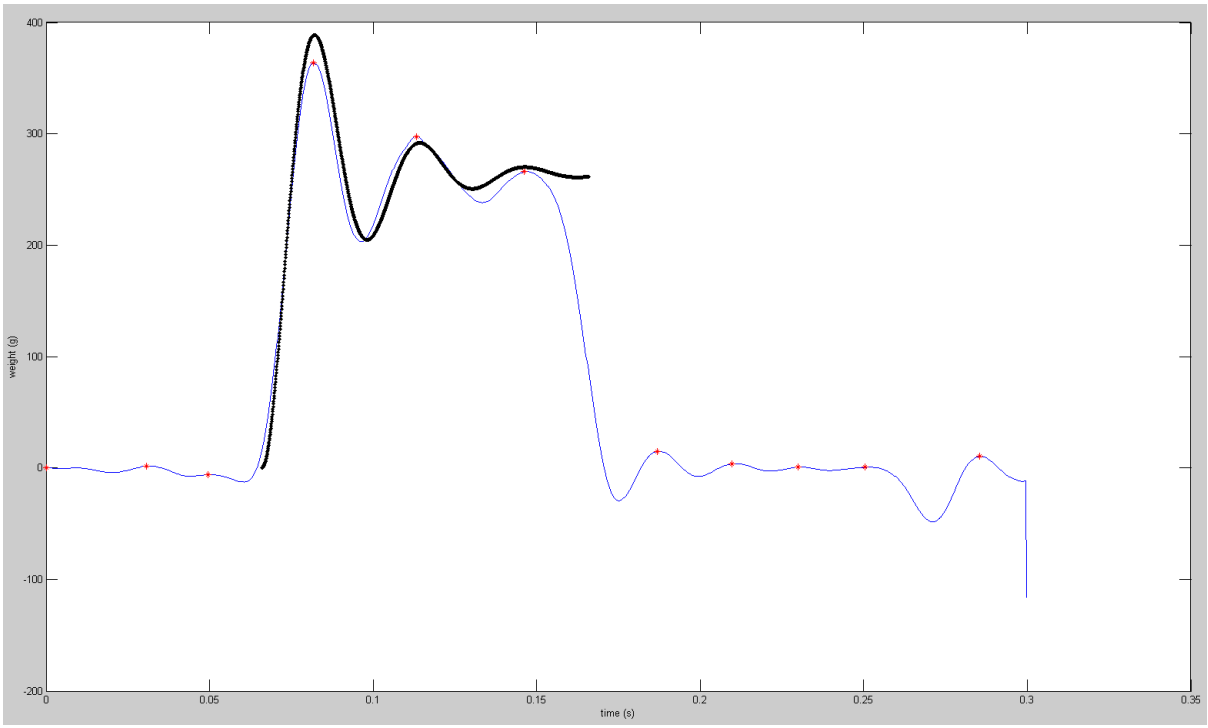

Figure 38: Actual vs Predicted for 264g at 600cpm

The model graph's oscillation frequency fit well onto the output graph's data from the weighing system but the amplitude does not. To make the models fit the data better, damping could be investigated as the model is sometimes consistently higher than the data at the peaks. This suggests that more damping would be beneficial. Although, some cases similar to the 264g at 300cpm, presented in Figure 37, shows that the model graph's amplitude starts of higher than the weighing system's output data, then it is lower after the first oscillation. This suggests that the data is being interfered with.

All forms of interferences and disturbances need to be eradicated from the system. There seems to be more than one form of interference as the data is not consistently affected the same way. These are investigated later in the chapter.

5.5 Frequency Method

To predict the weight utilising the Frequency method, a similar approach to the Damping method is applied. In addition to the 200g weight placed on both the lane's load cells, another static load was applied to get the load cell parameters which are used to predict the weight when an unknown mass is run on the dual load cell system. The graphs of 122g static loads on both load cells are presented in Figure 39 and Figure 40.

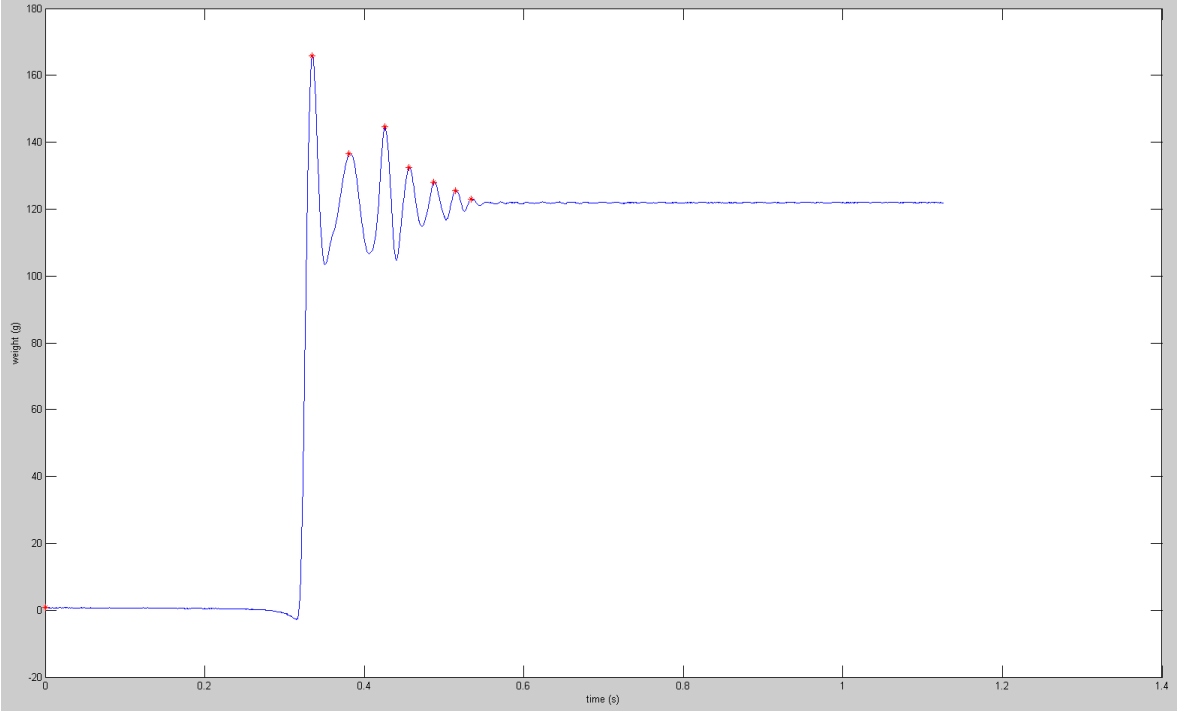

Figure 39: Weigh graph of 122g on third load cell

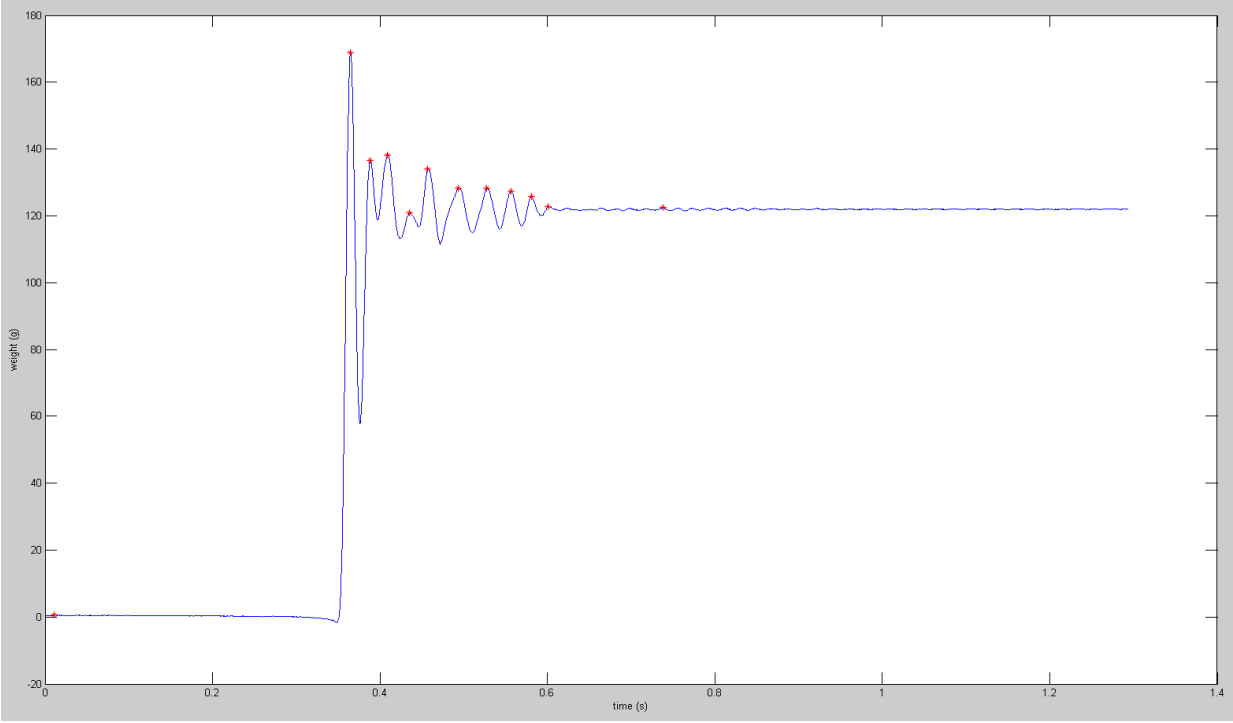

Figure 40: Weigh graph of 122g placed on fourth load cell

The frequencies acquired are presented in Table 18. The table also has the frequencies acquired from running a 283g weight at 399cpm on lane 2 (load cells 3 and 4) presented in Figure 33 and Figure 34 above. Approximately half the weight is going to be exerted on each load cell, therefore the actual frequencies on each load cell is that of a 141.5g weight.

Lane	Load Cell	Weight (g)	1st Peak	2nd Peak	Frequencies (Hz)
2	4	200	(0.3137, 247.6)	(0.3380, 220.4)	259.1
2	4	122	(0.3347,165.8875)	(0.3810, 136.6375)	135.85
2	4	141.5	(0.1492, 163.2075)	(0.1718, 151.9575)	279.25
2	3	200	(0.1530, 295.9)	(0.1660, 248.3)	483
2	3	122	(0.3648, 168.8875)	(0.3882, 136.6375)	284.1
2	3	141.5	(0.1495, 176.8875)	(0.1727, 165.1375)	279.25

Table 18: Frequency comparisons

The time it takes for the oscillations created by a static load placed on a load cell are very short. This means that the difference in time between the first two peaks is very small. Even though the system has a high sampling rate of 4 KHz, any disturbance to the load cell while applying the load leads to inaccuracies and wrong predictions of the weight. The Frequency method is highly dependent on accurate determination of the time between the first two peaks. This system is highly susceptible to small variations which have a big effect on the angular frequency determination of the graphs. As seen from the graphs above, the oscillations do not follow a harmonic motion with the oscillations being at constant frequency. A difference of 0.01s between the first two peaks causes a large difference in the angular frequency calculation using Equation (3.18). Therefore although the Frequency method might be very useful tool for other systems with fewer discrepancies, it is not the best option for this weighing system.

Various factors may be contributing to the discrepancies such as the mechanical assembly not being fully isolated, the mechanical component's variations, the mechanical setup and

external noise. When these factors are flagrant, the graph of the output of the load cell does not abide by the expected outcome of the system model. Therefore the algorithms do not give an accurate prediction of the weight.

5.6 Disturbances

5.6.1 Carrier Interference

The current system has the chain driven carriers travel along a hardened stainless steel plate which is mounted using a couple of button-head bolts to the Vishay 6Kg load cell. The stainless steel plate is hardened to withstand the carriers constantly running on top without cutting groves or wearing the steel. The frame of the carriers, which is the contact point to the stainless steel plate, is made of glass reinforced nylon plastic. The stainless steel plate is cut to the shape of a Z to allow the weigh pads on the frame of each carrier to enter, and exit, the stainless plate at the same time.

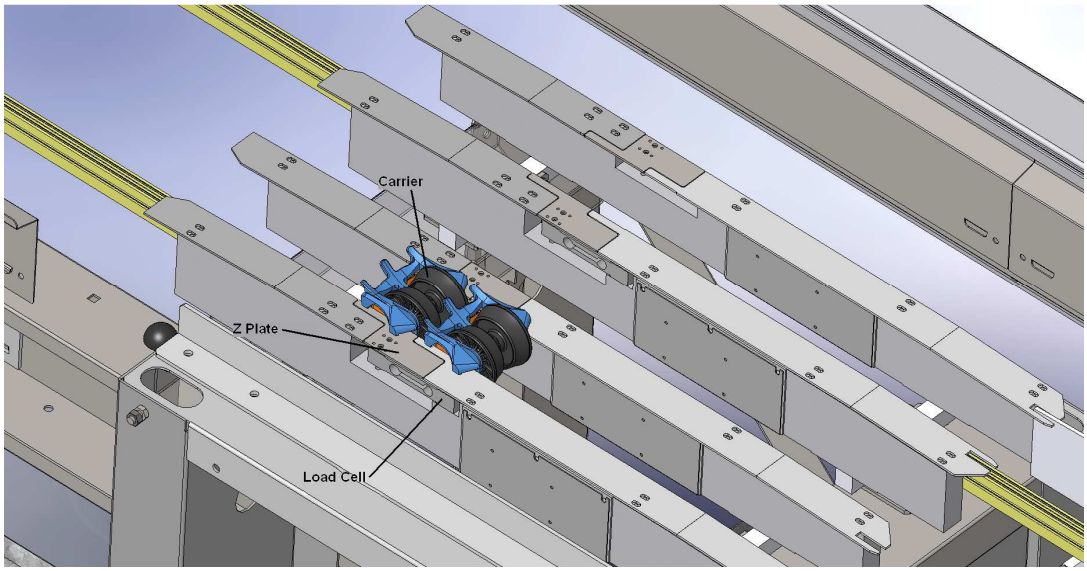

Figure 41: Carriers on z-plate

Each carrier is on the z-plate for a distance of 90mm to allow enough time for the deflection of the load cell to accrue an accurate measurement. Although, due to the distance between the carriers being 95.25mm as they are at 3.75” pitch means that the carrier prior to the one on the z-plate being weighed will enter the z-plate before the first one exits as presented in Figure 42. There is a gap of 1mm between the z-plate and the weigh plates. Therefore the interference lasts for 4.25mm as the carrier is introduced onto the z-plate (from the preceding

carrier), and a further 4.25mm as the carrier exits the z-plate (from the next carrier). Giving a total of 8.5mm, this equates to ~9% of the carrier duration while being weighed.

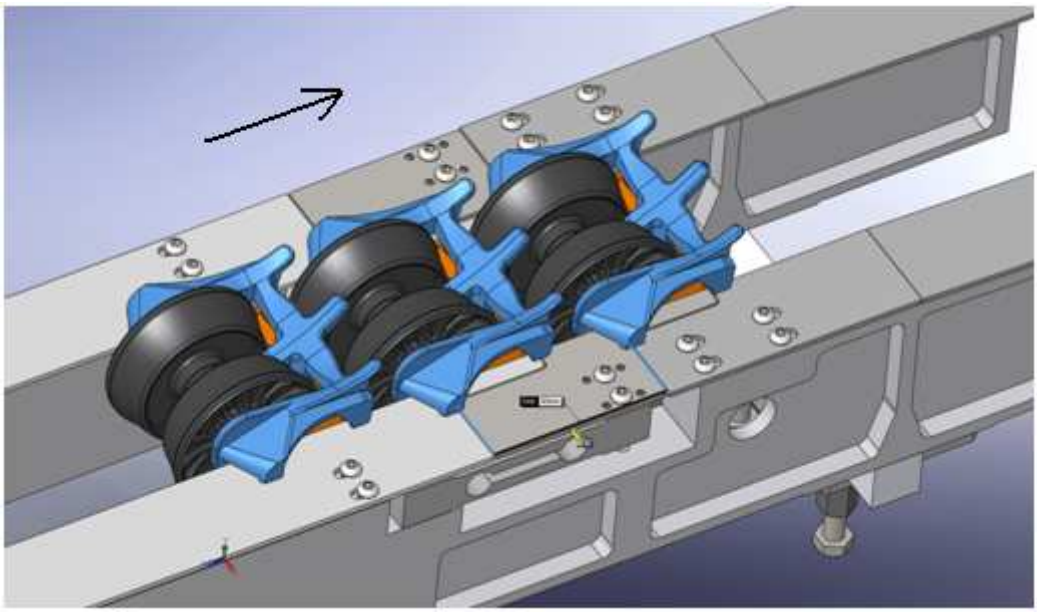

Figure 42: Carrier interference on the z-plate

To investigate this further an experiment was conducted whereby every second carrier was removed from the chain to allow only one carrier on the z-plate at any one time. This allowed the deflection of each load cell to have enough time to return to its neutral position before the next carrier arrived to be weighed.

A 166g weight was placed on the carriers twenty times while the machine was running at 300, 400, 500, 600 and 670cpm. The mean, standard deviation, range and error were calculated and presented in Table 19 for the case without missing carriers and Table 20 for the case with missing carriers;

Running 166g weight on carriers without missing carriers on the chain					
Speed	Mean	StdDev	Range	error (g)	error %
300	167.04	0.98	3.5	1.04	0.626506
400	167.20	1.24	4.6	1.2	0.722892
500	165.83	1.05	4.4	0.17	0.10241
600	166.81	1.92	6.7	0.81	0.487952
670	170.21	1.89	8.8	4.21	2.536145

Table 19: 166g Weight on Carriers without Missing Carriers

Running 166g weight on carriers where every second carrier is missing from the lane					
Speed	Mean	StdDev	Range	error (g)	Error %
300	166.41	0.82	3.1	0.41	0.246988
400	166.25	0.83	2.9	0.25	0.150602
500	165.13	0.73	6.9	0.87	0.524096
600	166.59	1.25	4.5	0.59	0.355422
670	169.09	2.03	6.2	3.09	1.861446

Table 20: 166g Weight on Carriers with Missing Carriers

Having every second carrier missing from the lane, therefore allowing the load cell to return to its neutral position before the next carrier with a weight is introduced, gave more accurate results at all speeds except at 500cpm. Further investigation shows that at 500cpm the range is bigger than expected due to two values having the values of 163.9 and 164g. These outliers

have skewed the mean. Disregarding this, the overall effect of allowing the load cell to settle before the next carrier is introduced leads to more accurate calculation of the weights.

5.6.2 Item's physical shape (stability)

If an item is not stable on the carrier while travelling over the load cells then the weight of the item is not split evenly between the two load cells of the lane. Similar to Figure 43 where the blue graph is from load cell 4, the green graph is from load cell 3 and the red graph is the total sum of both the blue and green. If an item is bouncing it may exert less force on a load cell if it has an upwards velocity component, or it may exert more force if it has a downward velocity component. In this case, the item was bouncing therefore less force was exerted on the fourth load cell, and more was exerted on the third load cell. This is evident from the graphs of both load cells starting and ending at the same position but moving further apart during the motion.

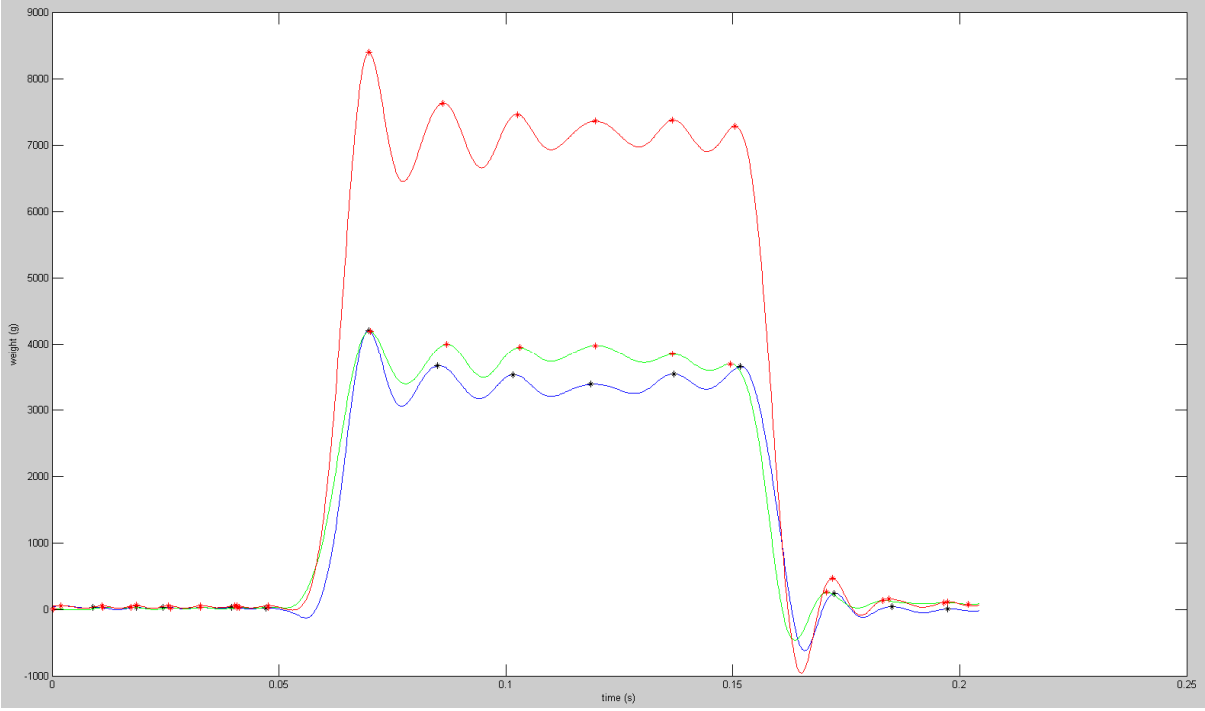

Figure 43: Load Cell output and their summation

The weights of graphs with interferences as such would be better calculated using the Damping method as it depends on the initial oscillation's amplitudes which might not have been affected by the unstable items. The Averaging method will predict the individual load cell's masses to be varying due to the bouncing, and depending on the intensity of the

unstableness, might give inaccurate results.

Due to the recent results implying that stability of the items on the carriers is crucial, a simple test experiment was carried out by adding foam to the carrier's frame. Ten carriers had low density, closed cell foam placed on the frame as shown in Figure 44.

It was expected that the foam should stabilise the items on the carriers therefore producing more accurate weighing. Tests were performed by running the carriers at two different speeds of 400 and 600 carriers per minute (cpm) and placing three weights of 88, 166 and 253g on empty standard carriers, and then on the carriers with the foam on the frame. Each weight was run 10 times on carriers with and without foam to compare. Table 21 outlines the results.

Figure 44: Carriers with Foam

Figure 45: Apple on Carriers with Foam

.	Speed (cpm)	Weight (g)	Mean (g)	StdDev (g)	Range (g)	Mean Error (g)	Mean Error %
Foam	400	88	89.76	1.38	3.6	1.76	2
No Foam	400	88	88.48	1.18	3.4	0.48	0.545454545
Foam	400	166	167.58	1.77	5.9	1.58	0.951807229
No Foam	400	166	166.02	2.44	7.9	0.02	0.012048193
Foam	400	253	254.76	0.96	3.1	1.76	0.695652174
No Foam	400	253	254.4	1.85	6.8	1.4	0.553359684
Foam	600	88	87.99	1.09	3.7	-0.01	-0.011363636
No Foam	600	88	88.89	1.45	4.3	0.89	1.011363636
Foam	600	166	167.72	2.06	7.5	1.72	1.036144578
No Foam	600	166	167.84	2.69	9.3	1.84	1.108433735
Foam	600	253	259.14	1.11	3.5	6.14	2.42687747
No Foam	600	253	259.98	4.07	13.8	6.98	2.758893281

Table 21: Results of Foam Vs No Foam on Carriers

Comparing the means between the two speeds, the carriers with no foam seemed to be closer to the actual weight being measured at the slow speed. This was differing to the results at higher speed where the carriers with foam seemed to be more accurate.

Comparing the standard deviations between the two speeds, the carriers with foam seemed to be more consistent every time, except for the case at 400cpm with 88g, although the standard deviations are very close (1.38 vs 1.18). It was very noticeable at higher speed (600cpm) using the heavy fruit (253g) that the foam had a big effect on the standard deviation (1.11 vs 4.07).

Comparing the range between the two speeds, again, the carriers with the foam gave better results by having a lower range. Except for the lower speed (400cpm) using the lower weight

(88g). Similar to the standard deviation in that case, the ranges are very close (3.6 vs 3.4). It was the most noticeable at the higher speed with the heavier weight (3.5 vs 13.8g).

When the foam and no foam experiments are compared in terms of weigh measurements error, the results were inconclusive. Generally, the foam had a positive effect on the weights, more so at higher speeds. As mentioned in the expected outcome, the foam seems to be effective in stabilising the fruit on the carriers. The low density property of the foam meant it moulded to the shape of the item placed on the carrier and gave it a soft surface contact rather than a line or point contact on the plastic frame of the carrier. Furthermore, the foam absorbed the shock of placing the fruit on the carriers quickly and so items managed to settle in one position.

Repeating this test with more weights and more frequent runs would be beneficial to draw sound conclusions.

5.6.3 External noise/vibration

External noise is one of the factors that can result in inaccurate determination of the weight of an item when using either of the methods. Even though the weighing system is isolated from the machine, noise can still propagate through the legs. When the noise is present the weigh graph of an item does not conform to a sinusoidal decay. It can be noticeable that the graph is increasing in amplitude of oscillations, or it fluctuates in a non-decaying form. Increasing in oscillations could be due to excitation of the natural frequencies of the structure. This is evident as in Figure 46 having the oscillations increase in amplitude. The natural frequencies of the structure could be researched further in terms of adding stiffness to increase the values of the natural frequencies. Although, this should be done with care as increasing the stiffness could be accompanied by increasing the mass, resulting in no change or even a decrease in the natural frequencies.

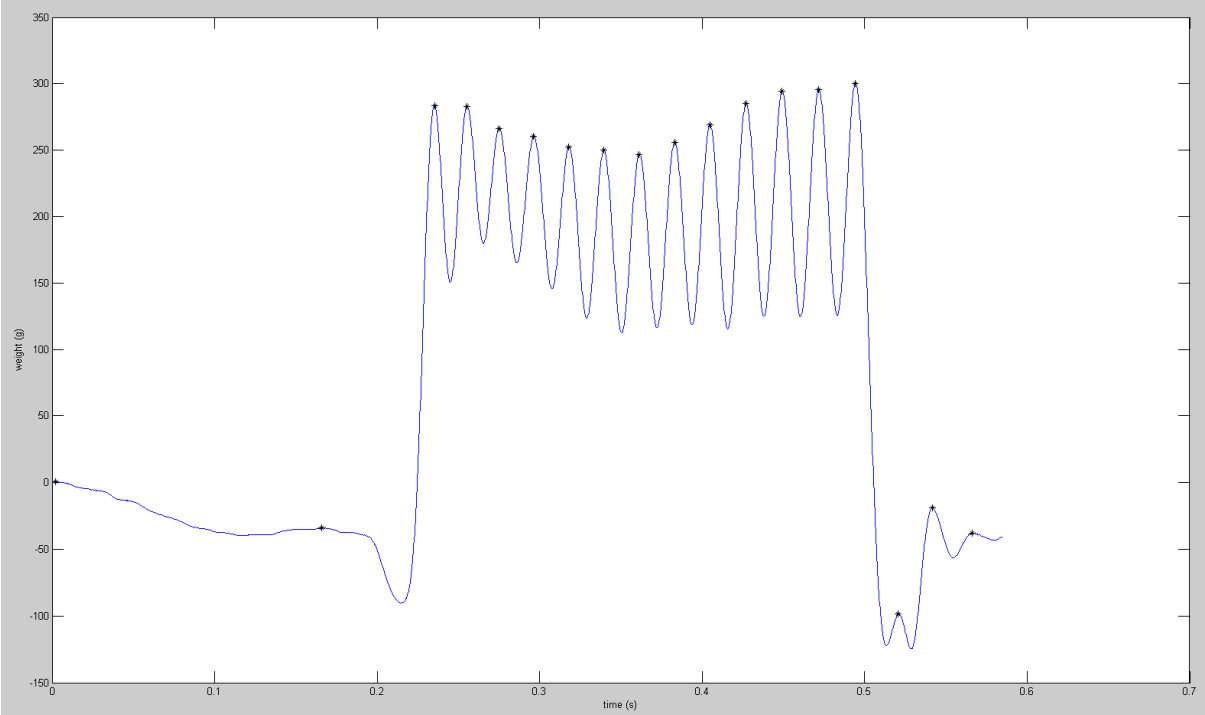

Figure 46: Disturbance due to excitation

5.6.4 External Disturbance – human interference

The load cells are designed to be very sensitive. Care needs to be taken when placing items onto each load cell to determine its parameters. External disturbance was noticed when trying to acquire the parameters of the load cell by placing a 200g load onto the fourth load cell on lane 2. Figure 47 shows that the weight was not placed correctly as it is evident that the weight was removed slightly after the initial contact with the load cell.

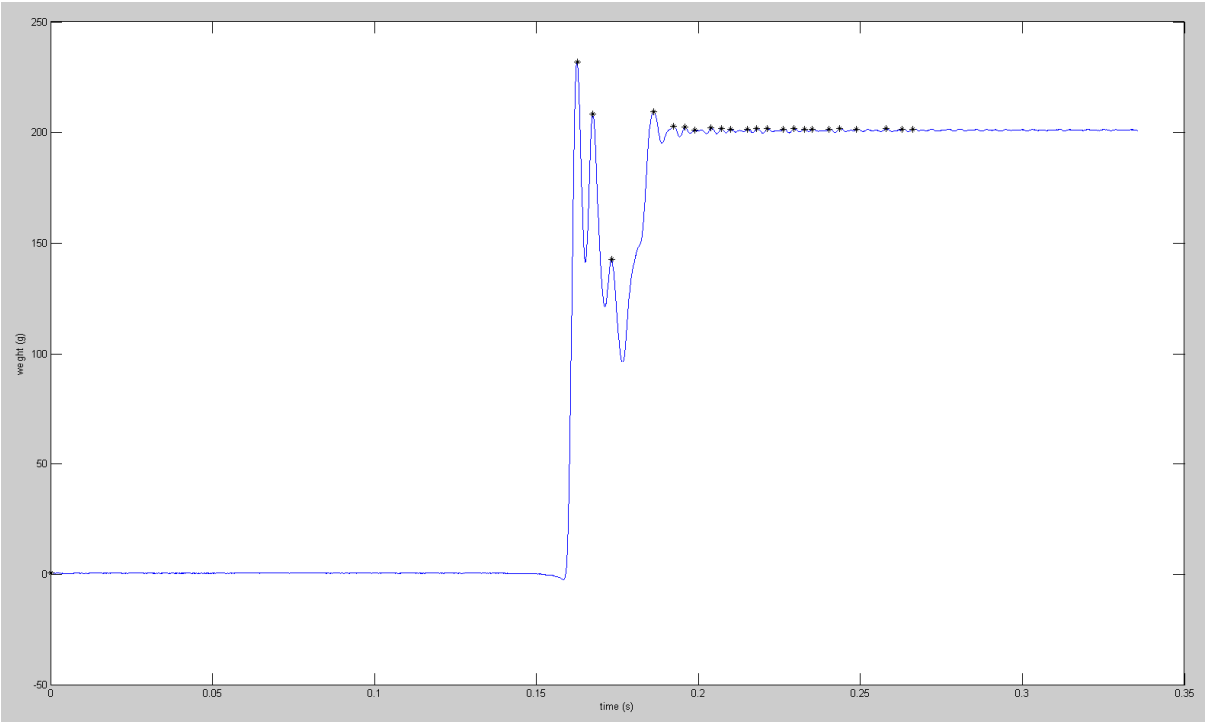

Figure 47: Disturbance due to human interference

When using the first three peaks in Figure 47 to calculate the damping factor and the spring constant, the coefficient values came out negative while using Equations (3.47) and (3.27). Therefore using either the Damping or Frequency methods would result in an inaccurate prediction of the parameters due to the misleading data.

Another way of acquiring the load cell parameters, instead of placing a known weight onto a load cell, is removing a known weight off a load cell. This seemed less likely to introduce disturbances in terms of human error adding extra weight or removing weight as seen in Figure 48.

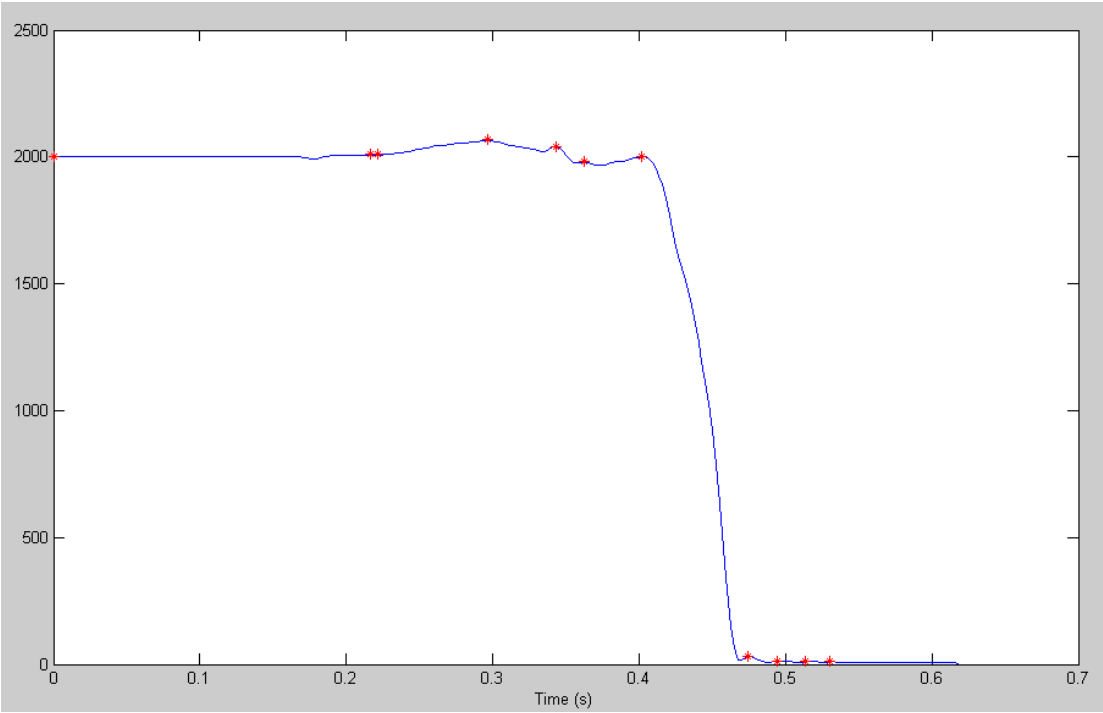

Figure 48: Weigh Graph from removing a 200g Weight off a Load Cell

This has been tested by removing a 200g weight from a load cell, and the two peaks captured after removing the load were at (0.4746, 32) and (0.4941, 12).

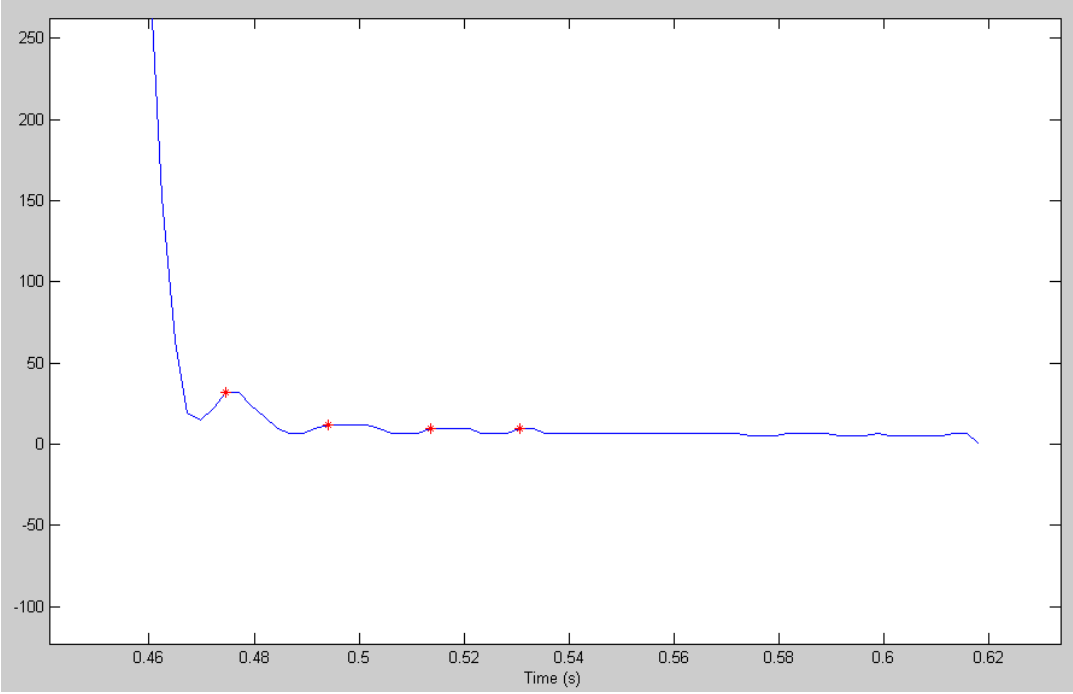

Figure 49: Peaks of interest from the 200g removed weight

Due to the resolution of the graph, the peaks are not accurately determined therefore the parameters of the load cell could not be calculated accurately. The load cell takes a very short time to reach a stable state when removing an item from the deflected position. Whereas

when an item is placed onto a load cell, it starts at its stable position, deflects to its maximum depending on the weight placed and oscillates back to its neutral state. There are more oscillations that have higher amplitude and take a longer time to settle when an item is placed onto a load cell. Therefore it is easier to get more accurate values for the peaks.

5.7 Spectral Analysis

Frequency of the weigh graphs from a load cell is dependent on the weight of the object being weighed regardless of speed, refer to Equation (3.4). Speed should theoretically only affect the time upon which the item to be weighed is applied to the load cell. Upon further experimentation, it was found that this is not necessarily the case for this system. This is explained in the following section.

An experiment was conducted to find the frequencies of the oscillations by running different weights 164, 379, 528 and 711g at different speeds 300, 400, 500 and 600cpm. The weigh graph data was captured and manipulated to be produced on the same graph. These tests were conducted on the second lane of the machine, hence using load cells three and four to capture the data. Figure 50 and Figure 51 show the weigh graphs of 379g on load cells three and four respectively. Refer to Figure 52 to Figure 57 in Appendix I for the weigh graphs of 164g, 528g and 711g. Throughout the figures, the x-axis denotes time (seconds) and the y-axis denotes weight (deca-grams).The peaks have been found using the peak detection algorithm presented in Appendix G. The graph colour codes are as follows; Blue = 300cpm, Green = 400cpm, Red = 500cpm and Magenta = 600cpm. The results are presented in Table 22.

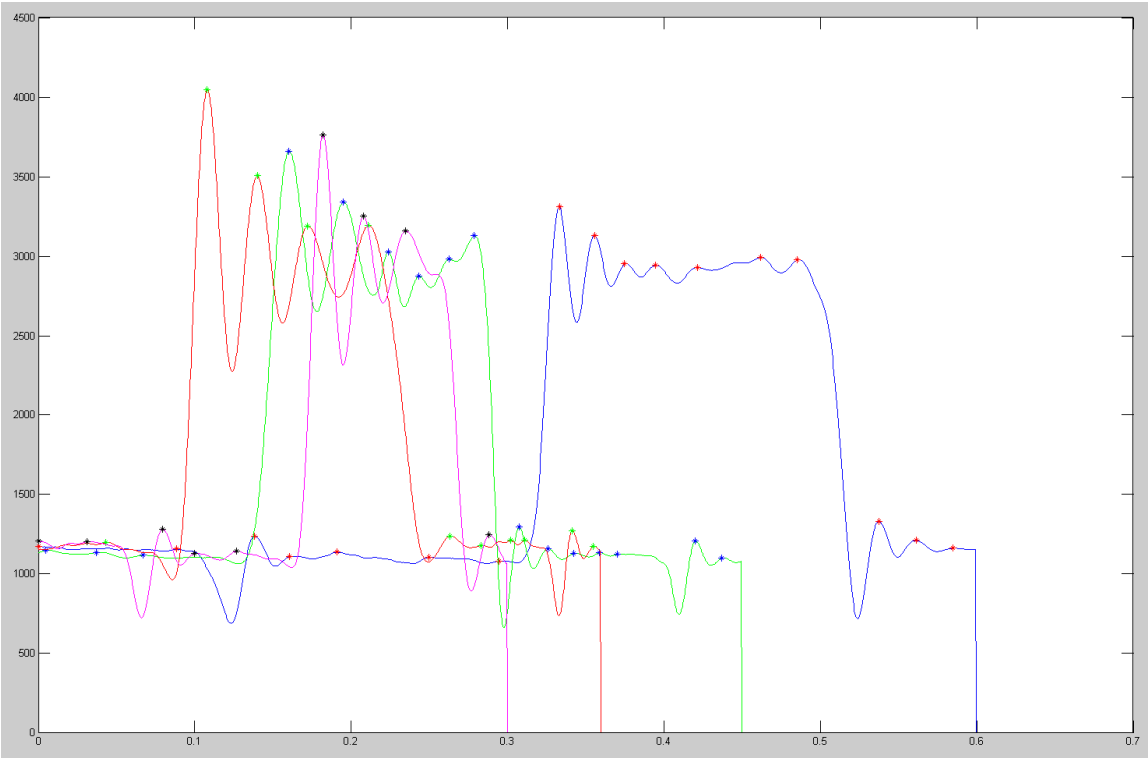

Figure 50: Weigh Graphs of 379g at 300cpm, 400cpm, 500cpm and 600cpm on Load Cell 3 (Lane 2, LC 1)

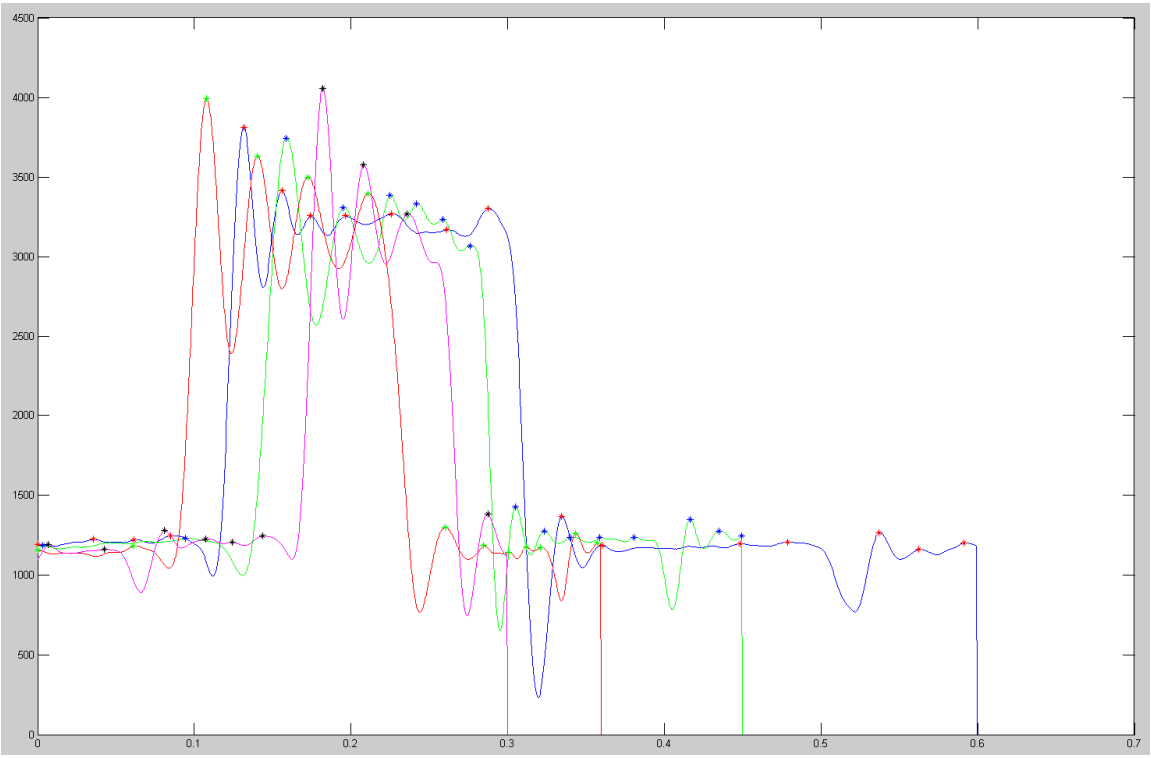

Figure 51: Weigh Graphs of 379g at 300cpm, 400cpm, 500cpm and 600cpm on Load Cell 4 (Lane 2, LC 2)

	Speed							
	300cpm		400cpm		500cpm		600cpm	
Weight	LC3	LC4	LC3	LC4	LC3	LC4	LC3	LC4
164g	47.3485	43.4028	27.2331	27.2331	39.0137	35.0730	42.5170	36.5497
379g	44.3262	40.8497	28.6369	27.5028	31.2813	30.7276	38.2263	38.2263
528g	38.5802	37.8788	27.2331	26.9687	29.6771	29.1783	31.8066	32.0513
711g	37.2024	37.2024	42.7350	42.7350	22.6943	22.4014	37.2024	35.3107

Table 22: Frequency (Hz) Depending on Speed and Weight

In general load cell 4 had a lower frequency from its outputs than load cell 3. LC3 and LC4 are both exposed to the same item at the same time; therefore the variation in their frequency at the same speed suggests that the weight on the cup might not be stable. It might be slightly rocking from side to side. Other possibilities are that the setup of the load cells is not level, or the carriers themselves are flexing and affecting the loadcell signals.

As expected, the frequency decreased with increasing weight at the same speed except for when running 379g and 711g at 400 and 600cpm. It was interesting that the frequency was not consistent using the same weight as speed increased. These discrepancies could be due to external interferences to the system. These interferences would have to be related to the speed of the machine. Increasing the speed would mean the motor runs faster to convey the chain around the sprockets faster. This also leads to the carriers transferring across the weighing system faster therefore causing more abrupt loading and unloading of the load cell.

Furthermore, running at different speeds would mean the carriers are introducing other forcing frequencies to the system themselves. In that,

- @300 cpm = 5 cups/sec, T = 0.2s, f = 5Hz
- @400 cpm = 6.67cups/sec, T = 0.15s, f =6.67Hz
- @500 cpm = 8.33 cups/sec, T = 0.12s, f = 8.33Hz
- @600 cpm = 10 cups/sec, T = 0.1s, f = 10Hz

Were T is the period, and f is the forcing frequency.

These forcing frequencies, and their harmonics, could be interfering with the natural frequency of the system therefore causing excitation. An overall frequency analysis of the weighing structure and the components in the system such as the carriers and the weigh plates

would be beneficial in further analysing these discrepancies. In general a stiffer structure is beneficial as it is less affected by the lower harmonics of everyday life.

Another factor that could affect this is the variance in tolerances between the different carriers. The carrier discrepancies were evident in the results presented before in Chapter 2.

Chapter 6: Results & Discussion

A weighing system was configured and built to allow testing and experimentation on acquiring the weight of items placed on the Compac carriers travelling at high speeds up to 600 items a minute.

The system has been modelled mathematically and different methods for predicting the weight have been established; the Averaging, Frequency and Damping methods. Each has its advantages and drawbacks. Also, each has its limitations. These were found through simulations using a programmed user interface and real world testing on the dual load cell system.

The simulations were successful in providing an easy and quick comparison between the three methods while presenting a visual graph of the load cell output for the weight applied. The real world testing allowed for a better understanding of external and internal variables unaccounted for using the simulations, while comparing the three methods for calculation of the unknown weights being run on the dual load cell system.

The Averaging method works best when the data output from the load cell is stable and there is enough time for the oscillations of the graph to reach steady state. This method involves utilising as much time as possible to get an accurate result. Therefore slower speeds and lighter weights work well using the Averaging method. At slower speeds the weight is subjected to the load cells for a longer period of time allowing the oscillations of the graph from the weighing data to settle. Lighter weights deflect the load cells less than heavier weights therefore they have lower amplitudes which reach steady state faster. The Averaging method does not require calculating the parameters of the load cell to acquire the weight.

The Frequency and Damping methods work well when the resolution is high so can determine the coordinates of the peaks accurately. They do not require waiting for all the oscillations to settle as they are based upon predicting the weight from the initial oscillations. The Damping method depends on the ratio of the peaks of the oscillations and consequently requires at least three peaks. The Frequency method depends on the frequency of the oscillations, and thus requires accurate determination of the period of the oscillations. This can be acquired from the first two peaks of the oscillations. These are an improvement over the Averaging method as the rest of the weigh data after the initial peaks are acquired can be

disregarded. An advantage of this is that processing power can be utilised elsewhere to calculate a prediction of the weight. This also means that speed of the machine can be increased as it is not necessary to wait to capture all the data from the load cell. When the initial three oscillations are captured accurately from the load of the first carrier onto the load cell, the next carrier can be subjected to the load cell directly after so time is not wasted. Another advantage is that heavier weights can be run over the weighing system. The Averaging method might not have had time to calculate the weight of heavier masses accurately due to the higher amplitudes, lower frequency and lower damping coefficient of oscillations taking a longer time to settle. Managing to predict the weight accurately in a shorter amount of time and having the ability to use heavier weights would be extremely beneficial for industry applications such as robotics, automation and food as it would increase throughput for production.

Simulations done on Matlab of different weigh graphs running with different weights between 55 and 400g showed that the Frequency method's error percentage is between 0.2 and 0.35%, the Damping method error percentage is between 0.3 and 0.45% and the Averaging method's error percentage is between 0.5 and 2.9%. The error increased with increasing weight, although the increase for the Frequency and Damping methods was less than the increase exhibited by the Averaging method. This is because the Averaging method's oscillations did not tend to reach steady state in the allocated time as weight increased. The Damping and Frequency method's errors were more consistent as they depended on the resolution of the graphs to acquire the peaks. Due to the consistency of the error, the error percentage of the Damping and Frequency method decreased with increasing weight, whereas the Averaging method's error percentage continued to increase with increasing weight.

Increasing the speed was another interesting factor investigated. This was simulated by decreasing the amount of time for each weigh capture as at faster speeds the items are subjected to the load cells in less time. Due to the Damping and Frequency methods depending on the initial oscillation's peaks, they were not affected by an increase in speed from 240 items a minute to 600 items a minute. Whereas the Averaging method's accuracy decreased due to the calculations being performed on higher amplitude oscillations of the graphs because of the decreased time. The error percentages were between 0.6 and 3.2%.

The Frequency and Damping methods are more suitable for a wider range of load cells. It was found that a higher damping factor of the load cells caused the oscillations of the graphs to reach steady state faster. Furthermore, a higher spring constant causes more oscillations with lower amplitude. Therefore having load cells with a higher damping factor and a lower spring constant that tends to reach steady state faster is preferred for the Averaging method as it depends on the start and finish position of the calculation of the graph data at the final 35%. Whereas, the Damping and Frequency methods do not depend on the behaviour of the graph after the initial oscillations; as long as the damping factor and the spring constant can be found accurately then it is a matter of obtaining the peak values of the initial oscillations.

Real world testing was performed to find the accuracy and reliability of the weighing system. Analysis using the Averaging method showed an increase of error between 0.1% and 0.5% due to speed while running various weights between 82g and 355.5g on the weighing system at 300cpm and 600cpm. There was a case when the error increased by 3% for the 355.5g weight. Repeatability tests showed that there were discrepancies when running a 100g weight as the ranges varied with increasing speed between 2.9g and 6.5g. The maximum range of 6.5g with a standard deviation of 1.83g was obtained while running at 600cpm. Part of this discrepancy was from the carriers and the z-plate that is placed on top of the load cell. This was shown through further repeatability tests performed by running empty carriers over the dual load cell system. Results ranged between 2.2g and 2.6g. The standard deviations seemed to be consistent between 0.71g and 0.77g.

The Damping method gave, while running the weights between 82g and 355.5g at 300cpm and 600cpm, varying results depending on how close the model outcome represented the actual outcome from the weighing system. There was an error between 0.22% and 0.86% for weights between 82g and 189.5g. The 264g weight gave better accuracy at 600cpm, and the 355.5g weight’s error increased to 2.84% with increasing speed. It was not consistent as the simulated outcome due to disturbances in the system. The general trend was that error increased with increasing weight and speed. Comparing this to the Averaging method showed that the Damping method had better accuracy in two cases while running at 300cpm and 600cpm. The difference between the accuracies was minimal, but due to the Damping method being calculated in a shorter duration, it is an improvement.

Spectral Analysis of the graphs of these weights at different speeds between 300cpm and 600cpm showed that the periods, and hence the frequencies, were not consistent for each weight at different speeds. This was due to disturbances to the system.

Modelling of the load cell as a second order mass spring damper system is similar to that applied by Gilman & Bailey (2006), Bahar & Horrocks (1997), Halimic & Balachandran (1995) and Shu (1993), although the results from the methods obtained here are better than those researched in the literature review. Shu (1993) has investigated a method similar to the Averaging method where the weight was acquired to 1% accuracy from 20% of the data measurements. The heaviest weight tested was 173.8g. The Averaging method, as mentioned above, has acquired accuracies of less than 0.5% up to a similar weight. Gilman & Bailey (2006) have shown that the weights can be calculated in 50ms periods while investigating weighing using impact on load cells. The Damping and Frequency methods were able to predict the weight from the first three peaks of the data while running at 600cpm. This equates to 1 cup in 0.1s, with the first three oscillations occurring in less than half that time (50ms). Generally, the weight accuracies acquired through Artificial Neural Networks were low such as Yasin & White (1999) investigating the tri beam load cell with accuracies of 1.5%, and Bahar & Horrocks (1997) investigating masses being dropped onto load cells with an accuracy of 2.3% while applying a 40g weight.

Disturbances and external interference were the main culprits for inaccuracies in determining the weight. It has been found that the system is susceptible to various factors including;

- The mechanical assembly and setup (isolation)
- Mechanical setup (heights, transition)
- The mechanical components (z-plate, material)
- External noise (disturbances)
- The carrier's tolerance
- Item's physical shape (stability)

When these factors are flagrant, the graph of the output of the load cell does not abide by the expected outcome of the system model. Therefore the algorithms do not give an accurate prediction of the weight as seen from the results.

Some precautions have been put in place to avoid disturbances such as isolating the mechanical assembly of the weighing section from the rest of the machine. Therefore

machine noise does not travel to the load cells and affect the accuracy. Also, the carrier design has a weighing position that is floating to avoid extra weight being added or removed. The transition plates, placed on either side of the carriers, shift the carriers to the correct floating height onto the weigh plates of the weighing section. These plates need to be setup at 10mm from the bottom of the chain extrusion. Refer to Figure 26. If they are setup less than 10mm then the carriers collide with the edge of the weigh plates causing them to bounce therefore affecting the stability of the items on top of the carriers. If they are setup higher than 10mm then the carriers drop onto the weigh plates causing the carriers and the items on the carriers to become unstable.

Disturbances from carriers were prominent due to the length of the z-plate that is placed on top of the load cells. Refer to Figure 42. The z-plates were 90mm long whereas the carriers placed on the chain were at a 95.25mm pitch. There is also a 1mm gap between the z-plate and the weighing plates. Therefore two carriers are on the z-plate at the same time for a distance of 4.25mm. A test was done by removing every second carrier from the chain and running a repeatability test by running a 166g weight twenty times over the load cell at different speeds. It proved that the accuracy improved when every second carrier was removed, as well as the standard deviation and the range decreasing between measurements.

External noise Disturbances were introduced from human interferences with the weights placed on the load cells while acquiring their parameters to predict the weight. This caused inaccuracies when trying to predict the weight using the Damping and Frequency methods.

Inaccuracies in the weighing were sometimes due to the carrier's tolerances. Measuring all the floating components of the carrier that are always part of the weight calculated had a variance of 1.8g. This included the frame ranging between 50.912 and 52.004g, the latch ranging between 16.301 and 16.469g and the rollers and axle ranging between 74.92 and 75.78g.

Inaccuracies to weighing occurred when an item was unstable on the carriers therefore exerting more pressure onto one load cell than the other. A test was performed whereby foam was placed on the lip of every frame of ten carriers and weights of 88, 166 and 253g were run at 400 and 600cpm. Results were inconclusive as they showed that the error was lower by having foam on at higher speeds, but not at lower speeds. Although, the foam was beneficial as the standard deviation and the range were generally lower from the results of carriers with foam than without, resulting in more consistent results with the foam.

Chapter 7: Conclusion & Future Recommendations

Constructing a mathematical model of the weighing system was a profitable activity. It allowed for the creation and comparison of different methods which were used as effective means of predicting the weight. The methods allowed accurate prediction of the weights passing a dual load cell system before the settling time of the oscillatory response.

These methods were used on data exported from the high speed weighing system that was designed and built to allow for experimentation and data analysis. In addition to this, simulations were performed on a programmed user interface that has produced an effective means of comparing the methods and presenting the user with results in an aesthetically pleasing manner.

It has been shown that the Damping and Frequency method were an improvement over the Averaging method currently used by Compac on their weighing inspection system, allowing for a faster measurement time thereby speeding up the process and increasing throughput.

Future work should be spent eliminating the noise disturbances which originate from various sources as seen throughout the thesis and improving the design of the weighing structure. I recommend concentrating on further research by splitting it into three sections; mechanical & design, noise vibration and method of calculation.

The z-plate should be made longer so two carriers are never exerting force on the load cell at any one time. Performing this would mean redesigning the weigh plates before or after the z-plate to avoid interference. I recommend further research being performed on the material of the z-plate and weigh plates. Hardened stainless steel at 2.75mm thickness is not a standard thickness that is readily available. A lighter and stiffer design would be beneficial and possibly more cost effective.

Stability of the items to be weighed on the carriers is crucial therefore further research should be performed on adding foam-like materials to the frame of the carriers. Minimising the bouncing and side rocking of the carriers and the items on them is critical. Furthermore, increasing the floating range in the carriers is recommended to avoid the tight tolerances that are currently needed during the setup, such as the 2mm gap needed between the load cell mounting block and the extrusion.

Noise vibration includes investigating the mechanical structure, the load cell system and the carriers. Having the weighing structure bolted to the floor isolated from the rest of the machine was successful in eliminating the noise from the rest of the machine when setup correctly. However, external noise was still evident in the data. Therefore further research on minimising this noise using such methods as rubber padding underneath the legs of the weigh structure to eliminate noise itinerant through the ground, and also, having a tuned mass damper to eliminate the external unwanted vibrations would be beneficial.

Investigation of stiffening and reducing the mass of the carriers themselves is recommended, as the presence of varying frequencies in the data raises the question of whether the flexing of the carriers might also be affecting the loadcell signals.

Furthermore, and possibly before the study on the carriers, it would be valuable investigating the natural frequencies of the load cell system and the mechanical structure. This would give further insight on the frequencies that would cause vibration problems due to excitation. This will probably influence the decisions in regards to further design done to the system, in terms of stiffening the weighing structure and carriers.

Further work should be done on other models of the system to provide alternative algorithms and methods of acquiring the weight run over the load cells. I would recommend investigating a mass, two springs, two damper system and a two mass, two springs, two damper system. This would allow comparing the models and determining which one is the most accurate representation of the system. The accuracy of the results of the model analysis is dependent upon how well the model represents the real system. The closer the model is to its actual counterpart, the more concise the predictions made and conclusions drawn about the system behaviour.

I would recommend investing time in creating a weighing diagnosis tool. This tool would ideally have the ability to capture raw as well as filtered data, and allow the application of various signal processing algorithms such as the Averaging, Frequency and Damping methods to allow easy and quick comparison through the use of statistical analysis of accuracy and precision. In addition to this, the tool can be used for investigating various filters, especially digital adaptive filters as recommended in the literature review.

Finally, a holistic improvement approach, whereby the whole system is analysed in terms of materials, manufacturing methods, design specifications and assembly installation

instructions, should be implemented on the weighing system. The future improvements need to be looked at from a cost benefit point of view, and depend on what is accepted for the application. The accuracy might be within the industry standard, and tolerances of variation allowed. As competition increases, and the demand for better accuracy and lower tolerances of variation are required, higher costs might be involved in improving the system.

References

Bahar, H. B., & Horrocks, D. H. (1997). Dynamic weight estimation using an artificial neural network. *Artificial Intelligence in Engineering, 12*, 135-139.

Balachandran, W., Halimic, M., Hodzic, M., Tariq, M., Enab, Y., & Cecelja, F. (1995). Optimal digital control and filtering for dynamic weighing systems. *Integrating Intelligent Instrumentation and Control*, 293-298.

Calpe, J., Soria, E., Martunez, M., Frances, J. V., Rosaldo, A., Gomez-Chova, L., et al. (2002). High-speed weighing system based on DSP. *Proceedings of the 2002 28th Annual Conference of the IEEE Industrial Electronics Society, 1-4*, 1579-1583.

Frances, J. V., Calpe, J., Soria, E., Martinez, M., Rosado, A., Serrano, A. J., et al. (2000). Application of ARMA Modelling to the Improvement of Weight Estimations In Fruit Sorting and Grading Machinery. *2000 IEEE International Conference on Acoustics, Speech, and Signal Processing, 1-4*, 1579-1583.

Gilman, A., & Bailey, D. G. (2006). High-speed weighing using impact on load cells. *Tencon 2005 IEEE Region 10 Conference 1-5*, 2443-2448.

Halimic, H., & Balachandran, W. (1995). Kalman filter for dynamic weighing system. *Proceedings of the IEEE International Symposium on 2*, 786-791.

Jafaripanah, M., Al-Hashimi, B. M., & White, N. M. (2005). Application of analog adaptive filters for dynamic sensor compensation. *IEEE Transactionss on Instumentation and Measurement, 54*(1), 245-251.

Mathworks. (2011). *Accelerating the pace of Engineering and Science*. Retrieved from http://www.mathworks.com/products/matlab/description1.html

McGuinness, M., Jenkins, D., & Senaratne, G. (2005). Modelling the physics of high-speed weighing. 1-20.

Muller, I., de Brito, R. M., Pereira, C. E., & Brusamarello, V. (2010). Load cells in force sensing analysis – theory and a novel application. *IEEE Instrumentation & Measurement Magazine, 13*(1), 15-19.

Robens, E. (1999). High-Speed Weighing. *Thermal Analysis and Calorimetry, 55*, 455-460.

Shu, W. Q. (1993). Dynamic weighing under nonzero initial conditions. *IEEE Transactions on Instumentation and Measurement, 42*(4), 806-811.

Solidworks. (2011). *Productivity Intuitive 3D design solutions let you focus on your product, not running the software*. Retrieved from http://www.solidworks.com/sw/why-solidworks/solidworks-productivity.htm

Windrow, B., & Lehr, M. A. (1990). 30 years of adaptive neural networks: perceptron, madaline, and backpropagation. *Proceedings of the IEEE, 78*(9), 1415-1442.

Yasin, S. M. T. A., & White, N. M. (1999). Application of Artificial Neural Networks to Intelligent Weighing Systems. *Science, Measurement and Technology, 146*(6), 265-269.

Appendices

Appendix A Load Cell Datasheet

Model LPS

Celtron

VISHAY PRECISION GROUP

Low-Profile Single Point

FEATURES

- Capacities: 0.6 to 200kg
- Small size with low profile
- Anodized aluminum
- NTEP Class III 5000S approval from 3kg to 30kg
- OIML C3 approval
- Platform size: 16"x16"/ 40cm x 40cm

OPTIONAL FEATURE

- FM approval available

APPLICATIONS

- Packaging machines
- Dosing/filling
- Belt scales/conveyor scales
- In-motion check weigher
- Retail scales/counting scales

DESCRIPTION

LPS is designed for electronic scales and platform scales where only one load cell can be used and low profile is required. It is the lightest model of Celtron single point load cell family. The design is most suitable for mass production operations.

LPS is constructed of anodized aluminum and is fully potted IP66 levels, providing excellent protection against moisture ingression.

OUTLINE DIMENSIONS

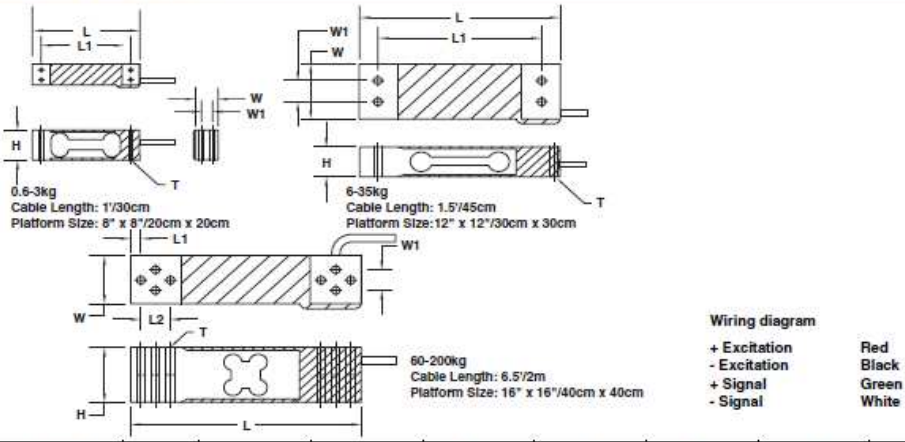

Wiring diagram

+ Excitation	Red
- Excitation	Black
+ Signal	Green
- Signal	White

CAPACITY (kg)		L	L1	L2	W	W1	H	T
0.6/1/2/3	mm	70.0	58.0	---	15.0	7.0	22.0	M3 x 0.5
	(inch)	2.76	2.28	---	0.59	0.28	0.87	
6/10/15/20	mm	130.0	106.0	---	30.0	15.0	22.0	M6 x 1.0
	(inch)	5.12	4.17	---	1.18	0.59	0.87	
30/35	mm	130.0	106.0	---	40.0	15.0	22.0	M6 x 1.0
	(inch)	5.12	4.17	---	1.57	0.59	0.87	
60/100/200	mm	150.0	7.0	19.0	35.0	15.0	40.0	M6 x 1.0
	(inch)	5.91	0.28	0.75	1.38	0.59	1.57	

www.vishaypgloadcells.com Technical contact in Americas: lc.usa@vishaypg.com, Europe: lc.eur@vishaypg.com, Document Number: 11707
136 China: lc.china@vishaypg.com, Taiwan: lc.roc@vishaypg.com Revision: 05-Feb-10

VISHAY PRECISION GROUP

Model LPS

Low-Profile Single Point — Celtron

SPECIFICATIONS				
PARAMETER	**VALUE**			**UNIT**
NTEP/OIML Accuracy class	NTEP III	Non-Approved	C3	
Maximum no. of intervals (n)	5000 single (1)	1000	3000 (2)	
$Y = E_{max}/V_{min}$	8000	1400	6000	Maximum available 12000
Standard capacities (E_{max})	0.6, 1, 2, 3, 6, 10, 15, 20, 30, 35, 60, 100, 200			kg
Rated output-R.O.	2.0 (3)			mV/V
Rated output tolerance	10			±% of rated output
Zero balance	3			±% of rated output
Non linearity	0.025	0.030	0.020	±% of rated output
Hysteresis	0.025	0.030	0.020	±% of rated output
Non-repeatability	0.020			±% of rated output
Creep error (20 minutes)	0.030	0.030	0.017	±% of rated output
Zero return (20 minutes)	0.030	0.030	0.017	±% of rated output
Temperature effect on min. dead load output	0.0026	0.0026	0.014	±% of rated output/°C
Temperature effect on sensitivity	0.0015	0.0015	0.008	±% of applied load/°C
Compensated temperature range	-10 to +40			°C
Operating temperature range	-20 to +60			°C
Safe overload	150			% of R.C.
Ultimate overload	200			% of R.C.
Excitation, recommended	10			Vdc or Vac rms
Excitation, maximum	15			Vdc or Vac rms
Input impedance	410±10			Ohms
Output impedance	350±3			Ohms
Insulation resistance	>5000			Mega-Ohms
Construction	Anodized aluminum			
Environmental protection	IP66			

Notes

(1) Capacities 3-30kg
(2) Capacities 6-35kg
(3) 1mV/V for 1kg and below

All Specifications subject to change without notice.

FM Approval
Intrinsically Safe: Class I, II, III; Div. 1 Groups A-G
Non-Incendive: Class I; Div. 2 Groups A-D

Appendix B Carrier Weights

Carrier	Frame Weight (g)	Latch Weight (g)	Roller and axle Weight (g)	Clip Weight (g)	Total Calculated Weight (g)	Total Calculated Weighing weight (g) (floating)
1	50.959	16.424	75.66	30.633	173.676	143.043
2	50.978	16.416	75.6	30.83	173.824	142.994
3	50.918	16.428	74.92	30.635	172.901	142.266
4	50.947	16.45	75.7	30.637	173.734	143.097
5	51.038	16.428	75.06	30.628	173.154	142.526
6	50.95	16.454	75.63	30.831	173.865	143.034
7	51.032	16.43	74.94	30.829	173.231	142.402
8	52.004	16.459	75.62	30.636	174.719	144.083
9	51.789	16.422	75.02	30.826	174.057	143.231
10	51.697	16.458	75.63	30.836	174.621	143.785
11	51.727	16.432	75.06	30.637	173.856	143.219
12	51.766	16.427	75.63	30.64	174.463	143.823
13	51.833	16.453	75.6	30.823	174.709	143.886
14	51.807	16.425	75.61	30.824	174.666	143.842
15	51.755	16.459	74.94	30.828	173.982	143.154
16	51.837	16.423	75.7	30.64	174.6	143.96
17	51.828	16.429	75.66	30.631	174.548	143.917
18	51.82	16.431	75.56	30.828	174.639	143.811

19	51.178	16.418	75.78	30.638	174.014	143.376
20	51.022	16.428	74.98	30.831	173.261	142.43
21	51.023	16.461	75.65	30.826	173.96	143.134
22	50.959	16.423	75.62	30.631	173.633	143.002
23	50.952	16.465	75.6	30.825	173.842	143.017
24	51.003	16.451	75.01	30.638	173.102	142.464
25	51.074	16.456	75.75	30.819	174.099	143.28
26	51.004	16.462	75.63	30.63	173.726	143.096
27	50.912	16.469	75.08	30.632	173.093	142.461
28	51.67	16.427	75.59	30.829	174.516	143.687
29	51.043	16.458	75.63	30.637	173.768	143.131
30	50.922	16.419	75.61	30.636	173.587	142.951
31	50.975	16.301	75.39	30.75	173.416	142.666
32	51.026	16.424	74.97	30.64	173.06	142.42
33	50.98	16.444	75.69	30.82	173.934	143.114
34	50.925	16.452	74.97	30.64	172.987	142.347
35	50.916	16.451	75.67	30.632	173.669	143.037
36	51.017	16.453	74.92	30.633	173.023	142.39
37	50.929	16.444	75.64	30.638	173.651	143.013
38	50.931	16.414	74.98	30.646	172.971	142.325
39	51.006	16.45	75.61	30.83	173.896	143.066
40	50.914	16.415	74.92	30.829	173.078	142.249

Appendix C Sample output weighing data file

The output weighing data files has the properties of capture scenario and then the samples in columns. Each column represents a Load Cell.

Below is a screenshot of the first page of a weighing data file representing 4 channels meaning four load cells active, with a weighing interval of 250 μs .The cycle percentage represents the number of carriers captured on screen at any time; 300 means three carriers captured. The screen shot shows the first 40 readings out of the 1250readings taken during that capture. The sampling rate is set to 4kHz.

	A	B	C	D	E	F
1	Channels	4				
2	Channel mask	15				
3	WeighInterval(us)	250				
4	CyclePercentage	300				
5	DesiredReadings	1250				
6	ActualReadings	1250				
7						
8	1	1171	1097	1126	1168	
9	2	1171	1095	1124	1168	
10	3	1171	1095	1124	1168	
11	4	1171	1095	1124	1165	
12	5	1173	1095	1124	1165	
13	6	1173	1095	1124	1163	
14	7	1173	1095	1124	1160	
15	8	1173	1095	1124	1160	
16	9	1173	1092	1124	1158	
17	10	1173	1092	1124	1155	
18	11	1175	1092	1124	1153	
19	12	1175	1095	1126	1153	
20	13	1175	1095	1126	1153	
21	14	1175	1095	1129	1150	
22	15	1178	1095	1129	1148	
23	16	1178	1095	1131	1146	
24	17	1178	1095	1134	1146	
25	18	1178	1097	1136	1143	
26	19	1178	1097	1139	1141	
27	20	1178	1099	1141	1141	
28	21	1178	1099	1144	1138	
29	22	1178	1099	1149	1136	
30	23	1180	1102	1151	1136	
31	24	1178	1104	1153	1133	
32	25	1180	1104	1158	1131	
33	26	1180	1107	1161	1131	
34	27	1180	1107	1166	1128	
35	28	1180	1109	1168	1128	
36	29	1180	1109	1171	1128	
37	30	1180	1112	1178	1126	
38	31	1180	1114	1181	1126	
39	32	1180	1114	1185	1123	
40	33	1180	1117	1190	1123	
41	34	1180	1119	1193	1123	
42	35	1180	1119	1198	1121	
43	36	1180	1122	1200	1121	
44	37	1180	1124	1205	1121	
45	38	1180	1124	1208	1121	
46	39	1180	1124	1212	1119	
47	40	1180	1124	1215	1121	

Appendix D Sampling Restrictions

The table shows the samples for 2 to 12 carriers running at 300, 342, 350, 400, 500, 600 and 700 carriers per minute. The second column represents the carriers per second. The cells highlighted pink are indicating missed samples.

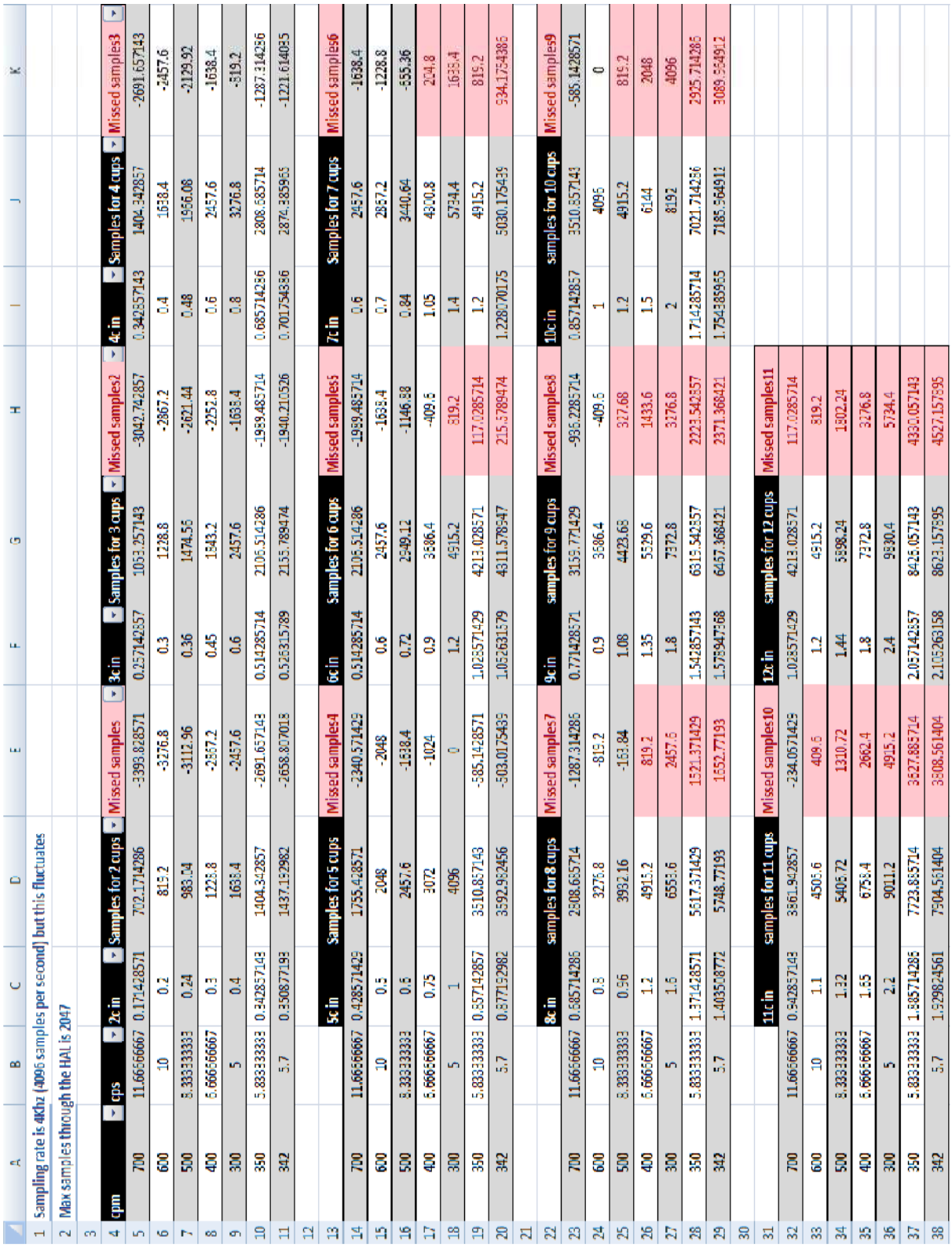

	A	B	C	D	E	F	G	H	I	J	K
1	Sampling rate is 4Khz (4096 samples per second) but this fluctuates										
2	Max samples through the HAL is 2047										
3											
4	cpm	cps	2c in	Samples for 2 cups	Missed samples	3c in	Samples for 3 cups	Missed samples2	4c in	Samples for 4 cups	Missed samples3
5	700	11.66666667	0.171428571	702.1714286	-3393.828571	0.257142857	1053.257143	-3042.742857	0.342857143	1404.342857	-2691.657143
6	600	10	0.2	819.2	-3276.8	0.3	1228.8	-2867.2	0.4	1638.4	-2457.6
7	500	8.333333333	0.24	983.04	-3112.96	0.36	1474.56	-2621.44	0.48	1966.08	-2129.92
8	400	6.666666667	0.3	1228.8	-2867.2	0.45	1843.2	-2252.8	0.6	2457.6	-1638.4
9	300	5	0.4	1638.4	-2457.6	0.6	2457.6	-1638.4	0.8	3276.8	-819.2
10	350	5.833333333	0.342857143	1404.342857	-2691.657143	0.514285714	2106.514286	-1939.485714	0.685714286	2808.685714	-1287.314286
11	342	5.7	0.350877193	1437.192982	-2658.807018	0.526315789	2155.789474	-1940.210526	0.701754386	2874.385965	-1221.614035
12											
13			5c in	Samples for 5 cups	Missed samples4	6c in	Samples for 6 cups	Missed samples5	7c in	Samples for 7 cups	Missed samples6
14	700	11.66666667	0.428571429	1755.428571	-2340.571429	0.514285714	2106.514286	-1939.485714	0.6	2457.6	-1638.4
15	600	10	0.5	2048	-2048	0.6	2457.6	-1638.4	0.7	2867.2	-1228.8
16	500	8.333333333	0.6	2457.6	-1638.4	0.72	2949.12	-1146.88	0.84	3440.64	-655.36
17	400	6.666666667	0.75	3072	-1024	0.9	3686.4	-409.6	1.05	4300.8	204.8
18	300	5	1	4096	0	1.2	4915.2	819.2	1.4	5734.4	1638.4
19	350	5.833333333	0.857142857	3510.857143	-585.1428571	1.028571429	4213.028571	117.0285714	1.2	4915.2	819.2
20	342	5.7	0.877192982	3592.982456	-503.0175439	1.052631579	4311.578947	215.5789474	1.228070175	5030.175439	934.1754386
21											
22			8c in	samples for 8 cups	Missed samples7	9c in	samples for 9 cups	Missed samples8	10c in	samples for 10 cups	Missed samples9
23	700	11.66666667	0.685714286	2508.685714	-1287.314286	0.771428571	3135.771429	-935.2285714	0.857142857	3510.857143	-585.1428571
24	600	10	0.8	3276.8	-819.2	0.9	3686.4	-409.6	1	4095	0
25	500	8.333333333	0.96	3932.16	-163.84	1.08	4423.68	327.68	1.2	4915.2	819.2
26	400	6.666666667	1.2	4915.2	819.2	1.35	5529.6	1433.6	1.5	6144	2048
27	300	5	1.6	6553.6	2457.6	1.8	7372.8	3276.8	2	8192	4096
28	350	5.833333333	1.371428571	5617.371429	1521.371429	1.542857143	6315.542857	2223.542857	1.714285714	7021.714286	2925.714286
29	342	5.7	1.403508772	5748.77193	1652.77193	1.578947368	6457.368421	2371.368421	1.754385965	7185.564911	3089.564912
30											
31			11c in	samples for 11 cups	Missed samples10	12c in	samples for 12 cups	Missed samples11			
32	700	11.66666667	0.942857143	3861.942857	-234.0571429	1.028571429	4213.028571	117.0285714			
33	600	10	1.1	4505.6	409.6	1.2	4915.2	819.2			
34	500	8.333333333	1.32	5406.72	1310.72	1.44	5898.24	1802.24			
35	400	6.666666667	1.65	6758.4	2662.4	1.8	7372.8	3276.8			
36	300	5	2.2	9011.2	4915.2	2.4	9830.4	5734.4			
37	350	5.833333333	1.885714286	7723.885714	3627.885714	2.057142857	8425.057143	4330.057143			
38	342	5.7	1.929824561	7904.561404	3808.561404	2.105263158	8623.157895	4527.157895			

Appendix E Peak Detection Algorithm

The Peak Detect (peakdet) function detects peaks in a vector. It finds the local maxima and minima peaks in the vector V.

With [MAXTAB, MINTAB] = PEAKDET (V, DELTA, X); MAXTAB and MINTAB consists of two columns. Column 1 contains the x-value (usually time) and Column 2 the found peak value. A point is considered a maximum peak if it has the maximal value, and was preceded by a value lower by DELTA.

```
function [maxtab, mintab]=peakdet(v, delta, x)

maxtab = [];
mintab = [];

v = v(:); % Just in case this wasn't a proper vector

if nargin < 3
  x = (1:length(v))';
else
  x = x(:);
  if length(v)~= length(x)
    error('Input vectors v and x must have same length');
  end
end

if (length(delta(:)))>1
  error('Input argument DELTA must be a scalar');
end

if delta <= 0
  error('Input argument DELTA must be positive');
end

mn = Inf; mx = -Inf;
```

```
mnpos = NaN; mxpos = NaN;

lookformax = 1;
 for i=1:length(v)
  this = v(i);
  if this > mx, mx = this; mxpos = x(i); end
  if this < mn, mn = this; mnpos = x(i); end

  if lookformax
    if this < mx-delta
      maxtab = [maxtab ; mxpos mx];
      mn = this; mnpos = x(i);
      lookformax = 0;
    end
  else
    if this > mn+delta
      mintab = [mintab ; mnpos mn];
      mx = this; mxpos = x(i);
      lookformax = 1;
    end
  end
end
```

Appendix F Damping Method

```
load_cell = 4; %4 is LC4

file1=load('Calibration_200g_1.csv');
Mass1=200;
g=9.8;
t=file1(1:end,1)
length(file1(:,load_cell))
length (t)
time1=t/1000;
%1st load cell output
figure; plot (time1,file1(:,load_cell))
[maxtab1,mintab1]=peakdet (file1(:,load_cell),1,time1);
hold on; plot (maxtab1(:,1),maxtab1(:,2),'k*')
%Run through to find first peak
r=1;
maxtab1(r,2)
while (maxtab1(r,2)<200)
    r=r+1;
end
r

% Interesting Max for 1st load cell are at
Max1_1st = maxtab1(r,1:2)
Max1_2nd = maxtab1(r+1,1:2)
Max1_3rd = maxtab1(r+2,1:2)

%1st load cell coordinates
Max1_t1 = maxtab1(r,1);
Max1_y1 = maxtab1(r,2);
Max1_t2 = maxtab1(r+1,1);
Max1_y2 = maxtab1(r+1,2);
Max1_t3 = maxtab1(r+2,1);
Max1_y3 = maxtab1(r+2,2);
```

```
%Calculating u from three peaks
delta_y_LC4 = (Max1_y1 - Max1_y2)/(Max1_y2 - Max1_y3)
delta_t_LC4 = ((Max1_t2-Max1_t1)+(Max1_t3-Max1_t2))/2
u_LC4= (log(delta_y_LC4))/delta_t_LC4
c_LC4_M2= 2*u_LC4*(M_LC4+m1)
m_200=c_LC4_M2/(2*u_LC4) - M_LC4
load_cell = 4;
file3=load('399cpm_283g_1_m.csv');
speed=399;
time3 =file3(:,1)/1000;

%1st load cell output
plot (time3,file3(:,load_cell)-67.5) %67.5 is the mass of
the  carrier on the load cell

% hold on;
[maxtab3,mintab3]=peakdet (file3(:,load_cell)
67.5,1,time3);
hold on;
plot (maxtab3(:,1),maxtab3(:,2),'r*')

%Run through to find first peak
z=1;
while (maxtab3(z,1:2)<50)
    z=z+1;
end
z

% Interesting Max for load cell are at
Max3_1st = maxtab3(z,1:2)
Max3_2nd = maxtab3(z+1,1:2)
Max3_3rd = maxtab3(z+2,1:2)
```

```
%1st load cell coordinates
Max3_t1 = maxtab3(z,1);
Max3_y1 = maxtab3(z,2);
Max3_t2 = maxtab3(z+1,1);
Max3_y2 = maxtab3(z+1,2);
Max3_t3 = maxtab3(z+2,1);
Max3_y3 = maxtab3(z+2,2);

%first, we have to find the new u from the peaks
delta_y_ = (Max3_y1 - Max3_y2)/(Max3_y2 - Max3_y3)
delta_t_ = ((Max3_t2-Max3_t1)+(Max3_t3-Max3_t2))/2
u_LC_= (log(delta_y_))/delta_t_
m_M2=c_LC4_M2/(2*u_LC_) - M_LC4
```

Appendix G Simulation UI

```
function varargout = Simulation2(varargin)
%      SIMULATION2('CALLBACK',hObject,eventData,handles,...)
calls the local  function named CALLBACK in SIMULATION2.M with
the given input arguments.
%
gui_Singleton = 1;
gui_State = struct('gui_Name',       mfilename, ...
                   'gui_Singleton',  gui_Singleton, ...
                   'gui_OpeningFcn', @Simulation2_OpeningFcn,
...
                   'gui_OutputFcn',  @Simulation2_OutputFcn,
...
                   'gui_LayoutFcn',  [] , ...
                   'gui_Callback',   []);
if nargin && ischar(varargin{1})
    gui_State.gui_Callback = str2func(varargin{1});
end

if nargout
    [varargout{1:nargout}] = gui_mainfcn(gui_State,
varargin{:});
else
    gui_mainfcn(gui_State, varargin{:});
end
% End initialization code

% Executes just before Simulation2 is made visible.
function Simulation2_OpeningFcn(hObject, eventdata, handles,
varargin)
handles.output = hObject;

% Update handles structure
```

```
guidata(hObject, handles);

function varargout = Simulation2_OutputFcn(hObject, eventdata,
handles)
% Get default command line output from handles structure
varargout{1} = handles.output;

% Executes on button press in plot_button.
function plot_button_Callback(hObject, eventdata, handles)

% Get user input from GUI

% mass of item
m = str2double(get(handles.m_input,'String'));
% Mass of Load Cell
M = str2double(get(handles.BigM_input,'String'));
% Spring constant
k = str2double(get(handles.k_input,'String'));
% Damping coefficient
c = str2double(get(handles.c_input,'String'));
% Gravitational constant
g = str2double(get(handles.g_input,'String'));
% time
t = eval(get(handles.t_input,'String'));
time = max (t)
res = max (t) / (size (t,2)-1)

w=0.5*sqrt((4*k*(M+m)-c^2)/((M+m)^2)); %Frequency
u=c/(2*(M+m)); %Damping factor

x=((-m*g/k)*exp(-u*t).*cos(w*t))-((m*g*u/(k*w))*exp(-
u*t).*sin(w*t))+((m*g)/k);

% Create time plot
```

```
axes(handles.time_axes)
plot(t,x)
grid on
Xlabel ('time (ms)')
Ylabel ('Load Cell Output (deflection)')
Title ('High Speed Weighing')

%Peaks using the Peak Detection Algorithm
[maxtab,mintab]=peakdet (x,0.001,t);
hold on;
plot (maxtab(:,1),maxtab(:,2),'r*')
hold off;
Max_1st_x = maxtab(1,1)
Max_1st_y = maxtab(1,2)

Max_2nd_x = maxtab(2,1)
Max_2nd_y = maxtab(2,2)

Max_3rd_x = maxtab(3,1)
Max_3rd_y = maxtab(3,2)

%%%%%%%%%%%%%%%%%%%%%%%

T=Max_2nd_x - Max_1st_x;
f = 1/T;
w1=2*pi*f;

T=Max_3rd_x - Max_2nd_x;
f = 1/T;
w2=2*pi*f;

w_actual=0.5*sqrt((4*k*(M+m)-c^2)/((M+m)^2)) %Frequency

%Total Mass of Load Cell and Item
```

```
M_= (k + sqrt(k^2-(w1^2*c^2)))/(2*w1^2)

%Mass of item
m_MSD_freq= M_-M

%Error
m_MSD_freq_error = abs(m-m_MSD_freq)
%m_MSD_freq_error_perc = abs((m-m_MSD_freq)/m * 100)
m_MSD_freq_error_perc = ((m-m_MSD_freq)/m * 100)

%%%%%%%%%%%%%%%%%%%%%%%%

%Averaging Method

Max_3rd_x = maxtab(3,1);
Max_3rd_y = maxtab(3,2);

total=0;
count = 0;

time
res
Tot_Time = time/res
avg_interval = time/res * 0.35

for i= (Tot_Time - avg_interval): 1 : Tot_Time % averaging the
last 35%
    total = total + x(i);
    count= count +1;
end

avg = total / count;

m_Avg= avg * k / g
```

```
%Error
m_Avg_error = abs(m-m_Avg)
%m_Avg_error_perc = abs((m-m_Avg)/m * 100)
m_Avg_error_perc = ((m-m_Avg)/m * 100)

%%%%%%%%%%%%%%%%%%%%%%

% Dsmping Method
del_y = (Max_1st_y - Max_2nd_y) / (Max_2nd_y - Max_3rd_y)
del_t = ((Max_2nd_x - Max_1st_x) + (Max_3rd_x - Max_2nd_x))/2

u_3peaks = log(del_y)/del_t % Damping coeffitient

%Total Mass of Load Cell and Item
M_3peaks = c / (2*u_3peaks)

%Mass of item
m_3peaks = M_3peaks - M

%Error
m_3peaks_error = abs(m-m_3peaks)
% m_3peaks_error_perc = abs((m-m_3peaks)/m * 100)
m_3peaks_error_perc = ((m-m_3peaks)/m * 100)

%%%%%%%%%%%%%%%%%%%%%%
r=[m_MSD_freq m_Avg m_3peaks m_MSD_freq_error m_Avg_error
m_3peaks_error m_MSD_freq_error_perc m_Avg_error_perc
m_3peaks_error_perc]
% dlmwrite ('results7.csv', r, '/t', '-append')

dlmwrite ('results21.csv', r,'coffset',1, '-append')

% output to excel file
```

```
% fid = fopen('results5.xls','wb')
% count = fwrite (fid , r)
% ST = fclose (fid)
% if m==50
%     r=[m_MSD_freq m_Avg M_3peaks]
% end
%
% r=[r; m_MSD_freq m_Avg M_3peaks]

%Output
set (handles.MSD_freq,'String', m_MSD_freq)
set (handles.Averaging,'String', m_Avg)
set (handles.MSD_damping,'String', m_3peaks)

set (handles.MSD_freq_error,'String', m_MSD_freq_error_perc)
set (handles.Averaging_error,'String', m_Avg_error_perc)
set (handles.MSD_damping_error,'String', m_3peaks_error_perc)

% Executes during object creation, after setting all
properties.
function m_input_CreateFcn(hObject, eventdata, handles)

if ispc && isequal(get(hObject,'BackgroundColor'),
get(0,'defaultUicontrolBackgroundColor'))
    set(hObject,'BackgroundColor','white');
end
```

Appendix H Frequency depending on speed

```
% Loading Data
load_cell = 4; %LC =1 (lane1 LC1), =2 (Lane1 LC2), =3 (Lane2
LC1), =4 (Lane 2 LC2)
load_cell = load_cell + 1;
samples = 1250; % number of samples
file1=load('300cpm_711g_1.csv');
speed=300;
x=file1;

% Getting time in x axis
t=0:3*60/speed/samples:(3*60/speed)-(3*60/speed/samples);
length(file1(1:samples,load_cell));
length (t);
%1st load cell output
figure; plot (t,file1(1:samples,load_cell),'b')
hold on;
[maxtab1,mintab1]=peakdet (file1(1:samples,load_cell),10,t);
hold on; plot (maxtab1(:,1),maxtab1(:,2),'r*')

%faster speed (400cpm)
file2=load('400cpm_711g_1.csv');
speed = 400;
t=0:3*60/speed/samples:(3*60/speed)-(3*60/speed/samples);
% figure;
plot (t,file2(1:samples,load_cell),'g')

[maxtab2,mintab2]=peakdet (file2(1:samples,load_cell),10,t);
hold on;
plot (maxtab2(:,1),maxtab2(:,2),'b*')

%faster speed (500cpm)
file3=load('500cpm_711g_1.csv'); speed = 500;
```

```
t=0:3*60/speed/samples:(3*60/speed)-(3*60/speed/samples);
%  figure;
plot (t,file3(1:samples,load_cell),'r')

[maxtab3,mintab3]=peakdet (file3(1:samples,load_cell),10,t);
hold on; plot (maxtab3(:,1),maxtab3(:,2),'g*')

%faster speed (600cpm)
file4=load('600cpm_711g_1.csv');
speed = 600;
t=0:3*60/speed/samples:(3*60/speed)-(3*60/speed/samples);
% figure;
plot (t,file4(1:samples,load_cell),'m')

[maxtab4,mintab4]=peakdet (file4(1:samples,load_cell),10,t);
hold on; plot (maxtab4(:,1),maxtab4(:,2),'k*')

%Finding the first peak
i=1;
maxtab1(i,2);
while maxtab1(i,2)<1500
    i=i+1;
end

%Calculating the frequncy
Max1_t1=maxtab1(i,1);
Max1_t2=maxtab1(i+1,1);

t1= Max1_t2-Max1_t1;
f_300cpm=1/t1

%Finding the first peak
m=1;
maxtab2(m,2);
```

```
while maxtab2(m,2)<1500
    m=m+1;
end

%Calculating the frequncy
Max2_t1=maxtab2(m,1);
Max2_t2=maxtab2(m+1,1);

t2= Max2_t2-Max2_t1;
f_400cpm=1/t2

%Finding the first peak
n=1;
maxtab3(n,2);
while maxtab3(n,2)<1500
    n=n+1;
end

%Calculating the frequncy
Max3_t1=maxtab3(n,1);
Max3_t2=maxtab3(n+1,1);

t3= Max3_t2-Max3_t1;
f_500cpm=1/t3

%Finding the first peak
p=1;
maxtab4(p,2);
while maxtab4(p,2)<1500
    p=p+1;
end

%Calculating the frequncy
Max4_t1=maxtab4(p,1);
```

```
Max4_t2=maxtab4(p+1,1);

t4= Max4_t2-Max4_t1;
f_600cpm=1/t4
```

Appendix I Weigh graphs at various speeds

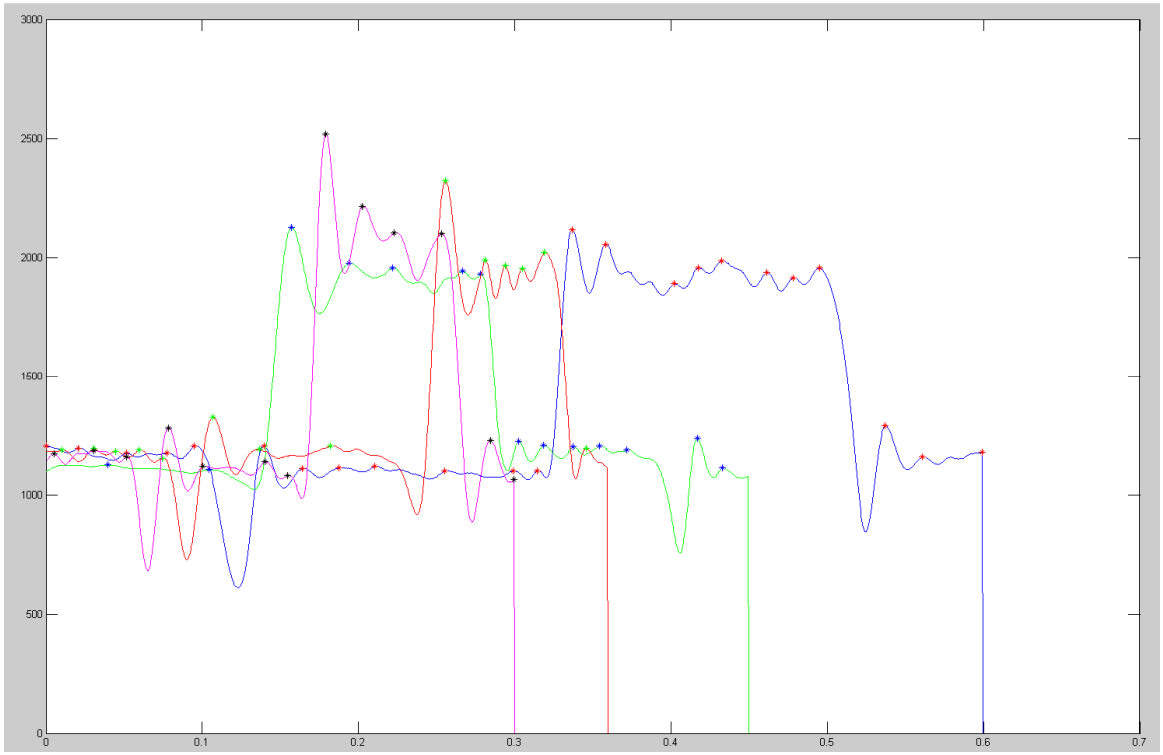

Figure 52: Weigh Graphs of 164g at 300cpm, 400cpm, 500cpm and 600cpm on Load Cell 3 (Lane 2, LC 3)

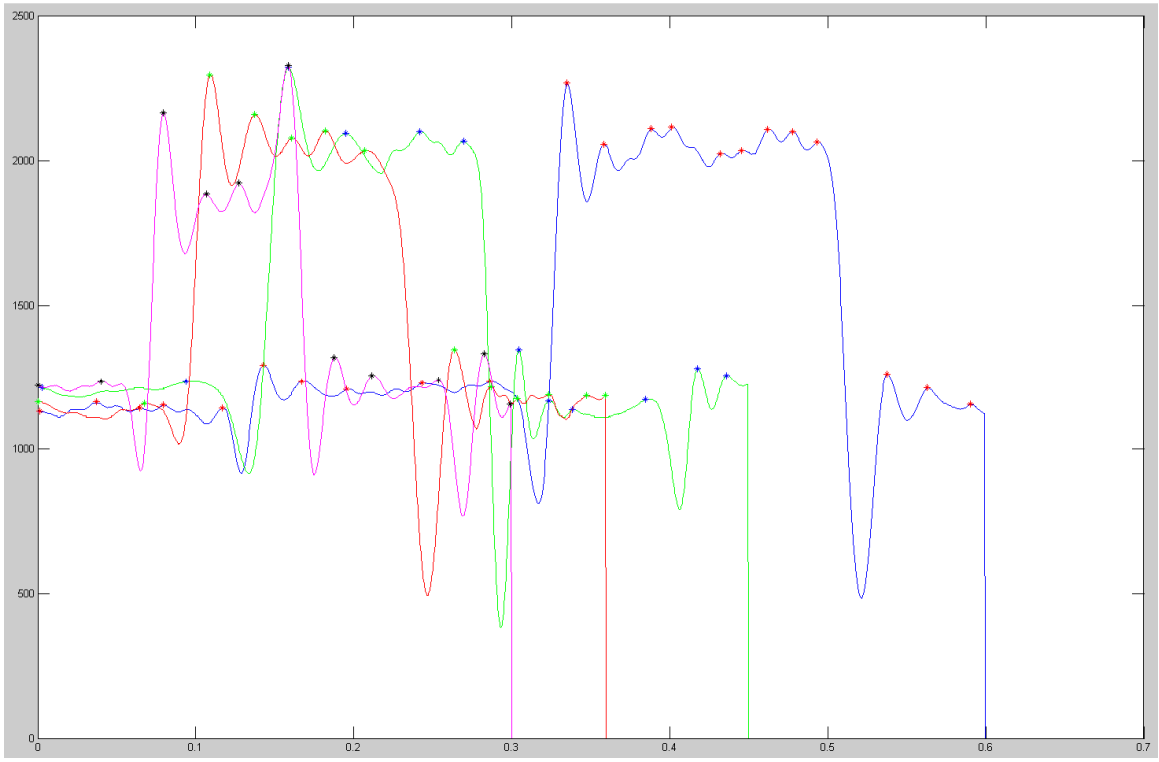

Figure 53: Weigh Graphs of 164g at 300cpm, 400cpm, 500cpm and 600cpm on Load Cell 4 (Lane 2, LC 4)

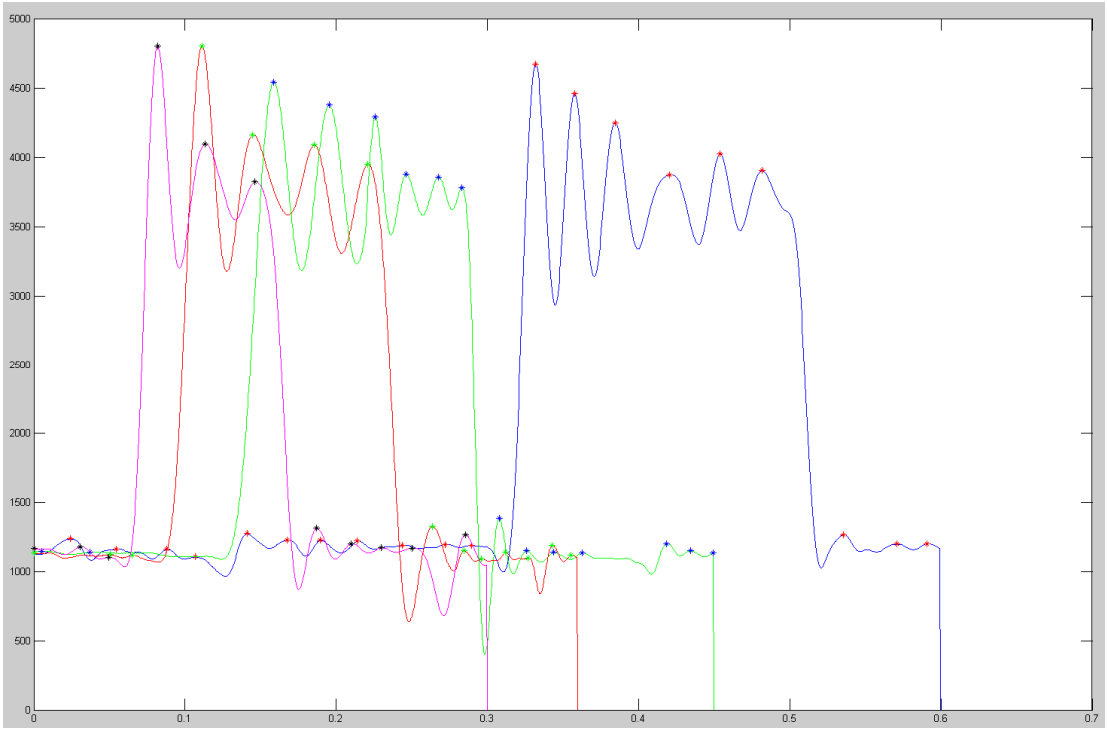

Figure 54: Weigh Graphs of 528g at 300cpm, 400cpm, 500cpm and 600cpm on Load Cell 3 (Lane 2, LC 1)

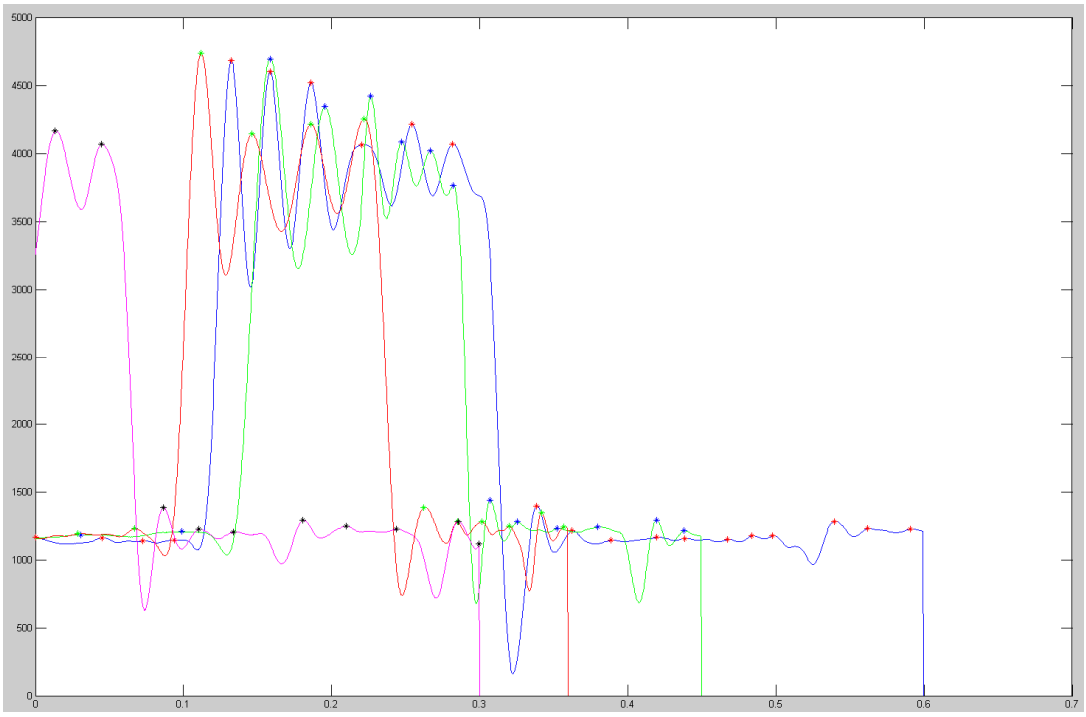

Figure 55: Weigh Graphs of 528g at 300cpm, 400cpm, 500cpm and 600cpm on Load Cell 4 (Lane 2, LC 2)

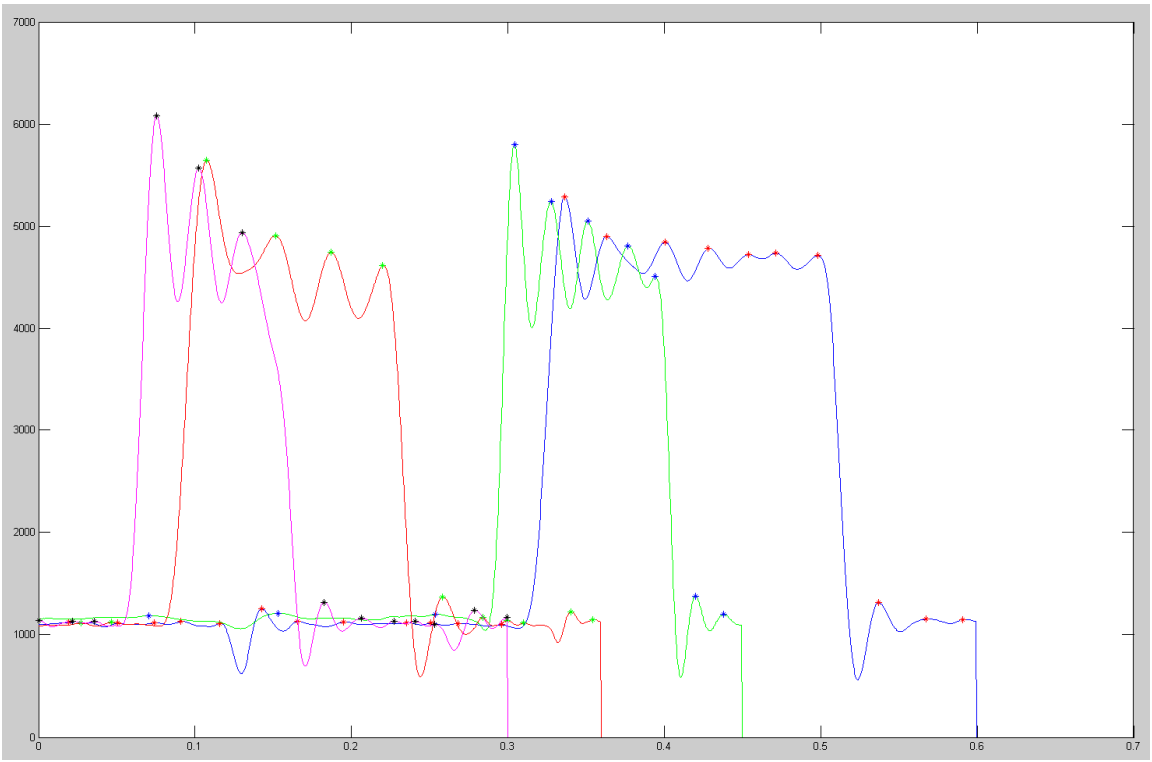

Figure 56: Weigh Graphs of 711g at 300cpm, 400cpm, 500cpm and 600cpm on Load Cell 3 (Lane 2, LC 1)

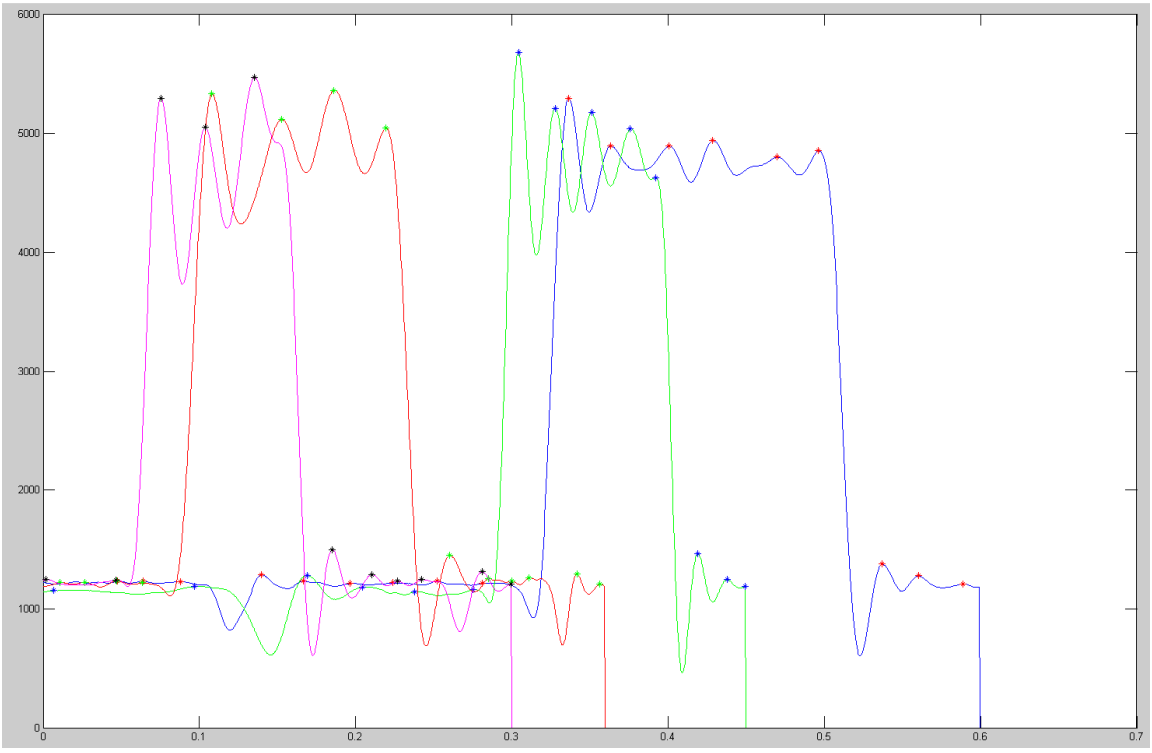

Figure 57: Weigh Graphs of 711g at 300cpm, 400cpm, 500cpm and 600cpm on Load Cell 4 (Lane 2, LC 4)